

# Permian integrative stratigraphy, biotas, paleogeographical and paleoclimatic evolution of the Qinghai-Tibetan Plateau and its surrounding areas

Shuzhong SHEN<sup>1\*</sup>, Yichun ZHANG<sup>2,3</sup>, Dongxun YUAN<sup>4</sup>, Haipeng XU<sup>1</sup>, Qi JU<sup>1</sup>,  
Hua ZHANG<sup>2</sup>, Quanfeng ZHENG<sup>2</sup>, Mao LUO<sup>2</sup> & Zhangshuai HOU<sup>1</sup>

<sup>1</sup> State Key Laboratory for Mineral Deposits Research, School of Earth Sciences and Engineering and Frontiers Science Center for Critical Earth Material Cycling, Nanjing University, Nanjing 210023, China;

<sup>2</sup> State Key Laboratory of Palaeobiology and Stratigraphy, Nanjing Institute of Geology and Palaeontology, Chinese Academy of Sciences, Nanjing 210008, China;

<sup>3</sup> University of Chinese Academy of Sciences, Nanjing 210049, China;

<sup>4</sup> School of Resources and Geosciences, China University of Mining and Technology, Xuzhou 221116, China

Received January 24, 2023; revised May 8, 2023; accepted May 31, 2023; published online September 1, 2023

**Abstract** The Permian Period was a critical time interval during which various blocks of the Qinghai-Tibetan Plateau have experienced profound and complex paleogeographical changes. The supercontinent Pangea was formed to its maximum during this interval, hampering a global east-to-west trending equatorial warm ocean current. Meanwhile, a semi-closed Tethys Ocean warm pool formed an eastward-opening oceanic embayment of Pangea, and became an engine fostering the evolutions of organisms and environmental changes during the Paleozoic-Mesozoic transition. Stratigraphy and preserved fossil groups have proved extremely useful in understanding such changes and the evolutionary histories of the Qinghai-Tibetan Plateau. Widely distributed Permian deposits and fossils from various blocks of the Qinghai-Tibetan Plateau exhibited varied characteristics, reflecting these blocks' different paleolatitude settings and drifting histories. The Himalaya Tethys Zone south to the Yarlung Zangbo suture zone, located in the northern Gondwanan margin, yields fossil assemblages characterized by cold-water organisms throughout the Permian, and was affiliated to those of the Gondwanaland. Most of the exotic limestone blocks within the Yarlung Zangbo suture zone are Guadalupian (Middle Permian) to Early Triassic in age. These exotic limestone blocks bear fossil assemblages that have transitional affinities between the warm Tethys and cold Gondwanan regions, suggesting that they most probably represent seamount deposits in the Neo-Tethys Ocean. During the Asselian to Sakmarian (Cisuralian, also Early Permian), the Cimmerian microcontinents in the northern part of Gondwana preserved glacio-marine deposits of Asselian to Sakmarian, and contained typical Gondwana-type cold-water faunas. By the middle Cisuralian (~290–280 Ma), the Cimmerian microcontinents rifted off from the Gondwanaland, and drifted northward allometrically due to the active magmatism of the Panjal Traps in the northern margin of the Indian Plate. Two slices of microcontinents are discerned as a result of such allometric drifting. The northern Cimmerian microcontinent slice, consisting of South Qiangtang, Baoshan, and Sibuma blocks, drifted relatively quickly, and preserved widespread carbonate deposits and warm-water faunas since Artinskian. By contrast, the southern Cimmerian microcontinent slice, consisting of Lhasa, Tengchong, and Irrawaddy blocks, drifted relatively slowly, and were characterized by widespread carbonate deposits containing warm-water faunas of late Kungurian to Lopingian (Late Permian). As such, these blocks rifted off from the northern Gondwanan margin since at least the Kungurian. Thus, it can be inferred that these blocks were incorporated into the low latitude, warm-water regions later than the northern Cimmerian slice. Such discrepancies in depositional sequences and paleobiogeography imply that the rifting of Cimmerian microcontinents resulted in the formation of both Meso-Tethys and Neo-Tethys oceans during the Cisuralian. By contrast, the North Qiangtang block, because of its further northern paleogeographical position, contains warm-water faunas throughout the whole Permian

\* Corresponding author (email: [szshen@nju.edu.cn](mailto:szshen@nju.edu.cn))

Period that are affiliated well with the faunas from the South China, Simao, and Indochina blocks. Together, these blocks belonged to the members of the northern Paleo-Tethys Ocean. Thus, an archipelagic paleogeographical framework divided by Paleo-, Meso-, and Neo-Tethys oceans was formed, fostering a global biodiversity centre within the Tethys warm pool. Since most of the allochthonous blocks assembling the Qinghai-Tibetan Plateau were situated in the middle to high latitude regions during the Permian, they preserved most sensitive paleoclimate records of the Late Paleozoic Ice Age (LPIA), the Artinskian global warming event, and the rapid warming event at the end-Permian. Therefore, sedimentological and paleontological records of these blocks are the unique window through which we can understand global evolutions of tectonic movement and paleoclimate, and their impacts on spatiotemporal distributions of contemporaneous biotas.

**Keywords** Permian, Tethys Ocean, Qinghai-Tibetan Plateau, Biotas, Paleogeography

---

**Citation:** Shen S Z, Zhang Y C, Yuan D X, Xu H P, Ju Q, Zhang H, Zheng Q F, Luo M, Hou Z S. 2024. Permian integrative stratigraphy, biotas, paleogeographical and paleoclimatic evolution of the Qinghai-Tibetan Plateau and its surrounding areas. *Science China Earth Sciences*, 67(4): 1107–1151, <https://doi.org/10.1007/s11430-023-1126-3>

---

## 1. Introduction

The Qinghai-Tibetan Plateau, the Earth's Third Pole, plays a pivotal role in regulating global environmental changes and effecting biological evolution of Southeast Asia. It once contained several now-vanished paleo-oceans (Yin and Harrison, 2000; Metcalfe, 2021) and holds the key to understanding the theories of Tethyan geodynamics (Wan et al., 2019; Wu et al., 2020; Zhu et al., 2022; Ding et al., 2022). The Permian Period (298.9–251.9 Ma) was a critical time interval during which major blocks of the Qinghai-Tibetan Plateau have experienced remarkable tectonic, paleogeographical and paleoclimatic changes. The unified Pangea supercontinent reached its zenith and hampered the east-to-west equatorial warm currents, and a semi-closed Tethys Ocean was formed as a vast east-opening warm pool around paleo-equator (Shields and Kiehl, 2018). This Tethys Ocean warm pool bears some similarities to the modern West Pacific-Indian Ocean warm pool (Roxy et al., 2019), which has been the most active region of tectonic activity, the center of energy exchange between the Earth's interior and surface matter, as well as the center of global biological diversity (Wan et al., 2019; Fan et al., 2020; Wu et al., 2020). Accompanied with large-scale volcanic activity along the northern margin of the Gondwana, a series of microcontinents were progressively detached from Gondwanaland and drifted northward, resulting in the formation of several oceans, including the Paleo-Tethys Ocean, the Meso-Tethys Ocean (also known as the Bangong-Nujiang Ocean), and the Neo-Tethys Ocean (Zhang et al., 2013a; Metcalfe, 2021; Wang et al., 2021). However, with the successive accretion and collision of the Gondwanan and Eurasian blocks, the Qinghai-Tibetan Plateau has been compressed, deformed, and uplifted, resulting in the disappearance of various paleo-oceans within the Qinghai-Tibetan Plateau (Figure 1). Consequently, reconstructing the evolutionary history of these past oceans, as well as the paleo-positions and drifting process of each microblock remains a focus in the studies of

Tethys geodynamics.

The spatial distribution of living organisms is obviously governed by their background environment, and as such, the factors such as latitudinal thermal gradient, ocean currents, and geographical barriers are the main controlling factors for spatial distributions of organisms (Saupe et al., 2019; Crame et al., 2022; Zhang and Torsvik, 2022). From a temporal and spatial perspective, climate change, configuration of continents and plate tectonics all played the major roles in controlling the distribution of organisms (Ke et al., 2016; Close et al., 2020; Xu et al., 2022). It has been well known that living organisms are highly sensitive to environmental gradients; however, it is a challenge with respect to how to recover the temporal and spatial distributions of organisms in deep time. Fossil assemblages and stratigraphic records provide a significant insight into this issue. The Qinghai-Tibetan Plateau consists of several independent blocks, from north to south: the North Qiangtang Block (also called the Qamdo Block), the South Qiangtang Block, the Lhasa Block, and the Himalaya Tethys Zone of the northern margin of the Indian Plate. These blocks were separated by the Longmu Co-Shuanghu, the Bangong-Nujiang, and the Yarlung Zangbo suture zones respectively (Figure 1). To Southeast Asia, these blocks are connected with the Simao, Baoshan, Tengchong blocks, etc. and to the west, they are connected to the Karakoram, Pamirs, and other blocks. The temporal and spatial relationships between these blocks and their geological evolution during the Permian have long been the controversial issues. The numerous blocks of the Qinghai-Tibetan Plateau and its surroundings preserved abundant Permian fossil assemblages and deposits (Figure 1), which served as a basis for unraveling the geological evolution of the various blocks in the Qinghai-Tibetan Plateau. This article aims to provide a state-of-the-art review of the Permian paleogeography, paleobiology, and paleoclimatic evolutions of various blocks in the Qinghai-Tibetan Plateau and its neighboring areas from the perspective of biostratigraphy and paleontology.

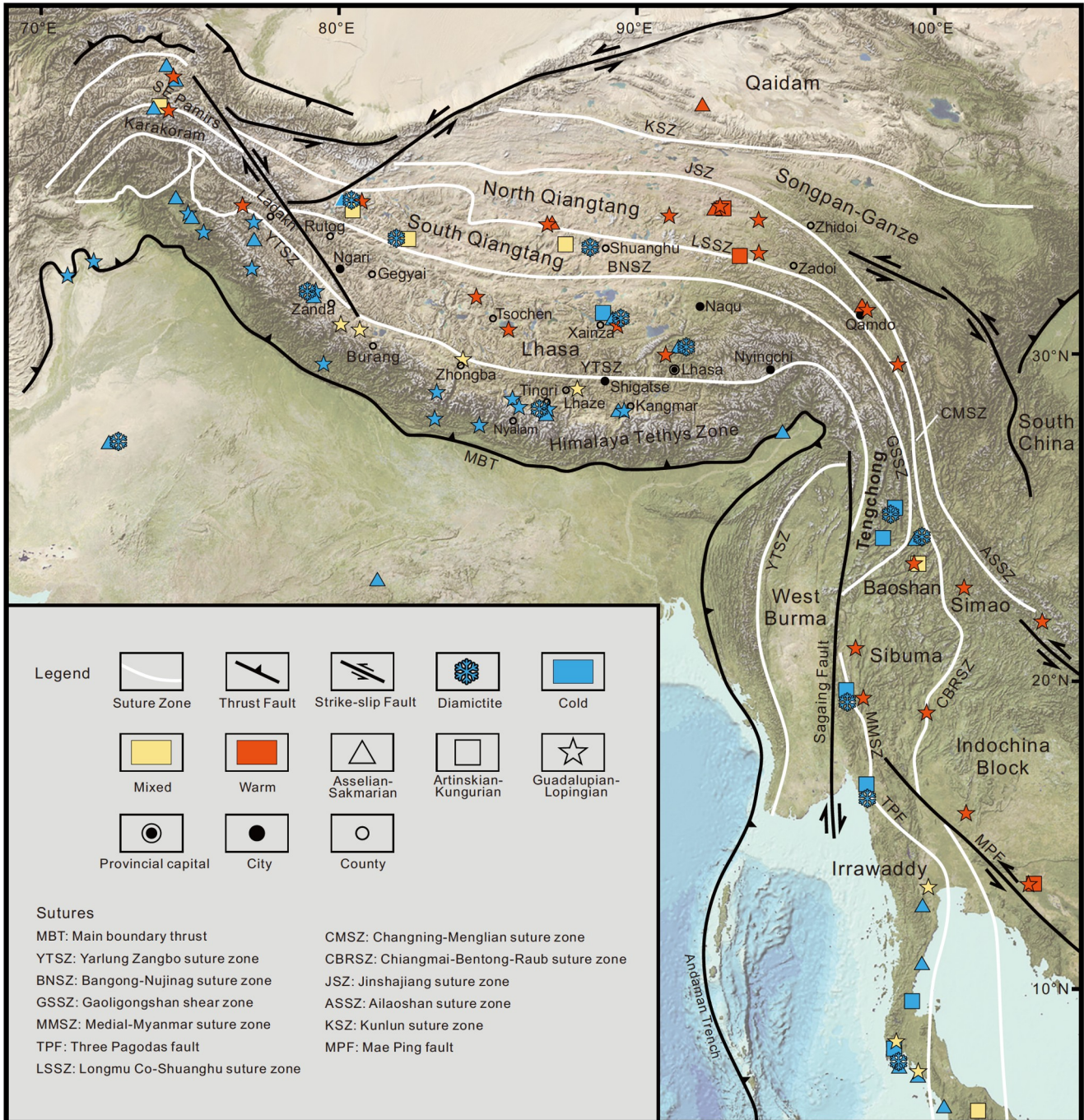


**Figure 1** Map of the Qinghai-Tibetan Plateau and Southeast Asia showing the various tectonic units, positions of suture zones superimposed with Permian fossil brachiopod faunas of different paleobiogeographical affinities. Gondwanan cold-water faunas are in blue, cold- and warm-water mixed faunas are in yellow and Tethyan warm-water faunas are in red. Base map from <http://www.gebco.net>. Divisions of the tectonic units are integrated from Angiolini et al. (2013), Ridd (2016), Wang et al. (2020), and Xu et al. (2022).

## 2. Lithostratigraphy, biostratigraphy and chronostratigraphic framework of the Qinghai-Tibetan Plateau

Reconstructing the evolutionary history of the Qinghai-Tibetan Plateau requires a united temporal-spatial scheme. Each block of the Qinghai-Tibetan Plateau belongs to dif-

ferent paleobiogeographic affinities during the Permian and contains different sediments and faunas, thus making stratigraphic correlation among various blocks difficult. The North Qiangtang Block was situated in the central Tethys region, and, therefore, belongs to the paleoequatorial zone as the South China Block during the Permian. The Himalaya Tethys Zone, located on the northern margin of the Indian

Plate, was always attached to the Gondwananland and situated in middle to high latitudes in southern hemisphere. It contains typical Gondwana-type cold-water faunas. Between them are a series of Cimmerian microcontinents, which drifted northward in different tempos and modes during the Permian, resulting in marked changes in sedimentary sequences and faunal assemblages. The lithostratigraphy, biostratigraphy, and chronostratigraphy are summarized as follows in different blocks (Figures 2–5).

## 2.1 North Qiangtang Block

The North Qiangtang Block lies between the Xijin Ulan-Jinshajiang suture zone in the north and the Longmu Co-Shuanghu suture zone in the south. Its western part is cut off by the Altyn Tagh fault, and its eastern part extends into Yunnan Province along the eastern Himalaya syntaxis (Figure 1). The North Qiangtang Block, also known as the Qamdo Block, contains widely distributed Mesozoic marine and terrestrial strata. The Permian strata are also well preserved and distributed mainly in the Qamdo area in eastern Tibet, the Tanggula area in Qinghai, and the Raggyorcaka area in Nyalam County.

### 2.1.1 Lithostratigraphy

The Cisuralian Series cropped out widely in the North Qiangtang Block, and is represented by the Licha Formation in the Qamdo area, the Zharigen Formation in the Tanggula-Zaduo area, and the Changshehu Formation in the Raggyorcaka area. All these formations are composed mainly of carbonates containing rich fusulines (Sichuan Regional Geological Survey, Nanjing Institute of Geology and Palaeontology, 1982; Liu, 1993; Li et al., 2016). In the Qamdo area, the Mangcuo Formation disconformably overlies the Licha Formation, and is dominated by pale gray thick-bedded limestone with gray-green mafic tuff (Rao et al., 1988). In the area of Jiaoga Town, Mangkang County and Chagyab County, the Jiaoga Formation overlies conformably on the Mangcuo Formation and is composed mainly of bioclastic limestone intercalated with tuff and tuffaceous sandstone (Rao et al., 1988; Qiao et al., 2021). In the Tanggula area, the Nuoribagaribao Formation conformably overlies the Zharigen Formation and consists of pebbly sandstone and tuff (Niu and Wu, 2016). Yet in the Zhiduo-Zaduo area of southern Qinghai, the equivalent strata are called the Gadi-kao Formation, which is composed mainly of basalt, volcanic agglomerates, volcanic breccia, and limestone (Niu et al., 2006a). The deposition in this area reflects a strong influence from extensive rifting (Niu et al., 2011).

The Guadalupian Series in the North Qiangtang Block is distributed mainly in the Tanggula and Zaduo areas, and rarely present in the Qamdo area. In the Tanggula area, it is represented by the Jiushidaoban Formation that overlies

conformably on the Nuoribagaribao Formation. The former consists of gray, dark gray silty limestone and bioclastic limestone, and locally interbedded with fine- to medium-grained feldspar sandstone (Liu, 1993). In the area of Garizharen, east of Tanggula, the Garijiaren Formation conformably overlies the Jiushidaoban Formation limestone deposits, and comprises quartzose sandstone and mudstone interbedded with limestone and basalt (Niu et al., 2006b). Upwards, overlying disconformably the Garijiaren Formation is the Suojia Formation, which is characterized by conglomerate in the lower member and limestone with chert bands/nodules in the upper member (Niu et al., 2006b).

In contrast to the limited distribution of the Guadalupian Series in the North Qiangtang Block, the Lopingian strata are widely distributed. In the Qamdo area, it is represented mainly by the Tuoba and the Xiayacun formations. The Tuoba Formation, also known as the Tuoba Coal Series, represents deposition in an alternated marine-terrestrial environment. It is composed mainly of mudstone and shale interbedded with sandstone and siltstone and coal beds, with abundant plant fossils such as *Gigantopteris*. The upper part of the Tuoba Formation, previously known as the Kaxiangda Formation, contains fusuline and brachiopod fossils in the limestone interlayers (Zhang et al., 1979; Rao et al., 1988). The overlying Xiayacun Formation is composed mainly of andesite. The Lopingian strata around the Tanggula region are known as the Wuli Group (Liu, 1993) and represented alternatively by the Nayixiong Formation and Lapuchari Formation (Liu, 1993; Niu and Wu, 2016). The Nayixiong Formation is composed mainly of quartz sandstone and mudstone, with multiple layers of bioclastic limestone and thin coal seams. This formation yields plant fossils, and is largely correlative with the lower part of the Wuli Group characterized by coal-bearing siliciclastic rocks. The Lapuchari Formation is dominated by bioclastic limestones with fusulines and is correlative with carbonate deposition of the upper part of the Wuli Group (Liu, 1993; Niu and Wu, 2016). The Lopingian strata in the Raggyorcaka area are named as the Xueyuanhe and Raggyorcaka formations (Qiao et al., 2021). The former is dominated by carbonate rocks and the latter is composed of siltstone, shale, and mudstone containing fossil plants in the lower part and with occurrence of limestone interbeds containing fusulines and brachiopods in the upper part. The Xueyuanhe Formation was once considered to conformably overlie the Lower Permian Changshehu Formation (Li et al., 2016). However, recent studies have shown that the boundary strata between these two formations are poorly exposed, and probably there is a stratigraphic discontinuity between them (Qiao et al., 2021). The Xueyuanhe Formation is dominated by carbonates. The lower part of the Raggyorcaka Formation is composed mainly of siltstone, shale, and mudstone with plant fossils; the upper part is interbedded with bioclastic limestone con-

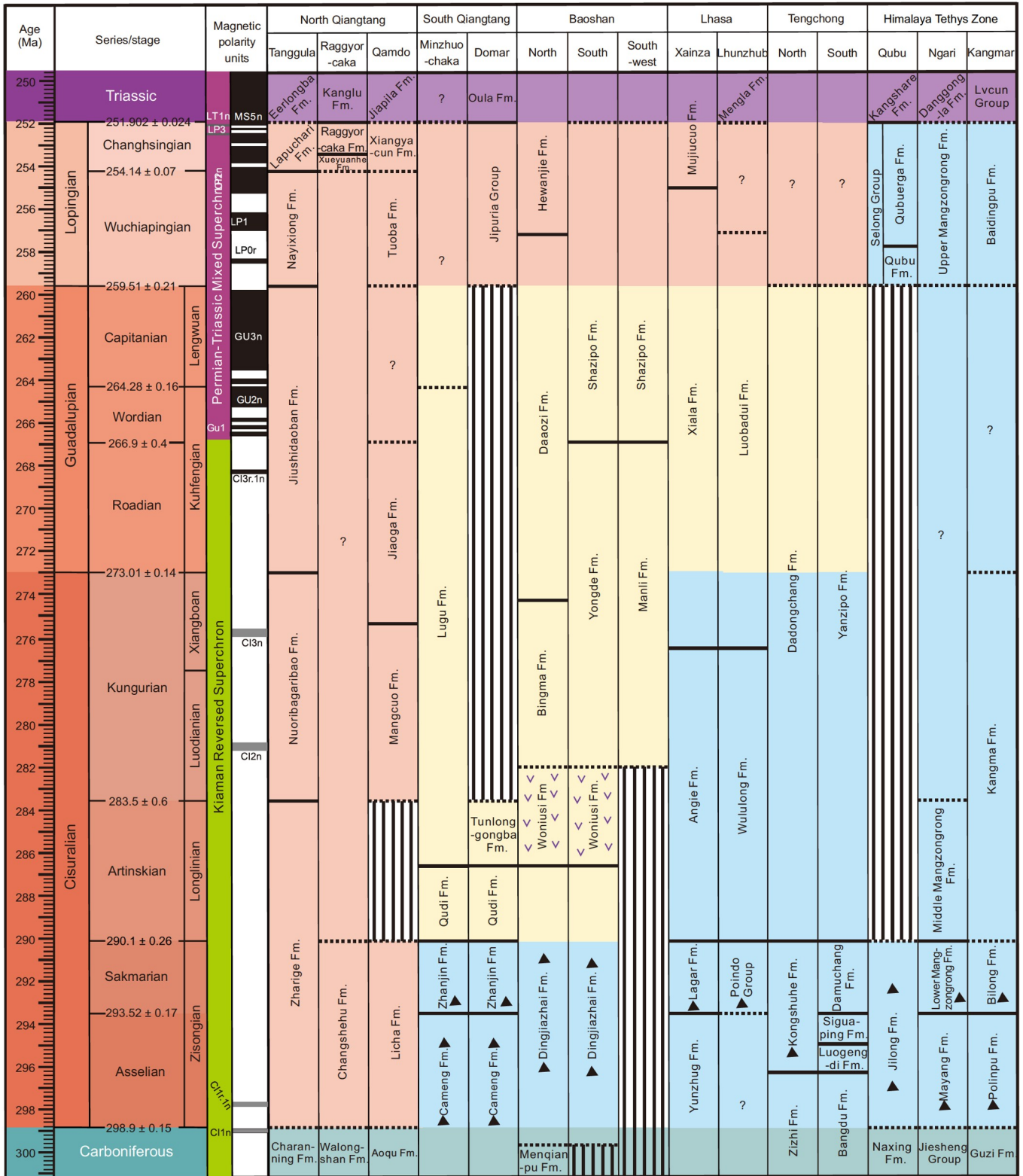


**Figure 2** Subdivision and correlation of the Permian sequences of different blocks in the Qinghai-Tibetan Plateau. Pale blue of background color suggests a cold-water Gondwanan affinity, pale red represents warm-water Tethyan affinity and pale yellow represents the mixed. Black triangle represents marine glacial deposits and v for basalts. Timescale after Shen et al. (2019).

taining fusulines and brachiopods. In summary, the Lopingian strata of the North Qiangtang Block are dominated

by the deposits in a marine-terrestrial environment (Qiao et al., 2021; Figure 2).

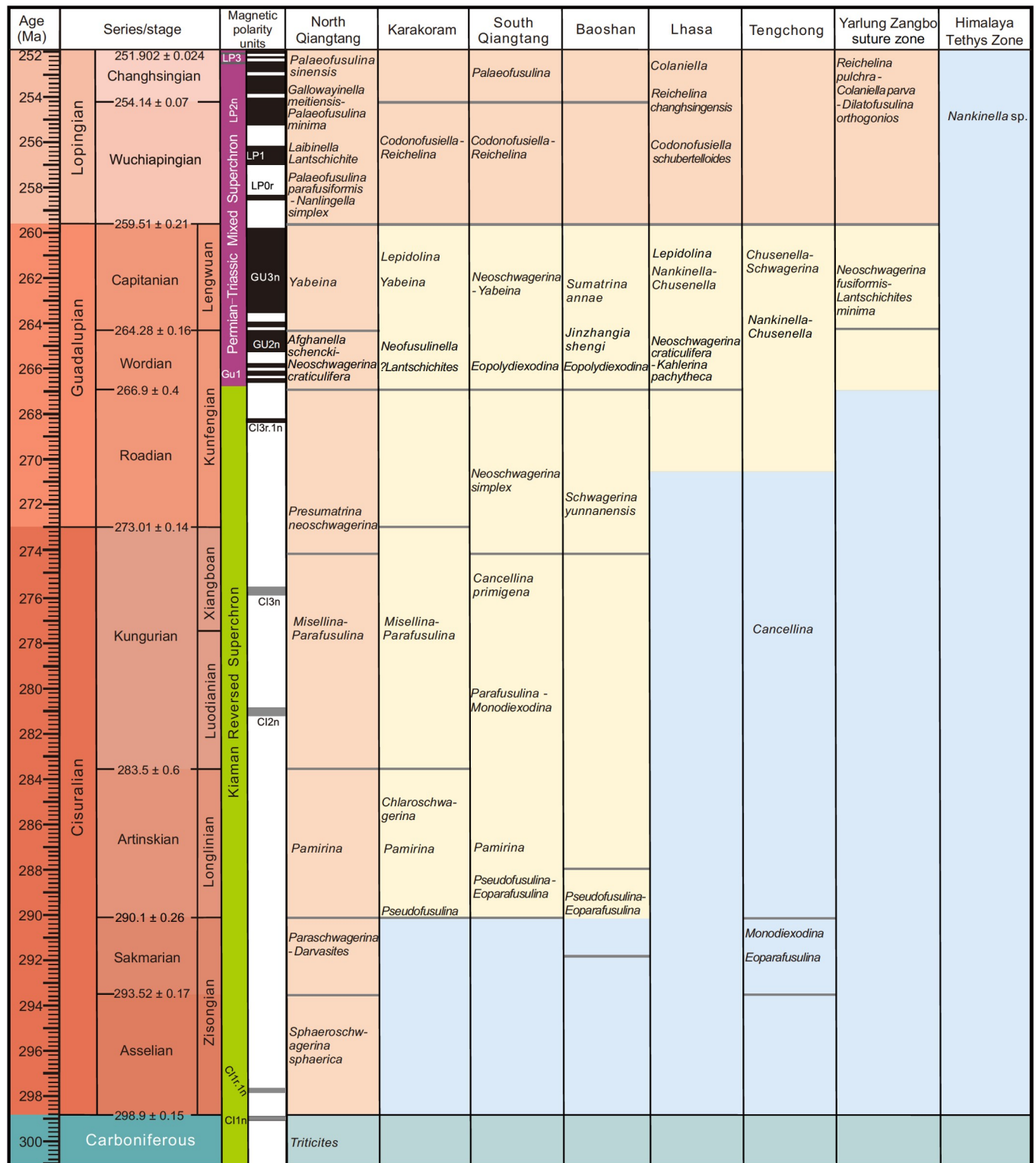


**Figure 3** Permian fusuline biostratigraphic framework and correlations between different blocks of the Qinghai-Tibetan Plateau. Background colors see explanation in Figure 2. The references are: North Qiangtang: Sichuan Regional Geological Survey, Nanjing Institute of Geology and Palaeontology (1982), Liu (1993), Niu et al. (2006a, 2010), Niu and Wu (2016), Zhang et al. (2016a), Zhang and Wang (2018), Wang et al. (2020), Qiao et al. (2021); Karakoram: Gaetani et al. (1995); South Qiangtang: Liang et al. (1983), Nie and Song (1983a, 1983b, 1983c, 1985), Wu and Lan (1990), Zhang (1991), Cheng et al. (2005), Zhang et al. (2012, 2013b, 2014a), Ju et al. (2022a), Yuan et al. (2022); Baoshan: Ueno (2001), Shi et al. (2011), Huang et al. (2009, 2017); Lhasa: Wang et al. (1981), Zhu (1982a, 1982b), Zhang et al. (1985), Wang and Zhou (1986), Huang et al. (2007), Ju et al. (2019), Zhang et al. (2010, 2016b, 2019a), Qiao et al. (2021), Huang et al. (2022), Ju et al. (2021, 2022b); Tengchong: Shi et al. (2008, 2017), Huang et al. (2020); Yarlung Zangbo suture zone: Wang et al. (1981), Zhang et al. (2009), Wang et al. (2010), Zhang and Wang (2019), Fan et al. (2023); Himalaya Tethys Zone: Zhang Y C's unpublished data.

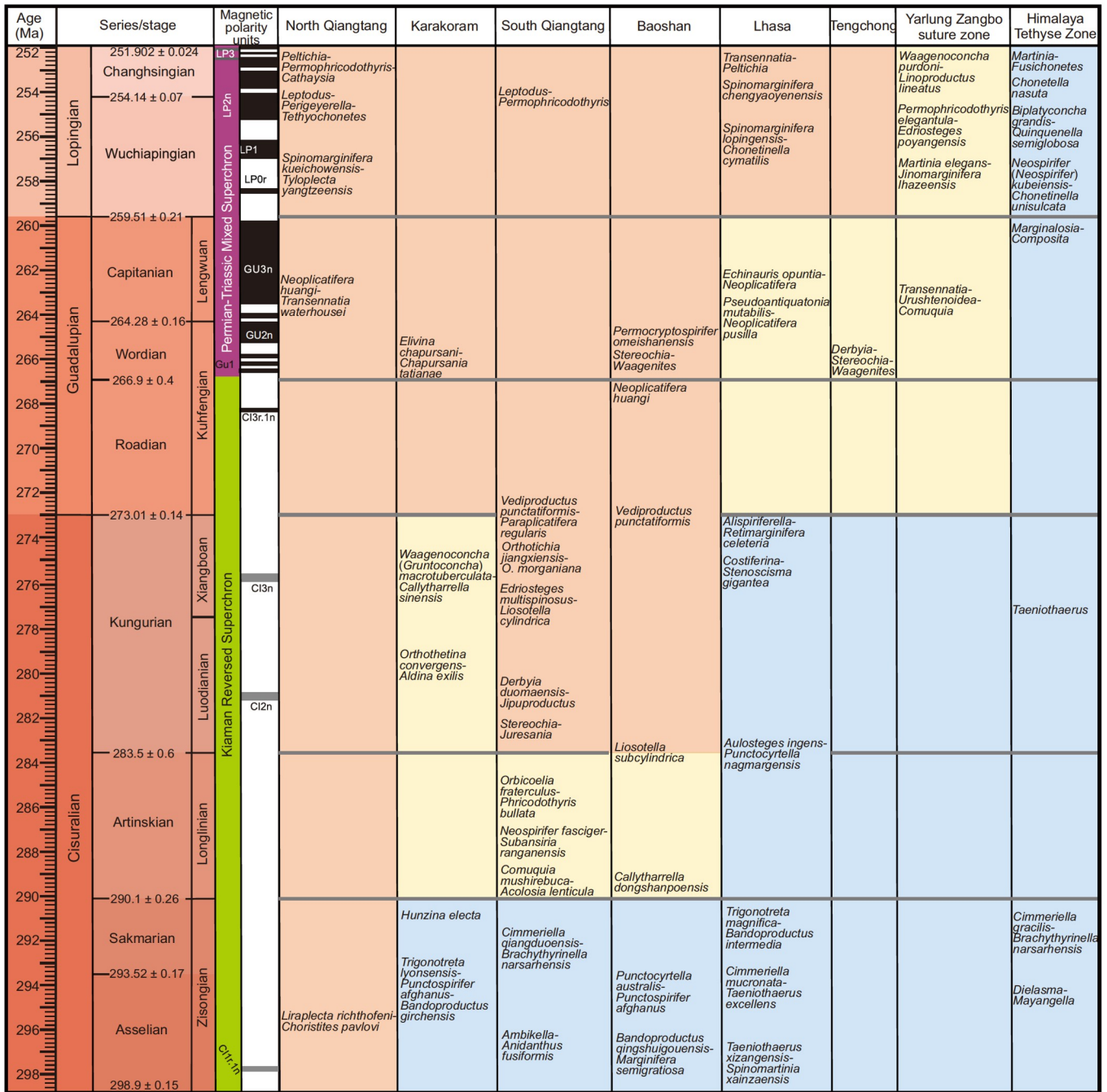


**Figure 4** Permian brachiopod biostratigraphic framework and correlations among different blocks of the Qinghai-Tibetan Plateau and its surrounding areas. Background colors see explanation in Figure 2. The references are: North Qiangtang: Jin and Sun (1981), Jin et al. (1985), Niu et al. (2003), He et al. (2008, 2009); Karakoram: Gaetani et al. (1995), Angiolini (1995), Angiolini et al. (2005); South Qiangtang: Liang et al. (1983), Shi and Shen (2001), Shen et al. (2000a, 2002); Lhasa: Jin and Sun (1981), Sun et al. (1981), Zhan and Wu (1982), Zhan et al. (2007), Xu et al. (2019); Tengchong: Fang and Fan (1994), Chen et al. (2000), Jin et al. (2011); Yarlung Zangbo suture zone: Jin and Sun (1981), Shen et al. (2003c, 2003d, 2010); Himalaya Tethys Zone: Jin et al. (1977), Yang et al. (1990), Shen et al. (2000b, 2001a, 2001b, 2003a), Xu et al. (2018).

2.1.2 Biostratigraphy and chronostratigraphy

Fusulines are the most abundant fossils in the North Qiangtang Block (Figure 3). The early Cisuralian fusuline fauna is represented by the *Sphaeroschwagerina sphaerica* Zone and has been reported in the Licha Formation in the Machala area of Qamdo, the Zharigen Formation in the Tanggula area, and the Changshehu Formation in the Rag-

gyorcaka area (Sichuan Regional Geological Survey and Nanjing Institute of Geology and Palaeontology, 1982; Liu, 1993; Zhang et al., 2016a). This zone consists mainly of *Sphaeroschwagerina sphaerica*, *S. parasphaerica*, *S. dachagouensis*, *Pseudoschwagerina* sp., and *Montiparus tobensis*, indicating an Asselian age (Zhang et al., 2016a; Zhang and Wang, 2018). The fusuline fauna is represented

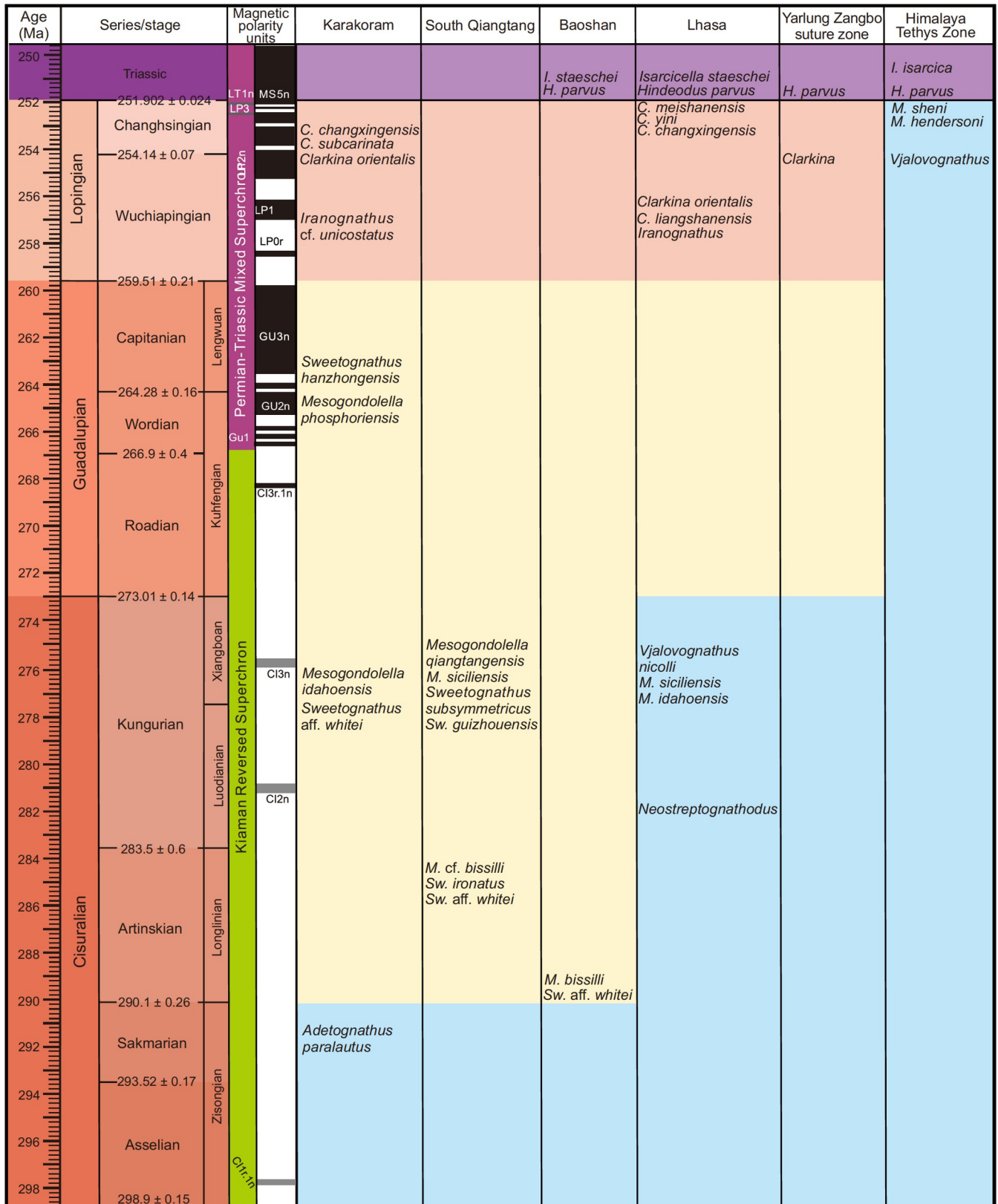


**Figure 5** Permian conodont biostratigraphic framework and correlation among different blocks of the Qinghai-Tibetan Plateau. Background colors see explanation in Figure 2. The references are: Karakoram: Gaetani et al. (1995); South Qiangtang: Ji et al. (2006), Yuan et al. (2022); Baoshan: Wang et al. (2001), Ueno et al. (2002), Ji et al. (2004), Wang et al. (2004), Dong and Wang (2006); Lhasa: Zheng et al. (2005, 2007), Ji et al. (2007), Yuan et al. (2014, 2016), Wu et al. (2014, 2021); Yarlung Zangbo suture zone: Shen et al. (2010); Himalaya Tethys Zone: Orchard et al. (1994), Mei (1996), Shen et al. (2006), Wang et al. (2017), Yuan et al. (2018).



by the *Paraschwagerina-Darvasites* Zone in the overlying strata (Zhang and Wang, 2018), and it contains *Paraschwagerina ishibajica*, *Darvasites sinensis*, and *Xizangia machalensis*, and indicates a Sakmarian age. This zone is distributed mainly in the Qamdo area of eastern Tibet (Sichuan Regional Geological Survey, Nanjing Institute of Geology and Palaeontology, 1982). The Artinskian fusuline fauna is characterized by the *Pamirina* Zone, and has been reported from the topmost part of the Zharigen Formation in the Tanggula area (Liu, 1993). Representative species of the *Pamirina* Zone include *Pamirina pulchra*, *P. nobilis*, and *P. orbiculoidea*. The Kungurian fusuline fauna is reported mainly from the Gadikao Formation in the Zhiduo-Zaduo area (Niu et al., 2006a) and the Mangcuo Formation in the Qamdo area (Sichuan Regional Geological Survey, Nanjing Institute of Geology and Palaeontology, 1982), which is represented by the *Misellina-Parafusulina* Zone. This zone contains *Sphaerulina hunanica*, *Nankinella orbicularia*, *Wutuella wutuensis*, *Misellina claudiae*, *M. sphaerica*, *Parafusulina yunanica*, *P. yabei*, and *P. splendens* (Niu et al., 2006a). The early Guadalupian deposits of the North Qiangtang Block are mostly siliciclastic rocks. Fusulines are rare and are reported only in the lower part of the Jiaoga Formation in the Qamdo area. They include *Neoschwagerina simplex*, *N. deprati*, *Parafusulina yalongica*, *P. tomuroensis*, *Armenina asiatica*, *Chusenella schwagerinaeformis*, *C. minguangensis*, *Pseudodoliolina ozawai*, and *Presumatrina neoschwagerinoides*. They are equivalent to the *Presumatrina neoschwagerinoides* Zone of a late Kungurian to early Roadian age (Qiao et al., 2021). The Wordian fusuline faunas are more widely distributed, and represented by the *Afghanella schencki-Neoschwagerina craticulifera* Zone from the Jiushidaoban Formation in the Tanggula area. Common species of this biozone includes *Neoschwagerina craticulifera*, *N. douvillei*, *Sumatrina annae*, and *Afghanella schencki* (Niu et al., 2010). The Capitanian fusuline fauna, represented by the *Yabeina* Zone, is found mostly in the upper part of the Jiushidaoban Formation in the Tanggula area and the Suojia Formation in the Zaduo area. This zone includes abundant *Yabeina gubleri*, *Sumatrina annae*, and *Chusenella schwagerinaeformis* (Liu, 1993; Niu and Wu, 2016). The Wuchiapingian fusuline fauna in the North Qiangtang Block is reported mainly from the Tuoba Formation in the Qamdo area and the Nayixiong Formation in the Tanggula area. Two fusulina zones were recognized, namely the *Laibinella-Lantschichites* Zone in the lower part and the *Palaeofusulina parafusiformis-Nanlingella simplex* Zone in the upper part (Niu and Wu, 2016; Wang et al., 2020). The Changhsingian fusuline fauna is distributed mainly in the Lapuchari Formation in the Tanggula area and the Xueyuanhe and Raggyorcaka formations in the Raggyorcaka area. It can be divided into the lower *Gallowayinella meitiensis-Palaeofusulina minima* Zone and the upper

*Palaeofusulina sinensis* Zone in the Raggyorcaka area. These two zones are largely equivalent to the *Gallowayinella meitiensis-Palaeofusulina sinensis* Zone in the Tanggula area, which includes *Gallowayinella meitiensis*, *G. cylindrica*, *Palaeofusulina sinensis*, *P. minima*, *P. simplex*, and *Reichelina changhsingensis* (Niu and Wu, 2016; Qiao et al., 2021; Figure 3).

Compared with fusulines, brachiopod fossils are relatively less investigated in the North Qiangtang Block. The Cisuralian brachiopods were reported only from the top of the Licha Formation in the Touba area of Qamdo and named the *Liraplecta richthofeni-Choristites pavlovi* Assemblage (Jin and Sun, 1981). The Guadalupian brachiopods have been reported only in the Zaduo and Zhiduo areas of Qinghai, and are called the *Neoplicatifera huangi-Transennatia waterhousei* Assemblage, which is similar to the coeval brachiopod assemblages in South China (He et al., 2008). The Lopingian brachiopods occurred commonly in the Raggyorcaka Formation in the Shuanghu area, the Tuoba Formation in the Qamdo area, and the Wuli Group in the Tanggula area. The Nayixiong Formation, also the lower part of the Wuli Group in the Tanggula area of southern Qinghai, contains brachiopods characterized by the *Spinomarginifera kueichowensis-Tyloplecta yangtzensis* Assemblage. On the basis of the associated fusulines *Nanlingella parafusiformis*, *N. simplex* and *Parananlingella laxa*, this brachiopod fauna is very likely of the Wuchiapingian age. Brachiopods in the Lapuchari Formation and the upper part of the Wuli Group are represented by *Leptodus nobilis*, *Perigeyerella costellata*, and *Fusichonetes* (Niu et al., 2003; He et al., 2009). Brachiopods in the Raggyorcaka Formation in the Shuanghu area and the Tuoba Formation in the Qamdo area include *Peltichia*, *Permophricondothyris* and *Cathaysia* (Jin and Sun, 1981; Jin et al., 1985). Given that brachiopods in the Lapuchari, Raggyorcaka, and Touba formations are all associated with the fusuline *Palaeofusulina*, they are probably of the Changhsingian age and are largely comparable with those of South China (Figure 4).

There are very few records of conodonts in the North Qiangtang Block. Therefore, the ages of the Permian strata are determined mainly by the widely distributed fusulines. The Licha Formation in the Qamdo area and the Changshehu Formation in the Raggyorcaka area are assigned to an Asselina-Sakmarian age (Sichuan Regional Geological Survey, Nanjing Institute of Geology and Palaeontology, 1982). In the Tanggula area, the Zharigen Formation contains fusulines ranging from Asselian to Artinskian (Liu, 1993). The *Misellina* Zone to the *Presumatrina neoschwagerinoides* Zone in the Mangcuo and Jiaoga formations in the Qamdo area is assigned to the Kungurian and Roadian. The Gadikao Formation in the Zaduo-Zhiduo area is the Kungurian (Niu et al., 2006a), and is overlain by the Guadalupian Jiushidaoban, Garijiaren, and Suojia formations (Niu et al., 2006b). The

Tuoba Formation in the Qamdo area, the Nayixiong Formation and Lapuchari Formation in the Tanggula area, and the Xueyuanhe and Raggyorcaka formations in the Raggyorcaka area are all assigned to the Lopingian (Niu and Wu, 2016; Qiao et al., 2021), among which the advanced forms of *Palaeofusulina* dominated the Xueyuanhe and Raggyorcaka formations. Thus, they are all Changhsingian in age (Qiao et al., 2021; Figure 3).

## 2.2 South Qiangtang Block

The South Qiangtang Block is bracketed by the Longmu Co-Shuanghu suture zone in the north and the Bangong-Nujiang suture zone in the south. Its western border is cut off by the Karakoram Fault and therefore its westward extension remains unclear, whereas the eastern part is complicated by the eastern Himalaya Syntaxis (Figure 1). The Permian strata are widely distributed in the Dongru, Lumajiangdongco, Xianqian and Shuanghu areas in this block.

### 2.2.1 Lithostratigraphy

The Carboniferous-Permian sequence in the South Qiangtang Block was first named the Horpatso Series (Norin, 1946). This series was later subdivided into the Cameng, Zhanjin, Qudi and Tunlonggongba formations in ascending order based on the outcrop in the Domar area (Liang et al., 1983) (Figure 2). In addition, the Longge Formation and the Jipuria Group were established in this area (Liang et al., 1983). The Cameng Formation is dominated by sandstone, slate, and diamictites with a thickness over than 500 m, representing glacio-marine deposits (Liang et al., 1983). The Zhanjin Formation is also represented by sandstone and slate, which resembles the Cameng Formation to some extent. However, the Zhanjin Formation bears convolute beddings suggesting flysch facies (Liang et al., 1983; Zhang et al., 2019b). Both formations are also widely distributed in the central Qiangtang Metamorphic Belt. Different from the strata in the western part of the South Qiangtang Block, both formations in the central Qiangtang Metamorphic Belt are strongly metamorphosed and contain multiple layers of basalt or basic dike swarm (Zhai et al., 2013; Li et al., 2016). The overlying Qudi Formation is characterized by calcareous sandstone with large-scale cross bedding, suggesting a shallow water depositional environment (Liang et al., 1983). The Tunlonggongba Formation overlies conformably on the Qudi Formation, and is composed mainly of dark gray bioclastic limestone with abundant compound corals, fusulines and brachiopods (Liang et al., 1983; Nie and Song, 1983a). The Longge Formation is dominated by gray limestone in rare outcrops. The Lopingian strata are represented by the Jipuria Group in the Domar area (Liang et al., 1983), or the Rehepan and Qingshuihe formations in the Rehepan area (Wu, 1991). The Jipuria Group unconformably overlies the

Tunlonggongba Formation and is composed of conglomerate in the basal part, sandstone and limestone in the lower part and dolomitic limestone in the upper part (Sun and Xu, 1991; Zhang et al., 2019b).

The Lugu Formation is widely distributed in the Lumajiangdongco and Shuanghu areas in the central South Qiangtang Block, and is composed mainly of basalt and limestone (Zhang et al., 2012, 2014a; Yuan et al., 2022). The equivalent strata in the Xianqian area were named the Cainaha and Xianqian formations (Sun and Xu, 1991).

### 2.2.2 Biostratigraphy and chronostratigraphy

Fusulines are abundant in the South Qiangtang Block and the oldest *Pseudofusulina-Eoparafusulina* Assemblage was reported from the Qudi Formation in the Domar area (Figure 3), which includes *Eoparafusulina regina*, *E. tibetica*, *Pamirina chinlingensis*, *Pseudofusulina insignis*, and *P. crassispira*. These fusulines indicate that the Qudi Formation is the Artinskian in age (Liang et al., 1983; Nie and Song, 1983b). Notably, the Qudi Formation at the Tuotala section is dominated by sandstone and slate with abundant brachiopod fossils (Liang et al., 1983). However, the same formation at the Nazhaxishan and Saerduoshan sections reportedly are dominated by gray limestone with abundant fusulines (Liang et al., 1983). Therefore, the Qudi Formation from these sections is not necessarily equivalent. Our field observation shows that the fusuline-bearing Qudi Formation is equivalent with the Tunlonggongba Formation. In other words, the earliest fusulines in limestone beds in the western part of the South Qiangtang Block actually began to occur in the Tunlonggongba Formation. Similar fusulines were also reported from the turbidites of the Qudi Formation in the central South Qiangtang Block (Zhang et al., 2013b). The Kungurian fusuline faunas are represented by the *Parafusulina-Monodiexodina* Assemblage in the Tunlonggongba Formation in the western South Qiangtang Block, which consists mainly of *Monodiexodina kattaensis*, *Parafusulina bosei*, *P. lata*, *P. undulata* and *Pseudofusulina hongziqianica* (Nie and Song, 1983a). However, based on our recent field investigation, the Artinskian fusulines such as *Monodiexodina*, *Pamirina*, and *Eoparafusulina* are abundant in this formation (Zhang Y C's unpublished data). In the Xianqian, Minzhuochaka, and Shuanghu areas, the Kungurian fusulines were summarized as the *Cancellina primigena* and *Neoschwagerina simplex* assemblages in the Lugu or Cainaha formations. The *Cancellina primigena* Assemblage is found mainly in the Shuanghu area and includes the species *Cancellina primigena*, *Pseudodoliolina ozawai*, *Chusenella schwagerinaeformis*, *Neofusulinella giraudi*, and *Pseudofusulina wangmoensis* (Zhang et al., 2012, 2014a). The *Neoschwagerina simplex* Zone was reported from Minzhuochaka, Xianqian, and the exotic limestone of the central Qiangtang Metamorphic Belt. This zone contains *Neosch-*

*wagerina simplex*, *Pseudodoliolina ozawai*, *Verbeekina furnishi*, *Pseudofusulina tchengkangensis*, *Yangchienia tobleri*, and *Presumatrina schellwieni*, indicating a late Kungurian-early Roadian age (Zhang, 1991; Ju et al., 2022a; Yuan et al., 2022). The upper part of the Lugu and Xianqian formations are characterized by abundant fusulines such as *Eopolydiexodina*, *Dunbarula*, *Yangchienia*, *Parafusulina*, and *Chusenella*, indicating a Wordian age (Zhang, 1991; Cheng et al., 2005). The Capitanian fusuline faunas are represented by the *Neoschwagerina-Yabeina* Assemblage, which is developed mainly in the Longge Formation of the Domar area but hardly found in the adjacent areas (Zhang et al., 2019b). This assemblage includes *Neoschwagerina guoi*, *Dunbarula pusilla*, *Sumatrina annae minima*, *Chusenella tingi*, and *Kahlerina pulchra* (Liang et al., 1983; Nie and Song, 1983c). In addition, the foraminifer *Shanita-Hemigordiopsis* Assemblage was also reported from the Longge Formation (Nie and Song, 1985). The Lopingian fusulines including *Codonofusiella* sp., *Reichelina tenuissima*, and *Palaeofusulina* sp. were recorded in the Rehepan and Qingshuhe formations (=upper part of the Jipuria Group) (Wu and Lan, 1990; Figure 3).

Permian conodonts are relatively less studied in the South Qiangtang Block. Only limited conodont fauna, including *Sweetognathus* aff. *whitei*, *S. ironatus*, and *Mesogondolella* cf. *bissilli*, was documented from the lowest part of the Tunlonggongba Formation (Ji et al., 2006). However, the conodont specimens of these species are fragmentary and quite different from the type specimens. In addition, the above-mentioned fauna has a long stratigraphic range (from the Asselian to Kungurian), making it difficult to precisely constrain the age. Based on the morphological characteristics of the specimens illustrated by Ji et al. (2006), they are closer to the Artinskian *Sweetognathus* species, but additional specimens are needed for a more reliable determination. Recently, the conodont fauna named as the *Sweetognathus-Mesogondolella* Assemblage was reported from the lower part of the Lugu Formation, which includes *Sweetognathus guizhouensis*, *S. subsymmetricus*, *Mesogondolella siciensis*, and *M. qiangtangensis* of a late Kungurian age (Figures 5, 6.12–6.13).

Permian brachiopods are quite abundant in the South Qiangtang Block, and relevant studies were performed mainly in the Domar and Mushirebuca areas in the western region and the Rongma area in the central part of the block. Four brachiopod assemblages were recognized in the Domar area by Liang et al. (1983). They are respectively the *Ambikella-Anidanthus fusiformis* Assemblage from the Zhanjin Formation, the *Neospirifer fasciger-Subansiria rangensis* Assemblage from the Qudi Formation, and the *Stereochia-Juresania* and *Derbyia duomaensis-Jipuproductus* assemblages from the Tunlonggongba Formation. In addition, five brachiopod assemblages were erected by Sun (1991) in the

Mushirebuca area. Three of them are from the Mushirebuca Group, namely the *Cimmeriella qiangduensis-Brachythyrinella narsarhensis* in the lower part, the *Comuquia mushirebuca-Acolosia lenticula* in the middle part, and the *Orbicoelia fraterculus-Phricodothyris bullata* in the upper part. These assemblages suggest a Sakmarian-Artinskian age. Other two assemblages, the *Edriostegea multispinosus-Liosotella cylindrica* and the *Orthotichia jiangxiensis-O. morganiana*, were reported respectively from the lower and upper parts of the Cainaha Formation and both are assigned to the Kungurian. In the Rongma area of the central South Qiangtang Block, the *Vediproductus punctatiformis-Paraplicatifera regularis* Assemblage was reported from the Lugu Formation, and can be well correlated with the late Kungurian-Roadian *Permocryptospirifer-Vediproductus punctatiformis* Assemblage in South China (Shen et al., 2016; Shen, 2018). Lopingian brachiopod fauna was found only in the Rehepan and Qingshuhe formations (=upper part of the Jipuria Group) in the Domar area (Wu and Lan, 1990). This fauna is similar to that of the North Qiangtang and South China blocks on the basis of the presence of *Leptodus* and *Permophricodothyris* (Figure 4).

In summary, based on the fusuline, conodont, and brachiopod faunas and strata described above, we can provide a general framework of the Permian stratigraphy in the South Qiangtang Block. The Zhanjin Formation is probably of the Sakmarian age based on the presence of the brachiopod *Ambikella-Anidanthus fusiformis* Assemblage and the bivalve *Eurydesma* (Liang et al., 1983). The age of the Qudi Formation is assigned to the Artinskian based on the brachiopod *Neospirifer fasciger-Subansiria rangensis* Assemblage. The fusulines *Pamirina* and *Eoparafusulina* as well as the conodonts *Sweetognathus ironatus* and *Mesogondolella* cf. *bissilli* jointly indicate an Artinskian age for the Tunlonggongba Formation. The lower part of the Lugu Formation is represented by the conodont *Sweetognathus-Mesogondolella* Assemblage and the fusuline *Cancellina primigena* and *Neoschwagerina simplex* zones, both indicating a Kungurian age; whereas its upper part is characterized by the Wordian fusuline *Eopolydiexodina*. The fusuline *Neoschwagerina-Yabeina* Zone and the foraminifer *Shanita-Hemigordiopsis* Assemblage from the Longge Formation are both indicative of a Capitanian age. The Jipuria Group is assigned to the Lopingian in terms of the coral *Waagenophyllum* sp. and the fusulines *Palaeofusulina* sp., and *Reichelina tenuissima* (Figures 2–5).

### 2.3 Lhasa Block

The Lhasa Block is bounded by the Bangong-Nujiang suture zone in the north, and the Yarlung Zangbo suture zone in the south. It is cut off by the Karakoram Fault to the west and extends into western Yunnan in the east (Figure 1). It is

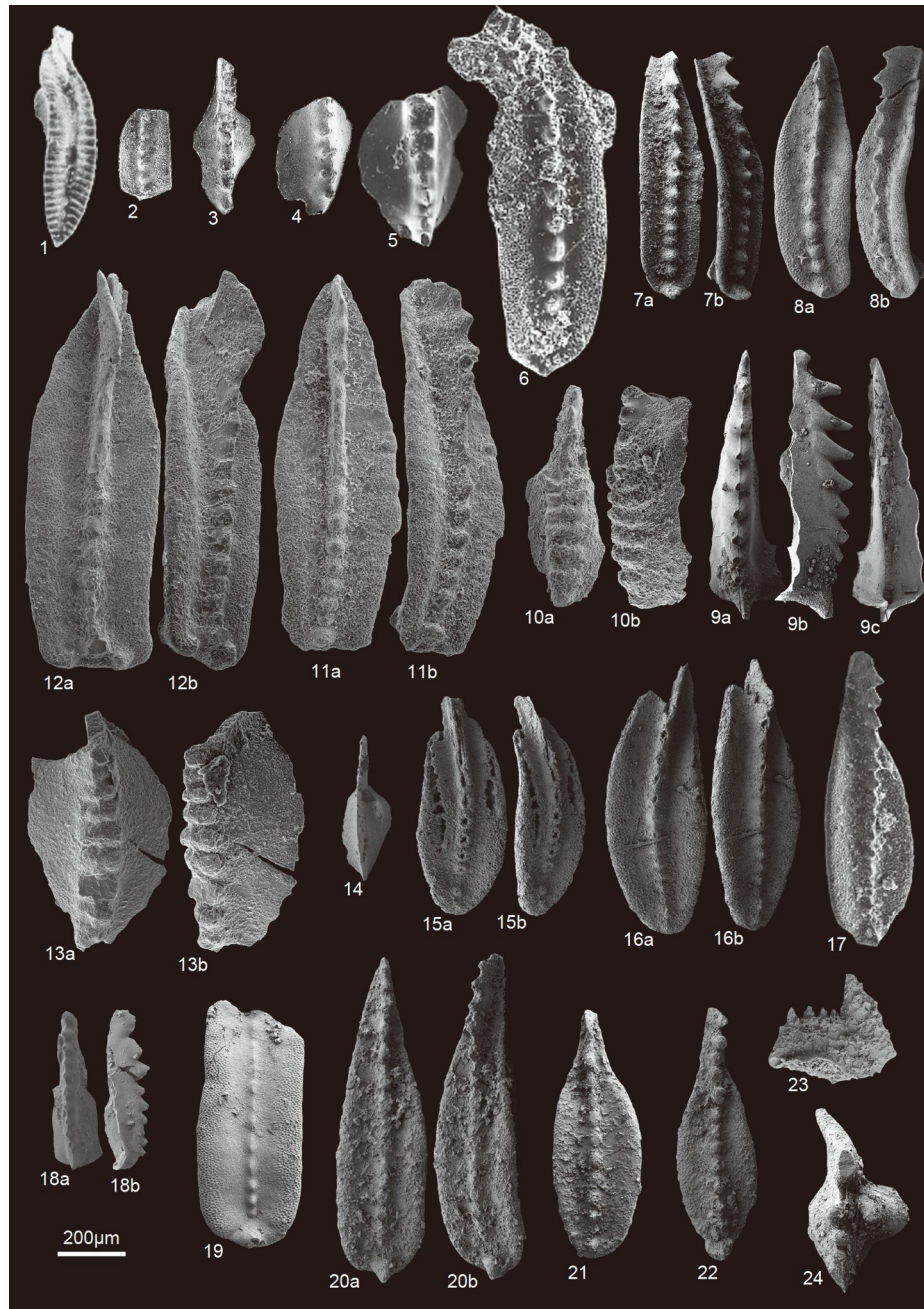


**Figure 6** Permian conodonts from different blocks in the Qinghai-Tibetan Plateau. 1, *Adetognathus paralautus*, from the top part of Member 1 of the Lashkargaz Formation in the northern Kalakoram Block (Gaetani et al., 1995). 2, *Mesogondolella* cf. *bisselli*, from the base part of the Tunlonggongba Formation in the South Qiangtang Block (Ji et al., 2006). 3, *Sweetognathus ironatus*, from the base part of the Tunlonggongba Formation in South Qiangtang Block (Ji et al., 2006). 4 & 5, *Sweetognathus* aff. *whitei*; 4 from the base part of the Tunlonggongba Formation in the South Qiangtang Block (Ji et al., 2006), and 5 from the top part of the Dingjiazhai Formation in the Baoshan Block (Ueno et al., 2002). 6, *Mesogondolella bisselli*, from the top part of the Dingjiazhai Formation in the Baoshan Block (Ueno et al., 2002). 7, *Mesogondolella idahoensis*, from the base part of the Xiala Formation in the Lhasa Block (Yuan et al., 2016). 8 & 11, *Mesogondolella siciliensis*; 8 from the base part of the Xiala Formation in the Lhasa Block (Yuan et al., 2016), and 11 from the lower part of the Lugu Formation in the South Qiangtang Block (Yuan et al., 2022). 9, *Vjalovognathus nicolli*, from the base part of the Xiala Formation in the Lhasa Block (Yuan et al., 2016). 10, *Sweetognathus guizhouensis*, from the lower part of the Lugu Formation in the South Qiangtang Block (Yuan et al., 2022). 12, *Mesogondolella qiangtangensis*, from the lower part of the Lugu Formation in the South Qiangtang Block (Yuan et al., 2022). 13, *Sweetognathus sub-symmetricus*, from the lower part of the Lugu Formation in the South Qiangtang Block (Yuan et al., 2022). 14, *Iranognathus* sp., from the upper part of the Xiala Formation in the Lhasa Block (Yuan et al., 2014). 15, *Clarkina orientalis*, from the top part of the Xiala Formation in the Lhasa Block (Yuan et al., 2014). 16, *Clarkina liangshanensis*, from the top part of the Xiala Formation in the Lhasa Block (Yuan et al., 2014). 17, *Clarkina yini*, from the top part of the Wenbudangsang Formation in the Lhasa Block (Wu et al., 2014). 18, *Vjalovognathus* sp., from the upper part of the Selong Group in Nyalam (Yuan et al., 2018). 19, *Mesogondolella hendersoni*, from the top part of the Selong Group in Nyalam (Yuan et al., 2018). 20, *Mesogondolella sheni*, from the top part of the Selong Group in Nyalam (Yuan et al., 2018). 21, *Clarkina orchardi*, from the top part of the Selong Group in Nyalam (Yuan et al., 2018). 22, *Clarkina carinata*, from the base part of the Kangshare Formation in Nyalam (Yuan et al., 2018). 23, *Hindeodus parvus*, from the base part of the Kangshare Formation in Nyalam (Yuan et al., 2018). 24, *Isarcicella staeschei*, from the base part of the Kangshare Formation in Nyalam of Himalaya Tethys Zone (Yuan et al., 2018).

subdivided into the Northern Lhasa, Central Lhasa, and Southern Lhasa by the Shiquan River-Nam Tso Mélange Zone and the Luobadui-Milashan Fault respectively (Zhu et al., 2013). The marine Permian strata are distributed mainly in the Central Lhasa such as Shiquanhe, Tsochen, Xainza, Lhunzhub, and Baxoi from west to east.

### 2.3.1 Lithostratigraphy

The Permian strata in the Xainza area are divided into the Yunzhug, Lagar, Angie, Xiala, and Mujiucuo formations in ascending order (Yao et al., 2007; Zhang et al., 2013a, 2019a). The Yunzhug Formation consists mainly of thin-bedded black shale, siltstone and sandstone. Its upper part has more limestone interlayers yielding abundant brachiopods. Most part of the Yunzhug Formation belongs to the Carboniferous, and only the top part is suggested an earliest Permian age (Zhang et al., 2013a). The overlying Lagar Formation is composed mainly of glacio-marine conglomerates, and preserve the dropstones that consist mainly of sandstone and granite. The top part of this formation has more sandstone (Zhang et al., 2013c). The overlying Angie Formation is represented by thick-bedded limestone yielding abundant bryozoans and brachiopods in the basal part (Xia, 1983; Zhang et al., 2013a). The upper part of the Angie Formation consists mainly of thin-bedded shale and mudstone, intercalated with calcareous sandstone and limestone, and the limestone is suggested to be hydrocarbon-seep deposits (Liu et al., 2021). The Xiala Formation can be divided into three parts. The lower part of the Xiala Formation, previously known as the Ria Formation (Lin, 1983), is composed of purplish limestone containing crinoids and intercalated with more cherty bands. Solitary corals and conodonts were also abundantly preserved in this part. The middle part of the Xiala Formation is dominated by bedded gray limestone with abundant fusulines, corals, and brachiopods. The upper part of the formation consists mainly of medium- to thick-bedded limestone with cherty nodules and bands, and yields conodonts and foraminifers (Zhang et al., 2014b). In the Aduogabu area, the top part of the Xiala Formation contains several sandstone beds (Qiao et al., 2019). Besides, the Wenbudangsang Formation in Gegyai County, Tibet may be equivalent to the top part of the Xiala Formation (Wu et al., 2014). In the Xainza area, the dolomite or dolomitic limestone of the Mujiucuo Formation conformably overlies the Xiala Formation, and yields compound corals (Cheng et al., 2002). The Permian Nazipo and Yangweishan formations established by Guo et al. (1991) in the Shiquanhe area are also referred later to the Lagar, Angie and Xiala formations (Ji et al., 2007; Zhang et al., 2013a; Figure 2).

The Permian strata in the Lhunzhub area are represented by the Poindo Group, Wululong, and Luobadui formations in ascending order (Tibetan Scientific Expedition Team and Chinese Academy of Sciences, 1984). The Poindo Group,

also termed as the Laigu Formation, is characterized by the widespread glacio-marine deposits and conglomeratic slates (Ji et al., 2005; Yang et al., 2016). It may be equivalent to the Lagar Formation in the Xainza area (Zhang et al., 2013a). The overlying Wululong Formation consists mainly of grayish black slates and gray carbonate rocks, with limestone yielding bryozoans, corals, and brachiopods (Tibetan Scientific Expedition Team and Chinese Academy of Sciences, 1984). The overlying Luobadui Formation is mainly composed of dark gray carbonate rocks interbedded with volcanic rocks (Wang et al., 2022). Limestones contain cherty nodules, and yield abundant fusulines, corals, and brachiopods (Tibetan Scientific Expedition Team and Chinese Academy of Sciences, 1984; Huang et al., 2022).

### 2.3.2 Biostratigraphy and chronostratigraphy

The earliest Permian fusulines in the Lhasa Block were reported from the middle part of Xiala Formation and its counterpart, the Luobadui Formation. In the Tsochen area, the middle part of the Xiala Formation yields the *Neoschwagerina craticulifera*-*Kahlerina pachythea* Assemblage, associated with *Yangchienia tobleri*, *Chusenella brevipola*, *C. schwagerinaeformis*, *Neoschwagerina craticulifera*, *N. cheni*, *Kahlerina pachythea*, and *K. tenuitheca*, which suggests a Wordian age (Ju et al., 2019). The overlying *Nankinella*-*Chusenella* Assemblage is widely distributed in the Tsochen area (Zhang et al., 2019a), Tangra Yumco area, and Yongzhu of the Xainza area (Zhu, 1982a; Zhang et al., 1985; Wang and Zhou, 1986; Huang et al., 2007), Mujiucuo of the Xainza area (Zhang et al., 2010). In particular, the abundant *Nankinella* and *Chusenella* species in this assemblage suggest a Capitanian age. The foraminifer *Shanita-Hemigordiopsis* Assemblage is also present in the Guadalupian of the Lhasa Block (Zhang et al., 2016a, 2019a; Ju et al., 2021). In the Lhunzhub area, the Luobadui Formation yields abundant *Lepidolina*, associated with *Dunbarula*, *Chusenella*, *Neoschwagerina*, and *Verbeekina* (Wang et al., 1981; Zhu, 1982b; Huang et al., 2022). Rare Lopingian fusulines have been found so far in the Lhasa Block. The *Codonofusiella*-*Reichelina* Assemblage, which includes *Reichelina changhsingensis*, *Codonofusiella tsochenensis*, and *Nankinella rarivoluta*, was described at Mujiucuo in the Xainza area and the south bank of Zhari Namco in the Tsochen area (Qiao et al., 2021; Ju et al., 2022b). The Changhsingian fusuline *Reichelina changhsingensis* and abundant foraminifera *Colaniella* Assemblage have been reported at Adogabu in the Tsochen area (Chen et al., 1999; Qiao et al., 2019; Figure 3).

Brachiopods were widely preserved in the Yunzhug, Angie, Xiala formations, and the Poindo Group. Three assemblage zones, respectively the *Taeniothaerus xizangensis*-*Spinomartinia xainzaensis*, *Cimmeriella mucronata*-*Taeniothaerus excellens*, and *Trigonotreta maginifica*-*Bando-*

*productus intermedia* assemblage zones, were established in the middle-upper part of the Yunzhug Formation by Zhan et al. (2007). All these assemblages represent the Gondwanan cold-water faunas and indicate an early Cisuralian age. The Poindo Group yields *Bandoproductus* fauna (Jin and Sun, 1981), which indicates approximately a Sakmarian age. The Angie Formation contains the *Aulosteges ingens-Punctocyrtella nagmargensis* Assemblage, which suggests an Artinskian to early Kungurian age (Zhan et al., 2007). The *Costiferina-Stenoscisma gigantean* Assemblage from the basal part of the Xiala Formation is similar to the assemblage in the Angie Formation. *Costiferina spiralis*, *Calliomarginatia orientalis*, and *Spiriferella salteri* in this assemblage are widely distributed in peri-Gondwanan region (e.g., Salt Range of Pakistan, Himalaya Tethys Zone and West Timor). However, the middle part of Xiala Formation contains *Pseudoantiquatonia mutabilis-Neoplicatifera pusilla* Assemblage (Zhan and Wu, 1982). Representative species include *Neoplicatifera pusilla*, *Leptodus nobilis*, *Permophricodothyris elegantula*, and *Haydenella minuta*, which are the common species in the paleoequatorial realm. In the Tsochen area, the top part of Xiala Formation contains the Changhsingian *Spinomarginifera* Assemblage, and about 70% species of this Assemblage have been reported from the Cathaysian fauna (e.g., South China) (Xu et al., 2019). In the eastern Lhasa Block, the Lielonggou Formation yields a Changhsingian *Transennatia* Assemblage, which also contains some warm-water species such as “*Peltichia*” sp., *Spinomarginifera* sp., and *Crenispirifer dzhulfensis* (Sun et al., 1981). However, the age and taxonomies of this assemblage require further studies (Figure 4).

The Permian conodonts in the Lhasa Block were reported from three horizons, the lower part of Angie Formation, the upper Angie and lower Xiala formations, and the upper part of the Xiala Formation. Zheng et al. (2005) reported *Neostreptognathodus* from the Angie Formation in the Xainza area, but did not provide any illustration. *Neostreptognathodus* is a dominant genus in the Kungurian, but it is also present in the late Artinskian and early Guadalupian. Thus, *Neostreptognathodus* indicates an age no earlier than Artinskian. Zheng et al. (2007) reported a *Mesogondolella-Vjalovognathus* Assemblage in the Shiquanhe area, western Lhasa Block and assigned it to a late Cisuralian to Guadalupian age. Apart from this, Ji et al. (2007) illustrated some *Mesogondolella idahoensis* from the equivalent strata in the same area and referred it to a late Kungurian age. Yuan et al. (2016) also illustrated some *Mesogondolella idahoensis*, *M. siciliensis*, and *Vjalovognathus nicolli* (Figures 6.9) from the central Lhasa Block. All those occurrences imply that this assemblage may be distributed in the whole Lhasa Block and consistently indicates a late Kungurian age. No conodonts have been reported from the middle part of the Xiala Formation so far. In the Xainza area, the Wuchiapingian con-

odonts *Clarkina liangshanensis*, *C. orientalis*, and *Iranognathus* sp. were described from the top part of the Xiala Formation (Yuan et al., 2014; Figure 6.14–6.16). Some Wuchiapingian conodonts *Clarkina liangshanensis* and *C. guangyuanensis* were also illustrated from the Longar area in western Lhasa Block, but these specimens are too fragmentary to be re-identified for certain. Some Changhsingian conodonts *C. changxingensis* and *C. meishanensis* were also reported above *C. liangshanensis* and *C. guangyuanensis* assemblages from the Longar area, but they were still referred to the Wuchiapingian by Wu et al. (2021). Therefore, these specimens from the Longar area require further investigations. Ji et al. (2007) described a few of *C. changxingensis* specimens from the top part of the Xiala Formation in western Lhasa Block, which is indicative of a late Changhsingian age. Wu et al. (2014) also reported abundant conodonts from the Wenbudang section, including the upper Changhsingian *C. changxingensis* and *C. yini*, the uppermost Changhsingian *C. meishanensis* and *Hindeodus praeparvus*, and the basal Triassic *Clarkina carinata*, *C. planata*, *Hindeodus parvus*, and *Isarcicella staeschei* (Figure 6.17). These records indicate that the Lhasa Block may preserve continuous marine carbonate sequences from the Wuchiapingian to the Lower Triassic (Figure 5).

On the basis of the fusuline, brachiopod, and conodont biostratigraphic data mentioned above, the ages of lithostratigraphic units in the Lhasa Block can be determined (Figures 2–5). The brachiopod *Bandoproductus* Assemblage in the Poindo Group and the sandstone in the top part of the Yunzhug Formation indicates a Sakmarian age (Zhan et al., 2007). The Lagar Formation has similar glacio-marine conglomerates to the Poindo Group, which implies that the Lagar Formation may be also Sakmarian. The conodont *Neostreptognathodus* from the limestone interval of the lower Angie Formation suggests a late Artinskian to Kungurian age (Zheng et al., 2005). The purplish limestone in the lower Xiala Formation yields the conodont *Mesogondolella-Vjalovognathus* Assemblage, indicating a late Kungurian age (Yuan et al., 2016). The occurrences of abundant fusulines including the *Neoschwagerina craticulifera-Kahlerina pachythea* and *Nankinella-Chusenella* assemblages in the middle part of the Xiala Formation and the *Lepidolina* assemblage in the Luobadui Formation suggest that they belong to a Wordian to Capitanian age (Zhang et al., 2010, 2019a; Ju et al., 2019). The conodont *Clarkina liangshanensis*, *C. orientalis* and fusuline *Codonofusiella-Reichelina* Assemblage in the upper Xiala Formation can be assigned to a Wuchiapingian age (Yuan et al., 2014; Qiao et al., 2021). The conodont *Clarkina changxingensis* and foraminifera *Reichelina changhsingensis*, *Colaniella parva* in the Wenbudang and the topmost part of the Xiala formations indicate a Changhsingian age (Wu et al., 2014; Qiao et al., 2019). The Mujiucuo Formation conformably overlies

the Xiala Formation, and its lower part yields compound corals *Waagenophyllum indicum crassiseptatum* and *Liangshanophyllum streptoseptatum*, which may suggest a late Wuchiapingian age (Cheng et al., 2002). The upper part of the Mujiucuo Formation has been assigned to the Lower Triassic by Wu et al. (2017) (Figures 2–5).

## 2.4 Baoshan Block

The Baoshan Block is bounded by the Nujian Fault and the Gaoligong Mountain in the west, and the Lancangjiang-Kejie-Nandinghe Fault in the east, and connects with the Changning-Menglian belt and the Simao Block (Figure 1). On the basis of the depositional sequences of the Permian System, three parts are divided for the Baoshan Block and they are the northern, southern, and southwestern Baoshan Block, respectively. Generally, the Permian strata in the northern Baoshan Block are well developed (Jin, 1994).

### 2.4.1 Lithostratigraphy

The Permian strata in the northern Baoshan Block were divided into the Dingjiazhai, Woniusi, Bingma, Daaози formations and the lower part of the Hewanjie Formation in ascending order (Wang et al., 2001, 2021; Jin et al., 2008; Figure 2). The Dingjiazhai Formation unconformably overlies the Lower Carboniferous strata, and is composed mainly of conglomerate, pebbly mudstone and shale interlayered with some bioclastic limestone at the top. The lower part of the Dingjiazhai Formation has few fossils whereas the middle and upper parts yield coral and brachiopod fossils (Fang and Fan, 1994; Shi et al., 1996; Shen et al., 2000a, 2002; Wang et al., 2001), and the top limestone interlayer contains corals, fusulines and conodonts (Ueno et al., 2002; Ji et al., 2004; Wang et al., 2004; Shi et al., 2011; Wang et al., 2013; Huang et al., 2015). The Woniusi Formation overlies the Dingjiazhai Formation, and is composed of marine basalt lava and pyroclastic rocks. Fusulines previously reported at the base of the Woniusi Formation were presumed to be derived from the limestone interlayer at the top of the Dingjiazhai Formation (Wang et al., 2001). The Bingma Formation lies unconformably over the Woniusi Formation, and is composed of red detrital deposits with beanlike bauxite and bauxite layers. A few of plant fossil fragments were collected from this formation. The overlying Daaози Formation is divided into two parts. The lower part is mainly marl and contains fossils of small foraminifers, corals, fusulines, and brachiopods (Sugiyama and Ueno, 1998; Wang et al., 2001; Jin et al., 2008) whereas the upper part is dolomitic limestone. The Hewanjie Formation overlies the Daaози Formation, and is dominated by dolomite in the lower part. The boundary between the two formations is not consistent in different studies. For instance, some studies assigned the calcareous dolomite unit of the upper part of the Daaози

Formation to the Hewanjie Formation. Jin et al. (2008) considered that the boundary between the Hewanjie and Daaози formations should be most suitable at the lithological interface between marl and dolomite. Notably, recent studies have reported conodont fossils near the Periman-Triassic boundary in the Hewanjie Formation (Dong and Wang, 2006).

The Permian strata in the southern Baoshan Block are divided into the Dingjiazhai, Woniusi, Yongde, and Shazipo formations in ascending order. The Dingjiazhai Formation lies unconformably over the Lower Devonian strata and has no limestone interlayer at the top. It contains bryozoan and brachiopod fossils (Wang et al., 2001). The Woniusi Formation is composed of basalt. Its contact with the underlying Dingjiazhai Formation may represent a disconformity. The Woniusi Formation is overlain by the Yongde Formation, also known as the Xiaoxinzhai Formation. This can be divided into two parts. The siliciclastic rocks in the lower part contain bivalves, brachiopods, and plant fossils, and are equivalent to the Bingma Formation in the northern Baoshan Block. The marl and shale in the upper part contain bryozoans and brachiopods (Fang, 1983; Fang and Fan, 1994). The Shazipo Formation directly overlies the Yongde Formation, and its lower part is dominated by marl and dolomitic limestone with fusulines (Ueno, 2003; Shi et al., 2005; Huang et al., 2015). The upper part of the Shazipo Formation is dominated by dolomitic limestone and dolomite, lithologically similar to the Daaози Formation in the northern Baoshan Block. However, the correlation among the Shazipo, Daaози, and Hewanjie formations still needs further study because of the inconsistency of the lithological subdivisions (Figure 2).

The Permian strata in the southwestern Baoshan Block include the lower Manli Formation and the upper Shazipo Formation. The Manli Formation unconformably overlies the Devonian or older strata, and is composed of siliciclastic deposits with bauxite layers. Its lithology is similar to the lower parts of the Bingma and Yongde formations. The overlying Shazipo Formation is dominated by dolomitic limestone and dolomite, and contains small foraminifers and fusulines in the lower part.

### 2.4.2 Biostratigraphy and chronostratigraphy

On the basis of the fusuline “*Triticites*” species, the Dingjiazhai Formation was previously assigned to the Upper Carboniferous (Chen, 1984). However, subsequent studies indicate that these so-called “*Triticites*” are actually *Pseudofusulina*. And fusulines in the Dingjiazhai Formation are dominated by the species of *Pseudofusulina* and *Eoparafusulina*, which belong to the Artinskian Kalaktash fauna (Shi et al., 2011). The Guadalupian fusulines were reported mainly in the Daaози Formation in the northern Baoshan Block and the Shazipo Formation in the southern Baoshan

Block, among which the lower *Yangchienia-Nankinella* Zone and the upper *Chusenella-Rugosofusulina* Zone are recognized in the Bawei area (Huang et al., 2017) and the *Schwagerina yunnanensis*, *Eopolydiexodina*, and *Sumatrina annae* zones were identified in the south Xiaoxinzhai area (Huang et al., 2009). By contrast, the fusulines are much less diverse in the Daozi Formation, and are represented mainly by the species *Jinzhangia shengi* (Ueno, 2001; Huang et al., 2015; Figure 3).

Brachiopods are found mainly in the Dingjiazhai, Yongde, and Shazipo formations. Three brachiopod assemblages were identified in the Dingjiazhai Formation: the *Bando-productus qingshuigouensis-Marginifera semigratiosa* Assemblage in the lower part, the *Punctocyrtella australis-Punctospirifer afghanus* Assemblage in the middle, and the *Callytharrella dongshanpoensis* Assemblage in the upper. They approximately indicate an age from Asselian to Artinskian (Shen et al., 2000a). Abundant brachiopods are present in the Yongde Formation, and were divided into three assemblages in ascending order. Assemblage A contains *Lisotella subcylindrica*, a typical species of the lower part of Chihsonian in South China. Assemblage B yields brachiopods *Tenuichonetes tengchongensis* and *Vediproductus punctatiformis*, and suggests a Kungurian-Roadian age. Assemblage C contains *Neoplicatifera huangi*, an index species of the Maokouan Stage in South China, approximately corresponding to the Wordian (Shen et al., 2002). This assemblage may be equivalent to the *Stereochia-Waagenites* Assemblage at the top of the Xiaoxinzhai Formation in the Gengma area (Fang, 1983). The Shazipo Formation in the southern Baoshan Block yields rich *Permocryptospirifer omeishanensis* and *Pseudoantiquatonia mutabilis*, which indicates a Wordian-Capitanian age. And the brachiopod assemblage also exhibits a mixed fauna characteristic, but is dominated by Cathaysian types (Shi and Shen, 2001; Figure 4).

Very few conodonts have been reported in the Baoshan Block. The *Sweetognathus* aff. *whitei-Mesogondolella bisSELLI* Assemblage in the limestone interlayer at the top of the Dingjiazhai Formation suggests an age from late Sakmarian to early Artinskian (Figure 6.5–6.6). However, the precise age of the fauna remains to be refined (Wang et al., 2001; Ueno et al., 2002; Ji et al., 2004; Wang et al., 2004). *Hindeodus parvus*, the index conodont species for the base of Triassic, was discovered in the dolomitic limestone of the Hewanjie Formation (Dong and Wang, 2006). And *Hindeodus parvus* and *Isarcicella staeschei* were also reported recently in the dolomitic limestone and dolomite of the Hewanjie Formation, suggesting that a considerable part of the lower part of the Hewanjie Formation belongs to the Lopingian age (Figure 5).

On the basis of all data mentioned above, the ages of Permian strata in the Baoshan Block can be well constrained. Brachiopods in the lower part of the Dingjiazhai Formation

indicate a possible Asselian-Sakmarian age, and fusulines and conodonts in the upper part are probably indicative of the Sakmarian-Artinskian. The Woniusi Formation is composed mainly of basaltic lava and pyroclastic deposits, which are thought to have been formed in a relatively short time. However, only a few specimens of *Sweetognathus* (= *Rabeignathus*) were reported in the limestone lens in the Woniusi Formation (Wang et al., 2004), and could indicate that the Woniusi Formation is of the upper Artinskian to the lower Kungurian. In addition, the zircon  $^{206}\text{Pb}/^{238}\text{U}$  ages for of the Woniusi Formation also indicate that it may have formed between 301 and 282 Ma (Liao et al., 2015). Therefore, the age of the Woniusi Formation should be no later than the early Kungurian. The fauna from the top of the Dingjiazhai Formation suggests a late Artinskian age. Brachiopods in the overlying Yongde Formation suggest a Kungurian-Wordian age (Shen et al., 2002). Abundant fusulines in the Daozi and Shazipo formations suggest a Wordian-Capitanian age. Recent discovery of conodonts from this formation suggests that it may range down into the late Kungurian. And conodonts in the lower part of the Hewanjie Formation are of the Lopingian age.

## 2.5 Tengchong Block

The Tengchong Block lies to the west of the Baoshan Block and is bounded by the Gaoligong Mountain in the east (Figure 1). Because of the large exposure of volcanic rocks, the Carboniferous-Permian strata have relatively limited outcrops in the Tengchong Block. Paleontologic and stratigraphic studies in this block were concentrated in the Kongshuhe and Dadongchang areas of the northern region as well as the Shuangheyuan area in the southern region.

### 2.5.1 Lithostratigraphy

The Carboniferous-Permian strata in the Tengchong Block consist of more than 1000 m thick siliciclastic rocks in the lower part and 400–600 m thick carbonates in the upper part. In the northern region, the siliciclastic rocks were called the Menghong Group, which includes the Zizhi and the Kongshuhe formations in ascending order (Jin, 1994). The 600–700 m thick Zizhi Formation is composed of brown or gray thick-bedded quartz sandstone whereas the 800–900 m thick Kongshuhe Formation is composed of diamictites and pebbly mudstone in the lower part and black mudstone, siltstone with limestone lens in the upper part (Jin, 2002). The upper part of the Kongshuhe Formation yields abundant sporopollens in the black mudstone and bryozoans, crinoids, and brachiopods in the limestone lens, all suggesting a Cisuralian age (Yang, 1999; Jin et al., 2011, 2014). The overlying Dadongchang Formation consists of bioclastic limestone with chert nodules or bands in the lower part and dolomitic limestone in the upper part. The lower part was



originally called the Guanyinshan Formation and contains abundant foraminifers, brachiopods, and corals (Fang and Fan, 1994; Figure 2).

The Menghong Group in the southern Tengchong Block includes the Bangdu, Luogengdi, Siguaping, and Damuchang formations in ascending order (Jin, 1994). The Bangdu Formation consists of 600 m thick gray mudstone and siltstone and is equivalent to the Zizhi Formation. The Luogengdi, Siguaping, and Damuchang formations are dominated by diamictites, pebbly mudstone and siltstone and can be correlated with the Kongshuhe Formation. The Damuchang Formation is rich in bryozoans, crinoids, and brachiopods. Above the siliciclastic rocks, the carbonates of the Yanzipo Formation yield abundant foraminifers, brachiopods, and bryozoans, and are the counterparts of the Dadongchang Formation in the northern region (Fan, 1993; Figure 2).

### 2.5.2 Biostratigraphy and chronostratigraphy

The studies of Permian fusuline faunas in the Tengchong Block are relatively few and their taxonomy and ages are still in dispute. Two fusuline faunas were reported from the Kongshuhe and Dadongchang formations by Fang and Fan (1994). The first one was from the limestone lens in the upper part of the Kongshuhe Formation and contained “*Triticites*” and *Schwagerina*, which were revised to *Eoparafusulina* of a Sakmarian age (Huang et al., 2020). The other fauna from the lower part of the Dadongchang Formation consists of *Cancellina*, *Nankinella*, and *Parafusulina* and clearly indicates a late Kungurian age. However, Shi et al. (2008) reported an *Eoparafusulina* fauna from the same horizon in the Kongshuhe area, including *Eoparafusulina tschernyschewi tschernyschewi*, *E. malayensis*, *Parafusulina* sp., and *Monodiexodina wanneri*, which was assigned to the Sakmarian. Therefore, further studies are necessary to clarify the exact horizons and relationships of these two faunas from the lower part of the Dadongchang Formation. Guadalupian fusuline faunas were found in the entire Tengchong Block: one is the *Nankinella-Chusenella* Assemblage from the middle part of the Dadongchang Formation in the Shanmutang area of the northern region and the other is the *Chusenella-Schwagerina* Assemblage from the Yanzipo Formation in the Shuangheyan area of the southern region (Shi et al., 2017; Figure 3).

Permian brachiopods were also reported from the lower part of the Dadongchang Formation (i.e., the original Guanyinshan Formation), namely the *Stereochia-Waagenites* Assemblage (Fang and Fan, 1994; Chen et al., 2000). Its age is probably Wordian on the basis of comparisons with the brachiopod faunas of the Baoshan Block and southern Thailand (Fang, 1983). Three brachiopod assemblages were established in similar horizons by Jin et al. (2011), but systematic paleontological studies and corresponding fossil

plates were absent. The *Derbyia grandis-Waagenites* Assemblage is the most reliable in age determination among these three assemblages, and its age can be restricted to Wordian by the occurrences of fusulines *Chusenella* and *Monodiexodina* from the overlying horizons (Shi et al., 2008; Figure 3).

The ages of the Carboniferous-Permian successions in the Tengchong Block are still controversial owing to insufficient studies of the fusulines and brachiopods. The upper part of the Kongshuhe Formation is probably Sakmarian in age on the basis of the presence of fusuline *Eoparafusulina* and the sporopollens *Jayantisporites* and *Microbaculispora* (Yang, 1999; Huang et al., 2020). The lower part of the Dadongchang Formation is likely Cisuralian in age based on the fusuline faunas, but also likely to be Guadalupian based on the brachiopod *Stereochia-Waagenites* Assemblage (Fang and Fan, 1994; Shi et al., 2008). The age of the middle part of the Dadongchang Formation is well-confined as the Roadian-Capitanian by the fusuline *Nankinella-Chusenella* and *Chusenella-Schwagerina* assemblages as well as the brachiopod *Derbyia grandis-Waagenites* Assemblage (Jin et al., 2011; Shi et al., 2008, 2017). The upper part of the Dadongchang Formation is dominated by dolomitic limestone with no fossils, and thus its age is difficult to determine and further studies are needed.

## 2.6 Himalaya Tethys Zone (Northern margin of the Indian Block)

The Himalaya Tethys Zone is separated from the Lhasa Block by the Yarlung Zangbo suture zone in the north, from the High Himalayas by the South Tibetan Detachment System in the south, and extends into Kashmir in the west and into the Indo-Myanmar Range in the east (Figure 1). Permian strata are distributed mainly in the southern and central part of the Himalaya Tethys Zone.

### 2.6.1 Lithostratigraphy

The Permian strata are most developed in the Qubu area of the northern slope of Mount Qomolangma (Mount Everest) in Tingri County, and are divided into the Jilong, Qubu, and Qubuerga formations in ascending order (Yin and Guo, 1976; Figure 2). The Cisuralian strata are represented by the Jilong Formation, which is composed mainly of marine diamictites in the lower part, siltstone in the middle part, and quartz sandstone in the upper part. Some basalt interlayers have also been found in this formation in the Jilong and Selong areas (Garzanti et al., 1999; Zhu et al., 2002). The Jilong Formation is in fault contact with the overlying Qubu Formation, which is characterized by the white quartz sandstone with a thickness of about 20 meters. In the Kujianla section in Qubu and Dingjie counties, plant fossil *Glossopteris* was reported in the shale of this formation (Xu,

1976). The Qubuerga Formation conformably overlies the Qubu Formation and is generally divided into two parts. The lower part is gray-brown siltstone interbedded with bioclastic limestone, and contains abundant brachiopods. The upper part is dominated by varicolored sandy shale with nodules, and is rich in gastropod and bivalve fossils. The equivalent strata of the Qubu and Qubuerga formations were named the Selong Group in the Selong Xishan section in the north of the Mount Shishapangma, Nyalam County, which represents a transgressive sequence consisting of coastal coarse to fine grained siliciclastic deposits, shallow marine fine siliciclastic rocks, and bioclastic limestone interbeds. Strata similar to those in the Tingri area were also found in the Nagri area, and are divided into the Mayang Formation, and the lower, middle, and upper Mangzongrong Formation in ascending order (Guo et al., 1991; Figure 2).

The Permian strata in the Kangma area is also relatively well developed, and consist of the Polinpu, Bilong, Kangma, and Baidingpu formations (Chen et al., 2002). The Polinpu Formation is composed of metamorphic sandstone, pebbly slate and conglomerate. The overlying Bilong Formation is characterized by gray-white gravel-bearing quartz sandstone containing typical Gondwanan cold-water brachiopod *Cimmeriella*. Both formations are possibly corresponding to the Jilong Formation in the Mt. Qomolangma area. The Kangma Formation is divided into two parts, the lower part is composed of pebbly sandstone with quartz sandstone and pebbled slate, and the upper part is silty slate yielding brachiopod fossils. The lower part of the Baidingpu Formation is composed of bioclastic dolomitic dalites and recrystalline limestone. The upper part is silty calcareous bioclastic slate with abundant brachiopods, and is close to that of the Qubuerga Formation in the Mt. Qomolangma area. Permian strata distributed in the Zhongba Block is collectively known as the Quga Group/Formation, and underwent strong metamorphism. They were subsequently divided into the Gangzhutang, Zhongba, and Kazhale formations in ascending order (Li et al., 2014; Figure 2).

### 2.6.2 Biostratigraphy and chronostratigraphy

Conodonts were poorly known in the Himalaya Tethys Zone of southern Tibet. The most intensively studied conodonts were from the Selong Group at the Selong Xishan section in Nyalam County (Figure 6.18–6.24), which has long been controversial of its biostratigraphic age (Zhang and Jin, 1976; Yao and Li, 1987; Xia and Zhang, 1992; Wang et al., 2017; Yuan et al., 2018). Abundant conodonts including *Clarkina changxingensis*, *C. carinata*, *C. taylorae*, *Hindeodus praeparvus*, *H. parvus*, and *Isarcidella isarcica* near the Permian-Triassic boundary in the southern Tibet have been described by Orchard et al. (1994), but there is still disagreement on the identification of some species. A similar conodont fauna in the same area has been reported by Mei

(1996) and Shen et al. (2006) at the top of Changhsingian. On the basis of a recent study, three conodont zones can be roughly identified in the Lopingian, respectively, the *Vjalovognathus carinatus* Zone, the *Mesogondolella hendersoni* Zone, and the *M. sheni* Zone (Wang et al., 2017; Yuan et al., 2018). Among them, the *Vjalovognathus carinatus* Zone belongs approximately to the Lopingian whereas the upper two zones belong to the Changhsingian. Because of the rapid global warming and transgression in the end of the Permian, the *Mesogondolella sheni* Zone became highly differentiated, with *Clarkina orchardi* and other *Clarkina* species in its upper part, followed by the emergence of *Hindeodus parvus*, an index fossil for the base of the Triassic (Figure 5).

Brachiopods are well studied in the Himalaya Tethys Zone. A relatively complete Cisuralian brachiopod succession is preserved in the Mayang area of Zanda County (Yang et al., 1990), and consists of three assemblages, namely, the *Dielasma-Mayangella* Assemblage of the Mayang Formation, the *Cimmeriella* Assemblage of the lower Mangzongrong Formation, and the *Taeniothaerus* Assemblage of the middle Mangzongrong Formation. In addition, the *Cimmeriella gracilis-Brachythyridella narsarhensis* Assemblage from the lower Mangzongrong Formation has also been reported in the Jilong Formation in Tingri County (Jin et al., 1977). The Lopingian brachiopods are widely distributed in the Himalaya Tethys Zone, mainly from the Selong Group, the Qubuerga Formation, and other equivalent strata (Shen et al., 2000b, 2001a, 2001b, 2003a; Xu et al., 2018). On the basis of the brachiopods of the Selong Group in the Selong Xishan section, Nyalam County and the lower part of the overlying Kangshare Formation, three brachiopod assemblages were recognized, namely the *Marginalosia-Composita* Assemblage in the lower part, the *Chonetella nasuta* Assemblage in the upper part of the Selong Group, and the *Martinia-Fusichonetes* Assemblage at the base of the Kangshare Formation (Shen et al., 2000b, 2001a). Two brachiopod assemblages, namely, *Neospirifer (Neospirifer) kubeiensis-Chonetinella unisulcata* and *Biplatyconcha grandis-Quinquenella semiglobosa* assemblages, were recognized in the Qubuerga Formation at the Qubu section in the Mt. Qomolangma area, and a Wuchiapingian to early Changhsingian age was assigned to them (Shen et al., 2003a). In addition, the *Costiferina indica-Neospirifer (Neospirifer) kubeiensis* Assemblage has been reported in the Quga Formation in the Zhongba Block, and has been assigned to the Capitanian-Wuchiapingian (Jin and Sun, 1981; Shi et al., 2003). However, this brachiopod fauna clearly belongs to the Gondwana brachiopod fauna, which is completely different from the mixed brachiopod fauna in the suture zone (Figure 4). On the basis of the abovementioned paleontological data, a conodont and brachiopod biostratigraphical framework for the stratigraphic units in the Himalaya Tethys Zone can be integrated. Marine glacial deposits are developed in the Ji-

long Formation in the Mt. Qomolangma area, the Mayang Formation and the lower Mangzongrong Formation in the southern Nagri area, and the Polinpu and Bilong formations in the Kangma area. The *Cimmeriella* brachiopod fauna, which is characteristic of the northern margin of Gondwana continent, is present in the middle part of the Jilong Formation, the lower Mangzongrong Formation, and the Bilong Formation, and is generally assigned to the early Cisuralian. Therefore, the age of Jilong Formation and its corresponding strata is determined to be the early Cisuralian, or possibly the Asselian-Sakmarian age. The Guadalupian strata in the Himalaya Tethys Zone have not been reported so far, except for a possible Quga Formation in the Zhongba Block. In contrast to the absence of the Guadalupian Series, the Lopingian strata are widely developed in southern Tibet, represented by the Qubu and Qubuerga formations at the Qubu and Tulong sections in Mt. Qomolangma area and the Selong Group in the Selong Xishan section in the Nyalam area. On the basis of the brachiopods and conodonts, the Lopingian is suggested. Similar brachiopods were reported from the upper Mangzongrong Formation in southern Nagri area and the Baidingpu Formation in the Kangma area as well as the Qubuerga Formation and the Selong Group (Figure 2).

## 2.7 Exotic limestone blocks within the Yarlung Zangbo suture zone

### 2.7.1 Lithostratigraphy

A series of Permian exotic limestone rock units of different sizes are scattered in the Yarlung Zangbo suture zone. From west to east, they were called the Gyanyima limestone block in Burang County, the Lasaila and Gaqoi limestone blocks in Zhongba County, and the Xiukang limestone block in Lhaze County, and were collectively known as the “Tibetan facies” (Diener, 1903; Yin and Guo, 1976; Lys et al., 1980; Yin, 1997; Shen et al., 2003a) or Chitichun-type deposits (Shen et al., 2003b). The Gyanyima limestone block in the western part of the suture zone consists of well-exposed Guadalupian-Lopingian carbonate sequences, which are divided into the Xilanta and Gyanyima formations (Wang et al., 1988). The Xilanta Formation is dominated by bluish-white medium-bedded limestone with basalt interlayers in the middle, and rich in compound corals, brachiopods, fusulines and foraminifers. The overlying Gyanyima Formation is divided into two parts. The lower part is dominated by reddish-purplish medium- to thick-bedded limestone with basalt units in the middle, and the upper part is represented by the blue-gray thin- to medium-bedded limestone rich in compound corals, brachiopods, fusulines, and foraminifers (Zhang et al., 2009; Zhang, 2010; Wang et al., 2019; Shen et al., 2010; Zhang and Wang, 2019). The Gaqoi limestone in the Zhongba area is outcropped as a small isolated hill and composed of pale red micritic limestone. The Lasaila lime-

stone consists mainly of breccia, pale gray massive bioclastic limestone, siliceous rock, and reddish limestone, with a thickness of about several hundred meters. It gently overlies the Jurassic reddish andesite and gray-black shale in the form of fault blocks. Both the Gaqoi and Lasaila limestone blocks are rich in brachiopods (Jin and Sun, 1981). The Xiukang limestone blocks are composed of gray and purplish limestones with poor beddings. They are covered by the Triassic limestone and shale in the south and are in fault contact with the Jurassic sandstone and shale in the north. There are abundant brachiopods in the Xiukang limestone blocks (Shen et al., 2003c; Figure 2).

### 2.7.2 Biostratigraphy and chronostratigraphy

The exotic limestone blocks within the Yarlung Zangbo suture zone usually contain rich fusulines, foraminifers, corals, and brachiopods (Wang et al., 1981; Shen et al., 2003b, 2003c, 2003d, 2010; Wang and Ueno, 2009; Wang et al., 2010; Zhang et al., 2009), and some yield ammonites (Sheng, 1984). Conodont fossils are rare in these exotic limestone blocks, and only a few juvenile specimens of *Clarkina* were reported from the reddish limestone of the Gyanyima Formation. However, abundant conodonts suddenly occur at the top of the Permian and the base of the Triassic, including *Hindeodus parvus*, *Clarkina carinata*, and *C. planata* (Shen et al., 2010; Figures 3, 5).

Fusulines are also relatively abundant in the exotic limestone blocks. Among them, the Xilanta Formation of the Gyanyima limestone block and the Lasaila limestone block in Zhongba County contain fusulines *Neoschwagerina*, *Chusenella*, *Yangchienia*, *Nankinella*, *Kahlerina*, and *Lantschichites*, which were named the *Neoschwagerina fusiformis-Lantschichites minima* assemblage, indicating a Capitanian age (Wang et al., 1981; Zhang et al., 2009). And the associated foraminifers are represented by the *Lysites biconcavus-Neoendothyra reicheli* Assemblage (Zhang and Wang, 2019). The Lopingian foraminifer faunas were widely reported in Ladakh of India, the Gyanyima Formation in the Gyanyima limestone block and the Gaqoi limestone, and are represented by the Changhsingian *Reichelina pulchra-Colaniella parva-Dilatofusulina orthogonios* Assemblage (Wang et al., 2010; Figure 3).

The Guadalupian brachiopod fauna in the exotic limestone blocks was reported from the Xiukang limestone in the Lhaze area, the Lasaila and Gaqoi limestones, and a collective *Transennatia-Urushtenoidea-Comuquia* assemblage was described on the basis of some common characteristic elements (Jin and Sun, 1981; Shen et al., 2003d). The Wuchiapingian brachiopods, namely, the *Martinia elegans-Jinomarginifera lhazeensis-Zhejiangospirifer giganteus* assemblage, were reported in the limestone blocks at Zhongbei in Lhaze County (Shen et al., 2003c). And some brachiopods have also been found in the Gyanyima lime-

stone, such as *Permophricodothyris elegantula-Edriosteges poyangensis* and *Waagenoconcha purdoni-Linoproductus lineatus* assemblages, and indicate a Changhsingian age (Shen et al., 2010; Figure 4).

On the basis of the fusulines and brachiopods above, the reddish or gray exotic limestones within the Yarlung Zangbo suture zone did not appear until the Guadalupian. The foraminifers from the Xilanta Formation in the Gyanmyima area, the Xiukang limestone in the Lhaze area and the Lasalia limestone in the Zhongba area all indicate a Capitanian age. The Changhsingian fusulines are reported from the Gyanmyima Formation (Wang et al., 2010; Shen et al., 2010) and the Gaqoi limestone (Wang et al., 1981).

### 3. Permian sequences in the surrounding areas of the Qinghai-Tibetan Plateau

#### 3.1 Salt Range, Pakistan

The sections outcropped in the Salt Range of Pakistan (Pakistan-Japanese Working Group, 1985; Wardlaw and Pogue, 1995; Shen et al., 2003e; Mertmann, 2003; Rahman et al., 2022; Figure 7) provide the best correlation scheme between the local Permian strata and the different tectonic blocks of the Qinghai-Tibetan Plateau. The Cisuralian (Nilawahan Group) is about 350 meters thick (Ghazi et al., 2012; Ali et al., 2021), and can be correlative with the lower Cisuralian glacial deposit in various tectonic blocks of the Qinghai-Tibetan Plateau. The Nilawahan Group is divided into four formations, of which the Tobra Formation is the lowermost. It unconformably overlies the Cambrian strata, and consists mainly of glacial and alluvial deposits containing Gondwanan flora such as *Gangamopteris*, *Glossopteris*, etc. The Tobra Formation was assigned to the Cisuralian (Asselian). Overlying the Tobra Formation is the Dandot Formation, a unit representing deposition of marginal marine environment and containing *Eurydesma* and *Conularia*. A marine regression occurred above the Dandot Formation, with the deposition of the Warchha alluvial sandstone. These alluvial deposits are probably the Artinskian but lack fossil evidence for this age determination. The Sardhai Formation was deposited during the following transgression, and thus represents the Kungurian deposition (Ghazi et al., 2012, 2015; Figure 7).

The overlying strata above the Nilawahan Group in the Gondwana region is known as the Zaluch Group in the Salt Range. The basal Amb Formation consists of shale, sandstone, and limestone, and contains the fusulines *Monodiexodina* (Douglass, 1970) and *Codonofusiella laxa* (Pakistan-Japanese Working Group, 1985). Wardlaw and Mei (1999) reported a complete conodont succession in the Guadalupian-Triassic sequence in the Salt Range, which is consistent with those of South China. However, these conodonts have never been illustrated. A large number of samples were collected by us from the Salt Range during the past years, but the results didn't confirm this conodont succession. The latest research on foraminifers shows that the Amb Formation contains the *Geinitzina araxensis* assemblage, and its age was assigned to the Wordian age on the basis of the co-occurring conodont fossils (Wardlaw and Mei, 1999). However, it is actually difficult to confirm this age since the derived conodonts such as *Vjalovognathus*, *Merrellina*, and *Hindeodus* cannot provide a precise age constraint. In fact, the *Monodiexodina* fauna of the Amb Formation is generally considered to be prevalent during the Artinskian and Kungurian in the southern hemisphere (Ueno, 2006). Therefore, the age of the Amb Formation is likely to be earlier than the Wordian, and more detailed research is necessary to determine a more precise age for this formation.

The Wargal Formation is composed primarily of limestone and has a distinct contact with the underlying Amb Formation. The lower part contains fusulines *Neoschwagerina* aff. *margaritae* and *Chusenella* sp., corals *Iranophyllum* sp. and *Wentzelella* sp. (Pakistan-Japanese Working Group, 1985), and the foraminifer *Baisalina pulchra* assemblage (Rahman et al., 2022). Therefore, it is clearly the Guadalupian, approximately equivalent to the Maokou Formation in South China. In the lower and middle parts of the Wargal Formation, there is a thin-bedded dolomite unit with abundant halite pseudomorphs and rare fossils, which may represent the response to the worldwide regression near the end of the Guadalupian. The upper part of the Wargal Formation is composed primarily of reddish limestone and contains numerous warm-water fossils including the fusuline *Nanlingella simplex* or *Codonofusiella schubertellinoides* zones, the coral *Waagenophyllum indicum* Zone, and numerous foraminifer *Colaniella minima* (Pakistan-Japanese Working Group, 1985; Rahman et al., 2022). Although the fusulines indicate the Wuchiapingian age, no conodont fossils have ever been recovered throughout our investigations.

The top of the Wargal Formation, which is characterized by rippled limestone known as the Kalabagh Member, yields abundant brachiopod fossils including *Oldhamina* and *Waagenoconcha*. Both the overlying Chhidru Formation and the uppermost Wargal Formation contain ammonoid *Cyclolobus*, indicating approximately the Wuchiapingian-Changhsingian boundary interval. The Chhidru Formation contains relatively few fossils in the upper part and is topped with the White Sandstone Unit containing numerous gastropods. Although no age indicative fossils have been found, the White Sandstone Unit represents deposits during the worldwide end-Permian regression, and similar deposits have been documented at the base of the *Waagenites* Unit at the Selong Xishan section in Tibet (Shen et al., 2006) and the *Clarkina yini* Zone in South China (Yin et al., 2014). Numerous investigations have been conducted on the Permian-

https://engine.scichina.com/doi/10.1007/s11430-023-1126-3

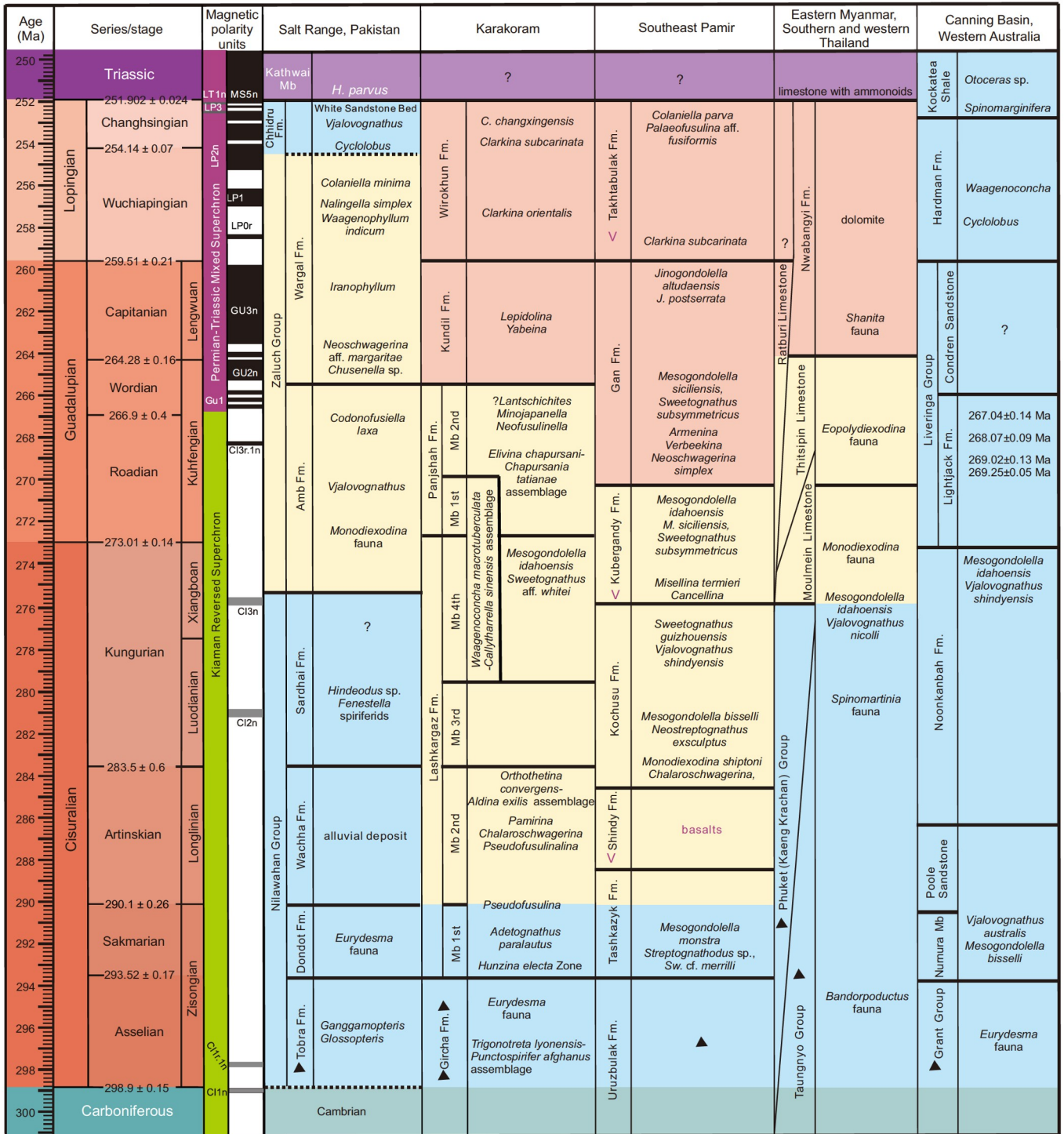


**Figure 7** Lithostratigraphy, biostratigraphy, and correlation of Permian System in the surrounding area of Qinghai-Tibetan Plateau. Background colors see explanation in Figure 2. The references are: Salt Range, Pakistan: Pakistan-Japanese Working Group (1985), Wardlaw and Pogue (1995), Wardlaw and Mei (1999), Shen et al. (2003e), Mertmann (2003), Ueno (2006), Ghazi et al. (2012, 2015), Ali et al. (2021), Rahman et al. (2022); Karakoram: Gaetani et al. (1995), Angiolini (1995), Angiolini et al. (2005); Southeast Pamir: Grunt and Dmitriev (1973), Grunt and Novikov (1994), Kozur (1994), Leven (1998), Angiolini et al. (2015), Chernykh et al. (2020); Eastern Myanmar, Southern and western Thailand: Brönnimann et al. (1978), Waterhouse (1981), Waterhouse (1982), Shi and Archbold (1995), Ueno (2003), Chaodumrong et al. (2007), Win et al. (2011), Yuan et al. (2020), Huang et al. (2020), Zhang Y C et al. (2020), Xu et al. (2021). Western Australia: Archbold (1999), Mory et al. (2008), Nicoll and Metcalfe (1998), Archbold (1999), Mory et al. (2008).

Triassic boundary in the Salt Range, Pakistan. On the basis of the FAD of *Hindeodus parvus* as well as the carbon isotope

chemostratigraphy, the Permian-Triassic boundary is within the dolomite (Kathwai Member) above the White Sandstone

Unit (Pakistan-Japanese Working Group, 1985; Schneebeli-Hermann et al., 2012, 2015; Figure 7).

### 3.2 North Karakoram, Pakistan

The North Karakoram region of Pakistan is closely related to the Qinghai-Tibetan Plateau, although it is still a subject of much controversy in terms of which particular block it connected to (Gaetani et al., 1995). The base unit of the Permian sequence in the Baroghil area is called the Gircha Formation and composed mainly of shale and sandstone with small pebbles. The middle and upper part of this formation contains typical Gondwanan cold-water brachiopod and bivalve fossils. Fossils found include *Eurydesma*, *Trigonotreta*, *Spirelytha*, and *Tomiopsis*, also known as the *Trigonotreta lyonensis-Punctospirifer afghanus* Assemblage (Angiolini, 1995; Angiolini et al., 2005). The Gircha Formation represents the cold-water deposits in the northern margin of the Gondwana during the early-middle Cisuralian, but lacks typical glacial characteristics. The Lashkargaz Formation lies above the Gircha Formation, and consists mostly of shale, sandstone, and limestone. It can be divided into four parts based on strata sequences. The first part contains abundant fossils characterized by the brachiopod *Hunzina electa* Zone. Typical Gondwana fossils (e.g., *Trigonotreta* and *Cimmeriella*) are also present. The conodont *Adetognathus paralautus* in this part also indicates an early Cisuralian age (Sakmarian). Fusuline fossils, mainly *Pseudofusulina*, begin to occur near the base of the second part, implying an age from the late Sakmarian to early Artinskian. The middle of the second part contains a second fusuline assemblage of the Artinskian age, including *Pamirina*, *Chalaroschwagerina*, and *Pseudofusulina*, etc. The top of the second part contains a third fusuline assemblage including *Darvasites* cf. *zulumartensis* and *Pseudofusulina krafftiformis*, which are associated with the brachiopod *Orthothetina convergens-Aldina exilis* Assemblage and *Retimarginifera praelecta* and *Magniplicatina* cf. *inassueta* as well as some other Gondwana type brachiopods. Thus, it is a transitional fauna with an obvious affinity to the Tethys warm-water fauna. The base of the fourth part is characterized by the brachiopod *Waagenoconcha macrotuberculata-Callytharrella sinensis* assemblage, in association with *Vediproductus* and *Enteletes* as well as abundant fusuline fossils including *Parafusulina yunnannica*, *Misellina parvicostata*, and *Pseudofusulina postkrafftiformis*. The third part is characterized by sandstone and no marine fossils have been reported so far. The top of the fourth part contains the conodont fossils *Mesogondolella idahoensis*, *M. phosphoriensis*, and *Sweetognathus* aff. *whitei*, etc. Although the taxonomy of these conodont fossils needs more detailed study, most species indicate that this part belongs to the Kungurian (Gaetani et al., 1995), but further study is ne-

cessary to confirm whether the top of the fourth part contains the Guadalupian strata. Similar succession also exists at the Chapursan Section, and the Lupghar Formation is equivalent to the Lashkargaz Formation in view of fully comparable fossil succession. Overlying the Lashkargaz Formation is the Panjshah Formation, which consists mainly of siliciclastic rocks intercalated with carbonate rock, and can be divided into two parts. In the lower part, the brachiopods still belong to the *Waagenoconcha macrotuberculata-Callytharrella sinensis* Assemblage whereas the brachiopod fossils in the upper part are known as the *Elivina chapursani-Chapursania tataniae* Assemblage, which contains a large number of Tethys warm-water fossils. In addition, fusulines such as *Lantschichites*, *Minojapanella*, and *Neofusulinella* were also associated with these warm-water brachiopods, and indicate a middle or late Guadalupian age. Above the Panjshah Formation is the thick dolomite unit named as the Ailak Formation. In the Chapursan to Shimshal region, the strata equivalent to the Ailak Formation are named the Kundil Formation, which is composed of thin-bedded limestone with pervasive chert bands/nodules. Fossils contained in this deep-water facies include fusulines *Lepidolina* and *Yabeina*. The upper part of the Kundil Formation preserves conodonts *Mesogondolella phosphoriensis*, *Sweetognathus hanzhongensis*, etc., possibly indicating a late Wordian or Capitanian age (Figure 7).

The Wirokhun Formation in the North Karakoram region of Pakistan is composed of shale and mudstone interbedded with limestone layers, and contains the conodonts *Clarkina orientalis*, *C. subcarinata*, and *C. changxingensis*. Therefore, it represents the Lopingian Series, including the deposits of both the Wuchiapingian and Changhsingian stages (Gaetani et al., 1995).

### 3.3 Southeast Pamir

Southeast Pamir, located north to the Karakoram Block, is separated from the latter by the Wakhan-Tirich fault zone (Angiolini et al., 2013). The faunas and sedimentary sequences in Southeast Pamir provide valuable clues in understanding the evolution of the Cimmerian microcontinents in the western part of the Qinghai-Tibetan Plateau, and yet little progress has been made in recent years as limited fieldwork was undertaken in this region out of security concerns. Southeast Pamir has long been a classical area for the establishment of the fusuline-based Permian biostratigraphic framework in the Tethys region (Leven, 2003, 2004; Angiolini et al., 2013, 2015). The Permian system consists of two different depositional sequences. One is represented by the Cisuralian Uruzbulak and Tashkazyk formations characterized by cold-water siliciclastic deposits (Grunt and Novikov, 1994), and the carbonate Kurteke formation of the upper Cisuralian to Lopingian. The other is represented by

slope to basinal facies, and consists of the Kochusu, Shindy, Kubergandy, Gan, and Takhtabulak formations in ascending order. These formations are composed primarily of bioclastic limestone, chert limestone, pyroclastic rock, basalt, sandstone, and conglomerate, and yield abundant fusulines, ammonoids, brachiopods, corals, and conodonts. These Permian strata are key sedimentary sequences for resolving the correlation between the Tethys and the international stratigraphic frameworks (Angiolini et al., 2015).

The Uruzbulak Formation consists of late Carboniferous black claystone, siltstone, and bioclastic limestone with a few cold-water brachiopods, belemnites, and ammonoids. The overlying Tashkazyk Formation consists of sandstone, siltstone, and black shale with a thickness of 200–295 m in the Kastenat Djilga area. This formation contains the ammonoids *Metapronorites* sp., *Marathonites* sp., *Emilites* sp., bivalves *Pseudomyalina* sp., *Megadesmus* sp., and abundant cold-water brachiopods including *Spirelytha*, *Tomioopsis*, and *Trigonotreta* (Grunt and Dmitriev, 1973). A recent study showed numerous conodont fossils at about 100 meters below the top of the Uruzbulak Formation, including *Mesogondolella monstra*, *Streptognathodus* sp., *Sweetognathus bucaramangus*, *S.* cf. *merrilli*, *S.* cf. *behnkeni*, and *S. whitei*. Among them, *Mesogondolella monstra* has been designated as the index species for the base of the Sakmarian stage (Chernykh et al., 2020). It is therefore suggested that the upper part of this formation belongs to lower Cisuralian, possibly Asselian to lower Sakmarian (Angiolini et al., 2015). The occurrence of *S. whitei*, an early form in North America (Lucas et al., 2022), further demonstrates that there are significant differences in depositional sequence and faunas between Southeast Pamir and Gondwana.

The Tashkazyk Formation is overlain by the Shindy and Kochusu formations. The former is composed mostly of basalt and the latter primarily of sandy limestone. These two formations represent either coeval deposits of different facies or superimposed relationship. Fossils contained within the Kochusu Formation include fusulines and two conodont faunas. Fusulines include *Monodioxodina shiptoni*, *Chalartoschwagerina*, *Darvasites*, and *Leeina*. The conodont fauna is represented by *Mesogondolella bisselli*, *M. shindyensis*, *Neostreptognathus exsculptus*, and transitional elements of *N. pequopensis* in the lower member; and *Pseudohindeodus nassichuki*, *Rabeignathus bucaramangus*, *Sweetognathus guizhouensis*, and *Vjalovognathus shindyensis* in the upper member of this formation (Kozur, 1994). The age of these faunas is the Bolorian, which approximately corresponds to the late Artinskian and early Kungurian (Angiolini et al., 2015; Gaetani and Leven, 2014). It is still unknown if the early Artinskian strata in this area are present or not. The Kubergandy Formation overlies the Kochusu Formation, and is named the Kubergandian Stage. The Kubergandy Formation contains the fusulines such as *Misellina termieri*,

*Neofusulinella* ex gr. *giraudi*, *Parafusulina* cf. *dzamantensis*, *Yangchienia* cf. *compressa*, and primitive species of *Cancellina*. Associated conodonts include *Mesogondolella idahoensis*, *M. lamberti*, *M. sicilensis*, *M. pingxiangensis*, *Pseudohindeodus ramovsi*, *Sweetognathus fengshanensis*, and *Sw. subsymmetricus*. There is disagreement with respect to the identification of these conodont fossils on species level, but the overall assemblage suggests a late Kungurian age, and the top part of the Kubergandy Formation may belong to the earliest Roadian. The Gan Formation lies above the Kubergandy Formation, which consists mostly of bioclastic limestone, siliceous rock, and shale, and contains multiple layers of volcanic ash. It is abundant in fusulines, foraminifers, and algae fossils. Fusulines in the Gan Formation include *Armenina*, *Presumatrina*, *Verbeekina*, and *Neoschwagerina simplex* in the middle part, ancestral *Yabeina* species in the upper part, and *Lantschichites*, *Neoschwagerina*, and *Yangchienia* in the gravels. Conodont fossils include *Mesogondolella pingxiangensis*, *M. sicilensis*, and the transitional elements of *Sweetognathus guizhouensis*-*S. subsymmetricus*. The topmost part of this formation also contains the Capitanian *Jinogondolella altdaensis* and *J. postserrata*. Thus, the Gan Formation may span from the upper Kungurian to the Capitanian Stage (Angiolini et al., 2015).

The Takhtabulak Formation, which lies above the Gan Formation, consists mostly of dark green volcanic breccia sandstone and hosts a great number of warm-water brachiopods (Grunt and Dmitriev, 1973). The base of this formation contains fusulines and foraminifers such as *Colaniella parva* and *Palaeofusulina* aff. *fusiformis* (Leven, 1998). Kozur (1994) reported the conodont *Clarkina subcarinata* in the upper part of this formation, suggesting that the Takhtabulak Formation may belong to the Changhsingian Stage or the undifferentiated Lopingian Series (Figure 7).

### 3.4 Eastern Myanmar and Western and Southern Thailand

The eastern Myanmar and the western and southern regions of Thailand have long been considered an integral Sibumasu Block (Metcalf, 2021). However, recent studies suggest that glacio-marine depositional sequence from the eastern and western region of the block shows a sharp difference, and two new terranes, the Irrawaddy Block (western part) and the Sibuma Block (eastern part) were introduced. According to Ridd (2016), the Irrawaddy Block encompasses the Phuket-Slate Belt of Myanmar and Thailand whereas Shan Plateau of Myanmar and the western region of Thailand are included in the Sibuma Block.

The Cisuralian in Phuket terrane of southern Thailand is referred to as the Phuket Group, and consists of a thick succession of glacio-marine deposits. Glacio-marine depos-

its in the lower part is characterized by pebbly mudstone and diamictites, with dropstone as well. Fossil are rare except for a few brachiopod fragments such as *Spinomartinia* sp., and *Costatumulus* sp. The upper part, approximately 200 m thick, consists of mudstone, thick-bedded sandstone, and shale. Brachiopods reported in this upper part include *Stereochia koyanensis*, *Spiriferellina modeta*, *Spinomartinia prolifera*, *Chonetinella andamanensis*, *Meekella bisculpta*, *Demonedys tricorporum*, *Costatumulus* sp., *Marginefera* sp., and *Cleiothyridina seriata*, and indicate an age ranging from the Sakmarian to Artinskian (Chaodumrong et al., 2007). The coeval Cisuralian in western part of Thailand is called the Kaeng Krachan Group, with deposits not showing typical glacio-marine features. This group is composed of mudstone, silty mudstone interbedded with occasional sandstone and diamictites. Fossils are abundant and represented by the typical cold-water *Bandoproductus* fauna (Waterhouse, 1982). Common taxa include *Spirelytha* and *Sulciplica*, and are assigned to the Asselian and Sakmarian ages. The upper part of the Kaeng Krachan Group is known as the Ko Yao Noi Formation, and contains the *Spinomartinia prolifera* fauna. Common species include *Retimarginifera alata*, *Stereochia koyaoensis*, *Vediproductus dissimilis*, *Urushtenia arguta*, and *Spiriferella modesta* (Waterhouse, 1981; Shi and Archbold, 1995). Equivalent strata in the Slate Belt of Myanmar are known as the Taungnyo Group, which contains a diverse *Spinomartinia prolifera* fauna at its top, and the late Kungurian conodonts *Mesogondolella idahoensis* and *Vjalovgnathus nicolli*. Hence, the age of this group seems substantially younger than previously recognized (Yuan et al., 2020; Xu et al., 2021).

The sedimentary succession above the Cisuralian siliciclastic rock in the Phuket-Slate Belt of Myanmar-Thai region is composed mainly of limestone. In the Phuket Belt of Thailand, this is represented by the Ratburi Limestone whereas in Myanmar, it is known as the Moulmein Limestone, which overlies the Taungnyo Group. The middle part of the Ratburi Limestone contains fusulines such as *Eopolydiexodina afghanensis*, *Rugososchwagerina* sp., *Chusenella* aff. *tumefacta*, and *Jinzhangia* whereas its upper part contains *Reichelina*, *Nanlingella*, and *Codonofusiella*. The age of this unit, based on these fossil occurrences, is assigned as the Guadalupian to Wuchiapingian (Ingavat and Douglass, 1981; Ingavat-Helmcke, 1993; Ueno, 2003).

The northeastern part of the Shan Plateau in Myanmar and western Thailand were included into the Sibuma Block (Ridd, 2016). The Permian strata in the northern Shan Plateau are typified by the Thitsipin Formation and Nwabangi Formation, but lack glacio-marine deposits (Oo et al., 2002). Diverse plant fossils including *Cordaites principalis*, *Annularia mucronate*, *Callipteridium* cf. *koraiense* were reported from the base of the Thitsipin Formation (Zhou et al., 2020). The Thitsipin Formation is also rich in fusulines, which

include *Eopolydiexodina*, *Jinzhangia*, *Rugososchwagerina*, and *Chusenella* (Huang et al., 2020; Zhang Y C et al., 2020). It is noteworthy that the Nwabangi Formation that overlies the Thitsipin Limestone in Myanmar is characterized by fragile, dark gray dolomites with rich *Shanita* but no other fossils. This well-known foraminifer was assigned to the late Guadalupian (Brönnimann et al., 1978; Win et al., 2011). However, this thick unit of dolomite is likely to contain the Lopingian strata. The field investigations in the Shan Plateau in eastern Myanmar show that the Lopingian sequence is characterized by a thick succession of dolomite or oolitic limestones, and is overlain conformably by the Lower Triassic gray-white limestone containing abundant ammonoids. However, further investigation is required to confirm the validity of this succession.

### 3.5 Western Australia

The Carboniferous-Permian sequence in Western Australia is distributed mainly in the Canning, Perth, Carnarvon, and Bonaparte basins. The lower part of the Pennsylvanian is absent, and glacial conglomerate deposits likely began to accumulate since the late Carboniferous. This is represented by the Nangetty Formation of the Perth Basin, the Lyons Group of the Carnarvon Basin, and the Grant Group and Paterson Formation of the Canning Basin. Fossils from these formations include typical cold-water faunas such as the widely distributed bivalve *Eurydesma* and the brachiopods *Lyonia*, *Tomiopsis*, and *Trigonotreta* (Archbold, 1999; Mory et al., 2008). Sandstone and coal sediment began to accumulate above the glacio-marine deposits in these basins, and are represented by the High Cliff Sandstone, Irwin River coal series, and Carynginia Formation in the north Perth Basin, the Callytharra Formation, Wooramel Group, Byro Group, and Kennedy Group in the Carnarvon Basin, the Poole Sandstone, Noonkanbah Formation, and Liveringa Group in the Canning Basin, and the Kulshill Group and Fossil Head Formation in the Bonaparte Basin. These strata contain typical Gondwanan cold-water faunas, including the brachiopods *Echinalosia*, *Fusispirifer*, and the conodont *Vjalovgnathodus* (Nicoll and Metcalfe, 1998; Archbold, 1999; Mory et al., 2008). The most useful fossils for age determination are the conodonts found in the Callytharra Formation, including *Vjalovgnathus australis*, *Mesogondolella bisselli*, and *Sweetognathus inornatus*, indicating an age from the Sakmarian to early Artinskian. The Coyrie Formation at the basal part of the Byro Group contains *Vjalovgnathus shindyensis*, which belongs to the Kungurian *Mesogondolella idahoensis-Vjalovgnathus shindyensis* Zone. The Wandagee and Coolkilya formations above contain advanced *Vjalovgnathus*, which is considered to be correlative with the *Jinogondolella nankingensis* zone (Nicoll and Metcalfe, 1998). The Noonkanbah Formation in the



Canning Basin contains the Artinskian-Kungurian conodonts *Vjalovognathus shindyensis* and *Mesogondolella idahoensis*. The Liveringa Group in the Canning Basin was previously assigned to the Lopingian. Recently, multiple high-precision ID-TIMS ages were obtained from the lower part of the Liveringa Group (the base of Lightjack Formation), with ages of  $267.04 \pm 0.14$  Ma,  $268.07 \pm 0.09$  Ma (Mory et al., 2017), and  $269.20 \pm 0.03$  Ma,  $269.02 \pm 0.13$  Ma, and  $269.25 \pm 0.05$  Ma (Laurie et al., 2016). Radiometric isotopic dating thus indicates a late Roadian age. The Hardman Formation consists primarily of sandstone and is rich in brachiopods represented mainly by cold-water elements (e.g., *Waagenoconcha*). Its age may be the Wuchapingian based on the occurrence of the ammonoid *Cyclolobus*. In the Bonaparte Basin, the equivalent unit is known as the Upper Marine Unit (Archbold, 1999). In the Perth Basin, the Changhsingian–Lower Triassic strata contain organic-rich source rocks called the Kockatea Shale. The top of the Changhsingian contains the brachiopod *Spinomarginifera*, and the base of the Triassic is composed mainly of mudstone interbedded with microbialites containing abundant bivalve *Claraia* and ammonoids including *Arctoceras* sp., *Proptychites* sp., *Prionites* sp., *Hemiprionites* sp., and *Anasibirites kingianus* (Skwarko and Kummel, 1972; Thomas et al., 2004; Shi et al., 2022). This assemblage suggests that the Tethyan fauna had invaded into Western Australia as a consequence of the end-Permian global climate warming (Figure 7).

#### 4. Implications of paleobiogeographical and paleogeographical evolutions

The Qinghai-Tibetan Plateau recorded the opening and closures of multiple oceans (including the Paleo-, Meoso- and Neo-Tethys Oceans) from late Paleozoic to Cenozoic. Evolutionary histories of these Tethys oceans, and plate subduction, collision, and accretions between European and Asian blocks thus become the frontier scientific issues among the global geoscientist community (Stampfli, 2000; Metcalfe, 2013; Keppie, 2015). The united supercontinent Pangea evolved to its maximum after collision between the Gondwana and Laurasia in the Early Carboniferous, making the Paleo-Tethys Ocean a semi-closed, east-opening ocean. Meanwhile, a series of continental blocks, including the Lhasa, South Qiangtang, Baoshan, Tengchong, Karakoram, Sibuma, and Irrawaddy blocks rifted off from the northern Gondwana and successively drifted northwards, forming the Cimmerian microcontinents (Şengör, 1979; Ridd, 2016). Recent studies suggest that the paleogeographic evolution of the Tethys oceans and various blocks assembling the Qinghai-Tibetan Plateau are much more complex than those of adjacent regions. On the one hand, the evolutionary history of the Tethyan oceans include the opening processes of

multiple paleo-oceans. On the other hand, the separating and rifting histories of these various blocks, and precise timing of opening and closure of Paleo-, Meso-, and Neo-Tethys Oceans remain highly controversial (Golonka and Ford, 2000; Stampfli, 2000; Muttoni et al., 2003; Metcalfe, 2013; Zhang et al., 2013a; Shen et al., 2013; Wang et al., 2021; Hu et al., 2022) (Figure 8).

It is well known that the current global biodiversity pattern shows remarkable latitudinal distributions (Mannion et al., 2014; Zhang and Torsvik, 2022). Notably, the temperature gradient is one of the most crucial factors shaping such latitudinal distribution of organisms. In general, low-latitude regions are characterized by more diverse biotas composed mainly of tropical and sub-tropical warm-water organisms. High-latitude and polar regions are dominated by cold-water organisms with a low biodiversity. A transitional zone between these two regions usually contains an admixture of faunas including both warm-water and cold-water organisms. With the strong influence of continental glaciers in the northern Gondwana superimposed with the pervasive latitudinal gradients in the Tethyan region, such phenomenon was extremely remarkable during the Permian (Shi et al., 1995; Shi and Grunt, 2000; Shen et al., 2013; Zhang et al., 2013a; Xu et al., 2022). Before rifting off from the northern Gondwana, the Cimmerian microcontinents was located in mid- to high-latitude regions, and contained typical cold-water fauna that can be correlated with those from Indian and Australian blocks. When the Cimmerian microcontinents started to break off from the northern Gondwana, and drifted northward to the low-latitude regions, its contained fauna then progressively transformed to those characterized by warm-water organisms correspondingly. In addition to temperature gradient that governs the latitude distribution of faunas, geographic isolation and current patterns are also responsible for the spatial distribution of marine organisms. In the case of the Lhasa and other Cimmerian microcontinents, all of them were separately situated in southern part of the Tethys Ocean, spreading in a northwest-southeast-trending along the margins of northern Indian and Australian Plate. As such, there was relatively less effect derived from geographic isolation on faunal compositions of these blocks. Meanwhile, these blocks were fundamentally influenced by an identical current pattern. The supercontinent Pangea united during the Carboniferous prevented a paleoequatorial ocean current from east to the west, which was divided into two currents flowing along the western side of the Tethyan Ocean. In the southern hemisphere, the diverted warm current flew approximately along the peri-Gondwana margin, and influenced faunal distributions in the southern part of the Neo-Tethys Ocean. Such effect has been manifested by the presence of mixed faunas along the northwestern part of the Indian Plate (e.g., the Salt Range region in Pakistan; and warm to mixed fauna in the Permian



**Figure 8** Paleogeographic reconstruction maps around the Tethys oceans during the Permian showing the paleogeographic evolution of various blocks in the Qinghai-Tibetan Plateau. Base map after [Wei et al. \(2022\)](#) and [Huang et al. \(2018\)](#). AF, central Afghanistan; BS, Baoshan Block; IC, Indochina Block; IR, Iranian Block; IW, Irrawaddy Block; KK, Karakoram Block; LS, Lhasa Block; NC, North China Block; NQ, North Qiangtang Block; SC, South China Block; SI, Sibuma Block; SP, Southeast Pamir; SQ, South Qiangtang Block; TC, Tengchong Block; HT, Himalaya Tethys Zone.

strata of Oman because these blocks were situated relatively in the northern part of Gondwana). To the southeast, the well developed mixed faunas from the exotic blocks and the Cimmerian continents clearly suggest that both Meso- and Neo-Tethys oceans had opened after the late Cisuralian. Otherwise, warm current could not go through between the Gondwana and the Cimmerian microcontinents. Over the past twenty years, paleontological and sedimentologic data have provided remarkable insights into paleobiogeographical and paleogeographical reconstructions of the Qinghai-Tibetan Plateau.

#### 4.1 The suture zone of the Paleo-Tethys Ocean

The Qinghai-Tibetan Plateau consists of a collage of blocks divided by major fault zones or suture zones. These suture zones, from south to north, include the Yarlung Zangbo, the Bangong-Nujiang, and Longmu Co-Shuanghu suture zones,

and have been regarded as representing closure of paleo-oceans ([Yin and Harrison, 2000](#); [Kapp et al., 2003](#); [Gehrels et al., 2011](#); [Pan et al., 2012](#); [Wu et al., 2020](#)). The Paleo-Tethys Ocean lies between the Eurasia and Gondwana continents. From a paleontological view, the most remarkable difference between these two continents lies in their obviously differential paleobiogeographic affinities, especially during the Asselian to Sakmarian (Early Permian). Continental glaciers were widespread in Gondwana during the early Cisuralian ([Fielding et al., 2008](#)). The wax of glaciation was displayed by glacio-marine deposits containing typical, Gondwana type cold-water faunas in the Himalaya Tethys Zone, Lhasa, South Qiangtang, Tengchong, and Baoshan blocks ([Liang et al., 1983](#); [Jin, 2002](#); [Zhang et al., 2013a](#); [Fielding et al., 2008](#); [Figure 9](#)). On the contrary, carbonates were the dominant sedimentary rocks (e.g., the Licha Formation and Changshehu Formation) accumulated in the North Qiangtang Block from the Late Carboniferous to Ci-



**Figure 9** Dropstone from the Permian strata indicating glacio-marine deposits in the Qinghai-Tibetan Plateau and its surrounding areas. Arrows in photos show the ice-rafted dropstone. (a) Glacio-marine conglomerate from the Tuotala section in the Duoma area in the South Qiangtang Block. (b) Dropstone from the Kongshuhe Formation of Cisuralian in Kongshuhe region of Tengchong Block (photo courtesy of Hao Huang). (c) Glacio-marine deposit from the PoindoPoindo Group in Wulong Village of Lhunzhub County, Lhasa Block. (d) Glacio-marine deposit from the Dingjiazhai Formation in Kongsongzhai in the Baoshan Block (photo courtesy of Xiangdong Wang). (e) Glacio-marine conglomerate from the Lower Permian Nilawahan Group in Salt Range of Pakistan. (f) Glacio-marine deposit from the Lower Permian Taungnyo Group at Mawachi section, Irrawaddy Block of Myanmar (photo courtesy of Kyi Pyar Aung). (g) Siltstone with dropstones, Kaeng Krachan Group in Khao Siin Village, southern part of Thailand Peninsula. (h) Glacio-marine conglomerate from the Cisuralian strata in the Canning Basin, Western Australia.

<https://engine.scichina.com/doi/10.1007/s11430-023-1126-3>

surian, where typical fusuline faunas (e.g., *Sphaerospiriferina*) are widespread in the Asselian or Sakmarina. As such, the faunal composition was remarkably different from those in the South Qiangtang and Lhasa blocks, both of which were parts of the northern Gondwana (Zhang et al., 2016a). In addition, *Gigantopteris* flora and fusuline fauna *Palaeofusulina* occurred in the Lopingian Raggyorcaka Formation in the Raggyorcaka area, the Nayixiong, and Lapuchari formations in the Tanggula area, and the Tuoba Formation in Qamdo County, suggesting a tropical paleobiogeographic affinity (Zhang et al., 2013a; Qiao et al., 2021). In view of the depositional sequence, the Permian strata in the North Qiangtang Block preserve alternated terrestrial-marine deposits with coal beds. Such sequences widely occur in the Tuoba, Nayixiong, Lapuchari, and Raggyorcaka formations and are very similar to the coeval depositional sequences in the Simao block, but are totally different from those of the South Qiangtang and Baoshan blocks (Qiao et al., 2021). Consequently, the stratigraphic sequences and faunas from both sides of the Longmu Co-Shuanghu suture zone are fundamentally different. Thus, the Longmu Co-Shuanghu suture zone represents the remnants of the Paleo-Tethys Ocean (Li et al., 1987, 1995; Zhang et al., 2013a, 2016a). Gehrels et al. (2011) suggested that the North and South Qiangtang blocks may have identical detrital source. However, it is worth noting that the sampling sites once considered within the North Qiangtang Block (e.g., the western part of Tuohepingcuo area, Gemuri area) in that paper were actually located at the accretion complex within the central uplifted belt. Only sampling localities in the northern part of Raggyorcaka area are representative of the North Qiangtang Block. Nevertheless, detrital zircon geochronology of the Permian and Triassic sandstones from these true North Qiangtang Block sites shows mid- to late Permian age peaks (Gehrels et al., 2011, Liu et al., 2022), and its pattern is remarkably different from that of the South Qiangtang Block.

Previous studies suggest that the Longmu Co-Shuanghu suture zone connects with the Changning-Menglian suture zone, with the latter representing its southeastern extension into Yunnan Province. The Changning-Menglian suture zone separates the Simao Block in the east from the Baoshan Block in the west. The seamount deposits reported from the suture zone were dominated by the Carboniferous to Permian carbonate deposits containing typical warm-water fusulines (Lan et al., 1983; Ueno et al., 2003). Such depositional sequence is in contrast to the Lower Permian glacio-marine deposits of the Dingjiazhai Formation. Faunas within these seamount deposits also differ remarkably from those occurred in the Guadalupian Shazipo Formation, which contains an admixture of fauna representative of the Cimmerian microcontinents. However, some studies also suggested that the sediments accumulated within the Changning-Menglian

suture zone represent deposition in a passive continental margin of the eastern Baoshan Block, and the seamount-type limestone and ophiolites in this suture probably represent exotic nappes from the east, and the real Paleo-Tethys suture is the Lancangjiang suture zone in the east (Ridd, 2015; Zheng et al., 2021). Glacio-marine deposits also occur in the Sibuma Block positioned in western side of the Chiang Mai-Inthanon and Bentong-Raub suture zones in Southeast Asia (Baioumy et al., 2020). By contrast, in the eastern side of these sutures, such as Sukhothai island arc and Indochina Block, the fossils were obviously of the low-latitude warm-water faunas (Metcalf, 2021).

As a result of the right-lateral strike-slip of the Karakoram Fault zone, the western extension of the Longmu Co-Shuanghu suture zone is difficult to discern. Paleobiogeography provides clues on the extension trajectory of this suture in the western part of the Karakoram fault zone (e.g., the Pamir Plateau). First, the small foraminifer *Shanita* was reported from the Central Pamir Block (Leven, 1991), which suggests an obviously Cimmerian paleobiogeographical affinity for this block. The North Pamir Darvaz region, however, contains abundant fusuline faunas from the Cisuralian to Guadalupian, suggesting a low-latitude paleobiogeographic characteristic (Leven, 1967; Leven et al., 1992). As such, the Tanyamas suture zone between the North and Central-Pamir most likely represents the remnants of Paleo-Tethys Ocean as well, and is equivalent to the Longmu Co-Shuanghu suture zone. Notably, the alternated terrestrial-marine deposits that were widely distributed in the North Qiangtang and Simao blocks have never been reported from the North Pamir region (Leven, 1967). Hence, the North Qiangtang and Simao blocks may connect with the Indochina Block instead of the Northern Pamir Block in the west (Qiao et al., 2021).

To sum up, the Longmu Co-Shuanghu suture zone in the northern part of Tibet may connect with other sutures. Its southeast extension is represented by the Changning-Menglian suture/Lancangjiang suture of Yunnan and the Chiang Mai-Inthanon and Bentong-Raub suture zones of Southeast Asia; whereas its west extension is represented by the Tanyamas suture of Pamir region. All these sutures most likely represent the remnants of the Paleo-Tethys Ocean that separates Eurasia from the Gondwana continent, corresponding to some key boundaries of paleobiogeography (Figure 8).

#### 4.2 The opening timing of the Meso-Tethys Ocean (Bangong-Nujiang Ocean)

The timing when the South Qiangtang Block rifted off from the northern Gondwana delineates the opening time of the Meso-Tethys Ocean. In the early Cisuralian, glacio-marine conglomerates occurred in several blocks such as the South Qiangtang, Lhasa, Baoshan, Tengchong, and Himalaya Te-

thys Zone (Figure 9). Similar glacio-marine deposits of the early Cisuralian age (Asselian to Sakmarian) were also reported from the Karakoram of Pakistan, the Southeast Pamir, and the Sibuma blocks. Furthermore, fossils from these marine glacial deposits were represented collectively by the bivalve *Eurydesma* and the brachiopods *Bandoproductus*, *Spirelytha*, *Puncocyrte*, and *Trigonotreta*, which are the typical cold-water elements that can be well correlated with those from Gondwana. Accordingly, it is inferred that all these above-mentioned blocks were situated in the northern Gondwanan margin, and accumulated deposits under the direct influence of the Late Paleozoic Ice Age (Wang et al., 2021). It clearly indicates that there was no such an ocean as the Meso-Tethys Ocean developed during the early Cisuralian (Figure 8a).

Widespread carbonate deposits with abundant fusulines and compound corals started to accumulate in the South Qiangtang, Baoshan, and Sibuma blocks from the Artinskian (middle Cisuralian) (Ingavat and Douglass, 1981; Shi et al., 2011; Zhang et al., 2013b). Meanwhile, warm-water conodont species such as *Sweetognathus* were also documented from the same interval in the Qiangtang and Baoshan blocks (Ueno et al., 2002; Ji et al., 2006). The fossil evidence suggests that there was a rapid paleoclimate warming in these three blocks after the LPIA (Figure 1). In contrast, there was only a change in lithology in the Lhasa Block in the Artinskian, with no records of warm-water faunas. Such characteristics suggest that warming climate may have not influenced the Lhasa Block yet during the Artinskian (Figure 8B).

Warm-water organisms such as the fusulines *Cancellina*, *Neoschwagerina* and the brachiopod *Vediproductus* occurred commonly in the basal part of the Lugu Formation at multiple sections from western to central regions of the South Qiangtang Block (Zhang et al., 2012, 2014a; Shen et al., 2016; Yuan et al., 2022). Meanwhile, the Kungurian fusulines were found widely in Peninsula Thailand of the Sibuma block (Ueno et al., 2015). On the contrary, fossils from the Angie and basal part of the Xiala formations are still characterized by abundant cold-water brachiopods, non-dissepimented solitary corals, and admixture of conodont faunas but with no fusulines (Zhan and Wu, 1982; Wang et al., 2003; Yuan et al., 2016). Similarly, in the western part of the Shan Plateau, the Kungurian strata in the Irrawaddy block also contain the brachiopod *Spinomartinia* fauna and the conodont *Vjalovognathus*, suggesting similar paleobiogeographic affinities with the Lhasa Block (Yuan et al., 2020; Xu et al., 2021). Paleobiogeographic analyses on more than ten Kungurian-Roadian brachiopod faunas from the northern Gondwana suggested that the South Qiangtang, Baoshan, and Sibuma blocks may have drifted to a paleolatitude of 30° in southern hemisphere. This is because warm-water faunas from these blocks have strong affinities with those from the

Cathaysian region. Paleomagnetic evidence documented from the Guadalupian deposits in the South Qiangtang Block also supports such drifting processes (Wei et al., 2022). On the other hand, the Gondwana-type, cold-water species (e.g., *Retimarginifera*, *Spirelytha*, *Trigonotreta*) and the Cimmerian endemic species (e.g., *Comuquia*, *Chonetinella*) were documented from the Lhasa, Tengchong, and Irrawaddy blocks of Myanmar in the Kungurian-Roadian interval (Xu et al., 2021). A mixed conodont fauna including *Vjalovognathus* and *Mesogondolella* were also characteristic for those blocks (Yuan et al., 2016, 2020). Thus, the Lhasa, Tengchong, and the Irrawaddy blocks of Myanmar were likely situated in the relatively high latitudinal regions in the southern hemisphere during the Kungurian. The evidence mentioned above suggests an allometric northward drifting of these peri-Gondwana microcontinents. An ocean, namely the Meso-Tethys Ocean (Bangong-Nujiang Ocean) may have been developed between the two slices of blocks (i.e., South Qiangtang, Baoshan, Sibuma blocks of the northern slice, and Lhasa, Tengchong, and Irrawaddy blocks of the southern slice) (Xu et al., 2022; see also Figures 2–5; 8b).

Therefore, different paleobiogeographic affinities between the South Qiangtang and Lhasa blocks started to appear from the Artinskian. This means that the Cimmerian microcontinents may have rifted off from the Gondwana since the mid-Cisuralian (Sakmarian-Artinskian). The difference in faunal composition between the South Qiangtang and Lhasa blocks in the Kungurian suggested there were obvious different paleolatitude settings between them. Such latitudinal discrepancy may represent the width of the Bangong-Nujiang Ocean. This recognition has been supported by paleomagnetic studies as well (Cheng et al., 2015; Zhou et al., 2016; Wei et al., 2022). As such, the opening of the Bangong-Nujiang ocean started from the Artinskian, which is closely linked with the drifting of the South Qiangtang, Baoshan, and Sibuma blocks off the northern Gondwana. Widespread basalt eruptions in the northern part of India, Himalaya Tethys Zone, South Qiangtang, and Baoshan blocks may have resulted in the rifting of a passive continental margin (Garzanti et al., 1999; Shellnutt et al., 2014; Liao et al., 2015; Dan et al., 2021). The rifting of the South Qiangtang Block also changed its detrital province, with detrital zircons coming from the South Qiangtang Block instead of the Gondwana continent (Fan et al., 2021; Figure 8).

The timing of appearance of warm-water faunas in various blocks may indicate that the blocks in the western part of the Tethys Ocean that drifted northward together with the South Qiangtang block may also include Central-Iran, Pakistan-Karakoram, and possibly Southeast Pamir and Central Pamir (Gaetani et al., 1995; Angiolini et al., 2015).

It is also to be noted that ophiolites were widespread along the Bangong-Nujiang suture zone (e.g., Qu et al., 2010; Zhong et al., 2017). Ophiolites along the southwestern part

of Yunnan Province, however, remains to be investigated. Liu et al. (2016) asserted that the Myitkyina ophiolite zones possibly represent the southern extension of the Bangong-Nujiang suture zone. Nevertheless, the Gualalupian fusuline faunas from Shan Plateau are close in composition to those from the Baoshan Block, implying the Gaoligongshan shear zone and its southward extension in Myanmar most likely represent the southern extension of the Bangong-Nujiang suture zone (Zhang Y C et al., 2020). Recent geophysical studies contended that an east-west subduction zone may exist in the western bounded area of Shan Plateau in Mandalay (Yang et al., 2022). Although it was interpreted as representing the northward subduction of the Neo-Tethys Ocean, its geographic location corresponds exactly to the diving boundary between the Irrawaddy and Sibuma blocks (Ridd, 2016; Xu et al., 2021). Hence, the possibility that this afore-mentioned subduction zone may otherwise represent the subduction of the Meso-Tethys Ocean cannot be excluded.

### 4.3 Opening time of the Neo-Tethys Ocean

The timing from which the Lhasa Block rifted off from the northern Gondwana indicates the opening of another ocean, the Neo-Tethys Ocean. One viewpoint suggests that the Lhasa Block drifted northward from the Gondwana during the Cisuralian (Shen et al., 2003b, 2013; Li and Shen, 2005; Zhang et al., 2013a; Xu et al., 2022). On the contrary, another point of view suggested that the Lhasa Block did not start to rift off from the north Gondwana until the Late Triassic (Muttoni et al., 2009; Metcalfe, 2013; Zhu et al., 2013; Jin et al., 2015; Meng et al., 2021).

Several lines of evidence from the Permian stratigraphic and paleobiogeographic records in the Lhasa Block argue against the view that it had a later drifting history (i.e., since the Late Triassic) off the northern Gondwana (Figures 2–5, 8). First, the fossil records of entire Permian in areas such as the Salt Range of Pakistan in the northern Indian Plate, Himalaya Tethys Zone of southern Tibet, and northwestern part of Australia were all dominated by the assemblages of cold-water brachiopod faunas, solitary corals, and cold-water conodonts (Waterhouse, 1978; Archbold, 1999; Shen et al., 2000b, 2003a; Xu et al., 2018; Wang et al., 2021). Although there were a few fusulines reported in the north Gondwanan region (e.g., Wargal and Chhidru formations of Salt Range; the Maubisse Group of Timor Island, northern Australia), the diversity is very low and the fusuline fauna overall shows a Gondwanan cold-water affinity (Pakistan-Japanese Working Group, 1985; Rahman et al., 2022; Haig et al., 2017). In addition, the Changhsingian Chhidru Formation in the Salt Range of Pakistan still contained abundant cold-water brachiopods and conodonts. On the contrary, carbonate deposits began to accumulate predominantly in the Lhasa Block from

late Kungurian, and contained a few warm-water conodonts such as *Mesogondolella* (Figures 3–5). Although there was still obvious difference in fauna compositions between Lhasa and South Qiangtang blocks during this time, the presence of sporadic warm-water faunas in the Lhasa Block implies that there was a gradual transformation of faunal composition toward warm-water types since the late Kungurian. In the Gualalupian, however, the fossil assemblages composed of diversified fusulines, small foraminifera, compound corals, and warm-water brachiopods occurred commonly in multiple regions of eastern and western part of Lhasa Block (Yuan et al., 2014; Zhang et al., 2010, 2016b, 2019a; Ju et al., 2021). As such, there were remarkable differences in faunal composition between Lhasa and Western Australia after the late Kungurian. In addition, the Wuchiapingian conodont *Clarkina-Iranognathus* Assemblage and the brachiopod faunas in the Lhasa Block are extremely similar to those in South China and Tengchong blocks (Yuan et al., 2014; Xu et al., 2019). Thus, there is a fundamental difference in faunal composition between Lhasa and the Salt Range of Pakistan, the basins in Western Australia, and the Himalaya Tethys Zone (Shen et al., 2000b; Ke et al., 2016). Secondly, the northern part of Western Australia, from north to south, contained the Timor Island, Canning Basin, south Carnarvon Basin and Perth Basin, representing an interior rift straddling from 35° to 55° of southern latitude (Haig et al., 2017). If the Lhasa Block remains connected with Western Australia (e.g., Meng et al., 2021; Metcalfe, 2021), similar depositional sequences and faunas would have been developed between the two before the Late Triassic. However, the Lhasa Block is a relatively stable terrane in terms of Permian stratigraphy (Zhang et al., 2013a, 2019b; Ju et al., 2022b). The Cisuralian Angie and Wululong formations are all characterized by mudstone and shales alternated with bryozoan limestone. From the Roadian, the Xiala and Luobadui formations are dominated by bioclastic limestone. Such depositional sequence can be correlated between different parts within the Lhasa Block, but is very different from that in Western Australia. Thirdly, the exotic limestone blocks within the Yarlung Zangbo suture zone also provides strong evidence indicating the primitive rifting of the Neo-Tethys. Some studies suggest that depositional processes of the exotic limestone were often influenced by input of terrigenous clasts (Jin et al., 2015). These authors thus suggested that these exotic limestone blocks were originally deposited in the peri-Gondwanan environment such as the Lhasa Block (Jin et al., 2015). However, depositional sequence combined with paleobiogeographic evidence derived from these exotic limestone blocks implies that they are more likely representing seamount deposit in the Neo-Tethys Ocean (Zhang and Wang, 2019; Fan et al., 2023). For instance, both the Lasaila and Gyanyima limestones contain abundant warm-water faunas. Specifically, the Lasaila limestone

contains the Guadalupian fusulines such as *Neoschwagerina*, *Verbeekina*, *Kahlerina*, *Yangchienia*, and *Verbeekina* (Wang et al., 1981). The Xilanta Formation in the Gyanyima limestone block contains the fusulines *Neoschwagerina*, *Chusenella*, and *Veeberkina*, etc. (Zhang et al., 2009). The Lopingian limestones (e.g., the Goqoi limestone, Gyanyima limestone) also contain abundant fossils consisting of warm-water brachiopods and foraminifers (Wang et al., 1981; Wang et al., 2010; Shen et al., 2010). Obviously, the Lopingian warm-water faunas within these exotic limestone blocks are very different from those in Himalaya Tethys Zone and the Salt Range, Pakistan. In addition, those exotic limestone blocks were embedded in the Yarlung Zangbo suture zone mélange (Cai et al., 2012), and often contain mafic volcanic rocks (Wang et al., 1988; Shen et al., 2003d, 2010; Fan et al., 2023). As such, the exotic limestone blocks are most likely formed in a seamount depositional setting (Zhang and Wang, 2019), suggesting that the Neo-Tethys Ocean had opened before the Guadalupian (Figure 8). Lastly, recent studies have found that a typical small foraminifer assemblage *Shanita-Hemigordiopsis* is commonly present in the Lhasa, Tengchong, Baoshan, South Qiangtang, Central Pamir and South Afghanistan blocks. Its distribution in these blocks implies a direct control from current patterns. Obviously, the ocean currents across the Neo-Tethys Ocean may have controlled the distribution of this small foraminifer assemblage (Ju et al., 2021).

In summary, the Permian depositional sequences and paleobiogeographic evolution of the Lhasa Block are remarkably different from those in the northern Gondwana (e.g., Himalaya Tethys Zone, Western Australia). Furthermore, the presence of Guadalupian to Lopingian seamount deposits as well as the evidence from ocean current pattern implies that the Neo-Tethys Ocean had opened at no later than the Kungurian (Cisuralian). Except for the evidence mentioned above, the Middle Triassic (Anisian) radiolarians including *Triassistephanidium laticorne*, *Eptingium manfredi*, *Triassocampe deweveri*, and *Pseudostylosphaera coccostyla* have recently been reported from the Yarlung Zangbo suture zone, suggesting that deep marine deposits have been accumulated in the Neo-Tethys Ocean (Chen et al., 2019). Furthermore, the Late Triassic granites were frequently reported from the Gangdese batholith (e.g., Ji et al., 2009; Meng et al., 2018). Their occurrences are most likely from the subduction within the Neo-Tethys Ocean.

It is particularly notable that the Salt Range in Pakistan, as a part of the Indian Plate, should have contained cold-water faunas during the entire Permian. Yet compound corals such as *Waagenophyllum*, *Iranophyllum*, and a few fusulines including *Neoschwagerina*, *Chusenella*, and *Nanlingella* occurred in the Wargal Formation in the Salt Range, all representing warm-water species. Presence of warm-water species in the Salt Range does not mean it once rifted off the

northern Gondwana together with the Cimmerian microcontinents, but rather because the Indian Plate spread northwest-southeastly, resulted in the western parts (such as Salt Range) being at relatively lower paleolatitude regions. This is why the Guadalupian and Lopingian strata contained warm-water faunas in the Salt Range, Pakistan. Similar paleontological features have also been reported from Iran and Oman (Viaretti et al., 2021, 2022). From a paleobiogeographic view of point, warm-water species contained in these areas were essentially different from those in the Cimmerian microcontinents, reflecting the complex paleogeographic framework of the northern Gondwana (Figure 7).

Additionally, it has been suggested that there was another ocean (Sumdo Ocean) between central and south Lhasa regions, as indicated by the discovery of the Guadalupian eclogites (Yang et al., 2009; Cheng et al., 2012). Sumdo Ocean was suggested to represent the southern branch of the Paleo-Tethys Ocean (Wang et al., 2022). The evolution of this ocean has been debated hotly, which focuses mainly on the timing of subduction (early versus late Permian), and the closure time (middle Permian versus Late Triassic) (Cheng et al., 2012; Xie et al., 2021; Wang et al., 2022). Stratigraphic and paleontological evidence discussed above provides an insight into the evolution of the Sumdo Ocean. First, marine glacio-marine deposits were predominantly preserved in the Lagar Formation and Poindo Group in Central Lhasa Block, suggesting the influence of northern Gondwana glaciers. In other words, the Sumdo Ocean might not exist. Secondly, the commonly occurred Guadalupian to Lopingian carbonate deposits with warm-water faunas in the central Lhasa Block, as well as the Neo-Tethys Ocean current patterns and the discovery of Middle Triassic radiolarians, all imply that the southern Lhasa Block had drifted away from the northern Gondwana before the Guadalupian. Hence, even if the Sumdo Ocean existed, it may only represent a small, limited ocean basin.

## 5. Paleoclimate change and major biotic events

The Carboniferous to Permian is a critical time interval as it archives a momentous paleoclimatic change from a global icehouse towards a greenhouse climate. Collision between Gondwana and Laurasia continents in the Early Carboniferous resulted in the closure of the Rheic seaway, forming the united supercontinent, Pangea. This supercontinent blocked the east-west paleoequatorial currents, and formed a semi-closed Tethys warm pool that opened to the east only. Such warm pool became a center for energy cycling between Earth's interior and surface and biodiversity, and had a crucial impact on global environments. This is somewhat comparable to the modern Western Pacific and Indo-Pacific warm pools (Zhang and Torsvik, 2022). The

biodiversity and paleoenvironmental changes in the Tethys warm pool provide informative clues for understanding the status of our modern ecosystem and global changes. The various blocks assembling the Qinghai-Tibetan Plateau were in middle to high latitude regions in the southern hemisphere during the Cisuralian, and were sensitive to the changes in paleoclimates and latitudinal temperature gradients. These blocks thus preserved important records of a series of significant biotic/paleoclimatic events that occurred during the Permian.

### 5.1 Records of the Late Paleozoic Ice Age in the Qinghai-Tibetan Plateau and adjacent areas

The Late Paleozoic Ice Age began from the Late Carboniferous and reached to its maximum in the Cisuralian (Sakmarian). Its records were fully preserved in the Qinghai-Tibetan Plateau. For instance, the Asselian to Sakmarian (early Cisuralian) strata in several blocks (e.g., South Qiangtang, Baoshan, Tengchong, Karakoram, Sibuma and Irrawaddy) consist of glacio-marine deposits with dropstones (Figure 9). Fossils consist correspondingly of cold-water fauna represented by the bivalve *Eurydesma* and the brachiopod *Bandoproductus* (Figure 4).

Glacio-marine diamictites have been reported from several blocks of the Qinghai-Tibetan Plateau, which include the Jilong Formation of Himalaya Tethys Zone (Yin and Guo, 1976), the Lagar Formation and Poindo Group in the Lhasa Block (Ji et al., 2005; Zhang et al., 2013a, 2013c), and the Cameng and Zhanjin formations in the South Qiangtang Block (Liang et al., 1983; Li et al., 2016).

In western Yunnan Province, marine glacial deposits have been documented from the Dingjiazhai and Kongshuhe formations in the Baoshan and Tengchong blocks respectively (Jin, 2002). Typical glacio-marine deposits have also been reported from the Irrawaddy block (e.g., the Mergui group in western part of the Shan Plateau, the Kaeng Krachan Formation in western Thailand, and the Bohorok Formation in the northeast part of Sumatra (Mitchell, 1992; Ridd, 2016). Similarly, glacio-marine deposits were also found in the Bonaparte, Canning, Carnarvon and Perth basins of Western Australia (Mory et al., 2008; Figure 9).

Glacio-marine deposits were also ubiquitously exposed in the western part of Qinghai-Tibetan Plateau, including the Tobra Formation in the Salt Range of Pakistan (Ghazi et al., 2012, 2015), agglomerated slates in Kashmir of India (Gupta, 1975), the Al Khilata Formation in Oman (Angiolini et al., 1997). Besides, the Gircha Formation characterized by pebbly sandstone and shale in the Karakoram Range may also represent glacio-marine deposits (Angiolini, 1995).

Thus, the Cisuralian glacio-marine deposits were widespread in the north peri-Gondwanan region (Oman, Himalaya Tethys zone, and Western Australia) and Cimmerian

microcontinents (South Qiangtang, Lhasa, Baoshan, Tengchong, Sibuma and Irrawaddy blocks). With the strong influence of glaciation, marine organisms from these blocks were dominated by cold-water brachiopods or bivalves during the early Cisuralian (Liang et al., 1983; Shen et al., 2000a; Zhan et al., 2007).

Notably, distribution of glacio-marine deposits may also be controlled by paleotopography (Isbell et al., 2012). This may explain the absence of such deposits in the Lagar Formation in the western Lhasa Block, the Cisuralian Uruzbulak and Tashkazyk formations in the South Pamir Block (Angiolini et al., 2015). Nonetheless, fossils from these blocks were still characterized by cold-water faunas, showing direct influence under cold climate that dominated the northern Gondwanan region (Grunt and Dmitriev, 1973).

### 5.2 Records of the Artinskian warming event in the Qinghai-Tibetan Plateau and adjacent areas

One of the most prominent climate changes in the Cisuralian was the transition from the Late Paleozoic Ice Age (LPIA) to a greenhouse climate. This climate change, known as the Artinskian Warming Event (AWE) (Marchetti et al., 2022; Hou et al., 2023), likely occurred during the Artinskian and lasted into the Kungurian, during which a persistent greenhouse climate prevailed. The occurrence of abundant carbonate rocks and warm-water biota in the South Qiangtang, Baoshan, and Sibuma blocks during the Artinskian was often interpreted as a consequence of such warming event (Figure 10). Although AWE cannot explain the delayed occurrence of warm-water faunas in the Lhasa and Tengchong blocks, the development of carbonate rocks and warm-water faunas in the northern Cimmerian microcontinent during the Artinskian was probably driven by the northward drift of these peri-Gondwana blocks superimposed by a gradual global warming in the wake of AWE. As the most comparable climatic warming event with our present global warming, the AWE has provided an important analog for evaluating potential consequences led by present climate warming. All the blocks assembling the Qinghai-Tibetan Plateau were located at the middle to high latitude regions during the Cisuralian. Therefore, these blocks were sensitive to climate changes and preserved reliable records of this climate warming event. The AWE in the Qinghai-Tibetan Plateau is demonstrated mainly by the replacement of diamictites by thick carbonate rocks during the middle-late Cisuralian in the South Qiangtang, Baoshan, and Tengchong blocks (Figure 10). Associated with such change in lithologies are the profound changes of biotas. For example, the fusulines *Pamirina*, *Eoparafusulina*, and *Pseudofusulina*, etc., occurred in strata above the diamictites in the South Qiangtang Block (Nie and Song, 1983b; Zhang et al., 2013b). Fusulines and conodonts also appeared in the top part of the Dingjiazhai Formation in





**Figure 10** Carbonate deposits from the Qinghai-Tibetan Plateau and adjacent areas indicating the transition from the icehouse state to the greenhouse state during the Cisuralian. (a) Carbonate rocks in the Tunlonggongba Formation from the South Qiangtang Block after the LPIA. (b) Carbonate rocks of the basal Angie Formation overlying the Lagar Formation in the Xainza area of the Lhasa Block. (c) Carbonate rocks of the Urulung Formation overlying the Poindo Group from the Lhunzhub area of the Lhasa Block. (d) Limestones from the top of the Dingjiazhai Formation at the Woniusi section in the Baoshan Block.

the Baoshan Block (Ueno et al., 2002; Ueno, 2003; Shi et al., 2011). Similarly, warm-water biota was reported from the second member of the Lashkargaz Formation in the Karakoram area (Gaetani et al., 1995). Moreover, abundant fusulines were found in the Cisuralian limestone blocks from southern Thailand and Malay Peninsula (Ingavat and Douglas, 1981).

Massive volcanism during the Artinskian has been proposed as one of the major drivers of the AWE (Hou et al., 2023). These volcanic activities were represented by the Panjal Traps in northern India (Shellnutt et al., 2014; Chen et al., 2023), the Wuoniusi basalt in the Baoshan Block (Liao et al., 2015), the Tarim LIP (Zhong et al., 2022), the Zado LIP in the North Qiangtang Block (Zhang and Torsvik, 2022). Eruptions of these Artinskian LIPs can release tremendous greenhouse gases leading to drastic transition from the icehouse state to greenhouse conditions (Hou et al., 2023). However, the detailed process and effects of LIP need to be further investigated (Figure 11).

### 5.3 Climate warming in the latest Permian recorded in the Qinghai-Tibetan Plateau

The end-Permian mass extinction (EPME) was the most severe catastrophic biological event in the geological history. Intensive volcanic activities (e.g., The Siberian Traps) during

the Permian-Triassic transition have released vast amounts of greenhouse gases, and led to a series of lethally climatic and environmental deteriorations such as a rapid increase of temperatures ( $\sim 8\text{--}10^\circ\text{C}$ ), ocean anoxia and acidifications. These extreme environmental events have been recognized as the most probable explanations for the EPME (Joachimski et al., 2012; Chen et al., 2016, 2020; Shen et al., 2019; Zhang F F et al., 2020). However, growing evidence suggests that volcanisms in and around the Tethys Ocean may have also played a pivotal role in leading to the EPME (Zhang et al., 2021). Temperature changes inevitably led to latitudinal shifts of marine faunal communities. When temperature rises, warm-water organisms in the fauna at low latitude regions tend to migrate towards bipolar regions; contrariwise, when temperature falls, organisms living in cold-water fauna of high latitude regions move towards equatorial areas (Shi and Grunt, 2000; Sun et al., 2012; Bernardi et al., 2018). The rapid global warming in the latest Permian has been well recorded by faunal changes in a series of blocks of the Qinghai-Tibetan Plateau (Shen et al., 2006; Figure 12). For instance, abundant conodonts and small warm-water brachiopod species suddenly began to appear in the *Waagenites* Bed at the Selong Xishan section and the basal part of the Kangshare Formation at the Tulong section; whereas fauna in the top part of the underlying Selong Group was still characterized by typical cold-water brachiopods (Shen and

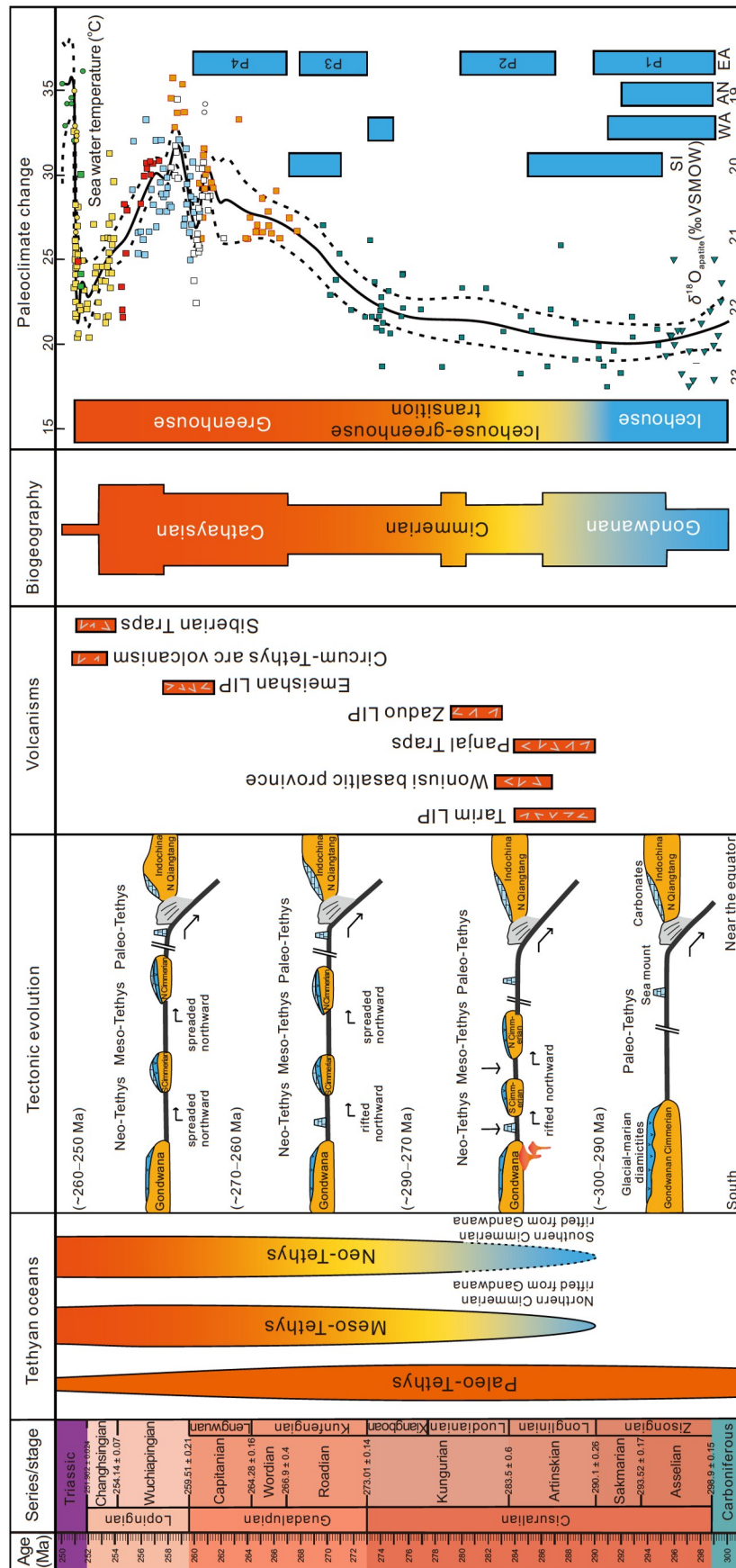


**Figure 11** Correlation of key evolution stages of tectonic paleogeography, paleoclimate, and major volcanic activities during the Permian. The conodont  $\delta^{18}O_{\text{apatite}}$  curve is from Chen et al. (2013).



**Figure 12** Records of rapid global warming and transgression in the latest Permian in the Qinghai-Tibetan Plateau. (a) Selong Xishan section from Nyalam County, Tibet; (b) Qubu section in the Mt. Qomolangma area, Tingri County, Tibet; (c) Tangla section from Tingri County, Tibet (photo courtesy of Hugo Bucher); (d) Nammal Road section in the Salt Range, Pakistan; (e) the Wenbudangsang section from Geji County, Tibet; (f) the Permian-Triassic boundary section in the Gyanyima exotic limestone from Pulan County, Tibet.

Jin, 1999; Shen et al., 2000b, 2001a; Xu et al., 2018). Such southward expanding event of warm-water faunas has also typified the Permian-Triassic boundary (PTB) sections in the Salt Range, Pakistan. The White Sandstone Unit at the top of the Changhsingian Chhidru Formation contains large proportions of cold-water brachiopods and cool-water conodonts such as *Vjalovognathus* and *Merrillina* (Pakistan-Japanese

Working Group, 1985; Wardlaw and Mei, 1999) whereas the base of the overlying Mianwali Formation is characterized by abundant cosmopolitan conodonts and bivalves akin to the Tethys warm-water faunas. Similarly, a remarkable change in faunal composition has also been documented across the PTB in Kashmir. The top of the Permian Zewan Formation still contains a large number of Gondwana-type

brachiopods and lacks conodont fossils, but the basal part of the overlying Lower Triassic Khunamuh Formation is characterized by containing abundant conodonts (Nakazawa et al., 1975; Lyu et al., 2021; Brookfield et al., 2022). In the Perth Basin of Western Australia, the lower Changhsingian contains Gondwanan cold-water brachiopods such as *Auritusinia*, “*Cimmeriella*”, and *Etherilosia*, with warm-water brachiopods (e.g., *Spinomarginifera*) emerging at the top of the Permian strata (Thomas et al., 2004; Shi et al., 2022). In the Gyanyima exotic limestone within the Yarlung Zangbo suture zone, the Changhsingian Gyanyima Formation contains a highly diverse Lopingian fauna dominated by foraminifera, admixture of cold- and warm-water brachiopods, compound corals, and fewer conodonts. By contrast, in the basal part of the Lower Triassic, the fauna is characterized by a rich conodont and bivalves as a result of rapid warming in the latest Permian (Shen et al., 2010). Thus, there was a rapid warming event throughout the northern margin of Gondwana at the end of the Permian, which was marked by the burst of conodonts and amonoids in the *Clarkina meishanensis* Zone. Such warming event has also been indicated by the oxygen isotope excursion of conodonts from the stratigraphic intervals in other regions such as South China and Iran (Chen et al., 2016, 2020; Joachimski et al., 2012; Figure 12). With the rapid pace of this warming event, obviously it was not related to the drifting-induced temperature changes in these blocks during the latest Permian.

Another remarkable manifestation of the rapid warming event at the end of the Permian in northern Gondwana is rapid transgression indicated by the changes in lithology and biotas at the top of the Permian (Figure 12). At the Selong Xishan section, there is a short hiatus between the underlying Coral Bed and overlying *Waagenites* Bed, and the lithology changes from bioclastic limestones to micrites upwards (Jin et al., 1996; Shen et al., 2006). At the Tulong and Qubu sections, the basal limestone unit of the Kangshare Formation directly overlies the Qubuerga Formation and contains abundant conodonts and amonoids (Zhang et al., 2017; Xu et al., 2018; Liu et al., 2020). In the Spiti area at the northern margin of Indian Plate, the lowest Triassic limestone directly overlies the Kuling Shale deposits (Orchard and Krystyn, 1998). In the Salt Range of Pakistan, the White Sandstone Unit at the top of the Chhidru Formation represents deposition of accelerated terrigenous supply in a global regression. The overlying Kathwai Member is composed of dolomite and limestone containing rich conodonts and amonoids, indicating a rapid transgression starting from the latest Permian (Mertmann, 2003). Such corresponding changes in lithologies as a result of rapid transgression have also been recorded in the Gyanyima section in the Yarlung Zangbo suture zone and the Wenlongdang PTB section in the Lhasa Block (Shen et al., 2010; Wu et al., 2014), which are comparable to those

from South China and other parts of the world (Shen et al., 2006; Yin et al., 2014; Figure 12).

## 6. Conclusions

The present Qinghai-Tibetan Plateau, consisting of a series of allochthonous blocks, experienced extremely complex tectonic activities during the Permian, through which underwent the paleogeographical evolutions of the Paleo-, Meso-, and Neo-Tethys oceans (Figure 1). The Permian lithological sequences and faunas in the Qinghai-Tibetan Plateau can be grouped into three main types. The North Qiangtang Block (Qamdo Block) is characterized by predominant carbonate deposits containing low-latitude warm-water faunas throughout the Permian. Lithological sequence and paleobiogeography of this block is mostly close to those in the South China and Simao blocks, all representing the continental slices of north Paleo-Tethys Ocean. The Permian depositional sequence and faunal composition in the Cimmerian microcontinent are relatively complex. The Cisuralian strata were dominated by typical glacio-marine deposits with cold-water faunas. Widespread carbonate deposits with warm-water faunas were not accumulated in the northern Cimmerian microcontinent (e.g., South Qiangtang Block, Baoshan Block) until the Artinskian. As for the southern Cimmerian microcontinents (e.g., the Lhasa Block, Tengchong Block), widespread carbonate deposits began to accumulate in the late Kungurian. The Guadalupian strata were well preserved in all blocks. And the Guadalupian and Lopingian were both represented by thick carbonate deposition containing warm-water biotas. The exotic limestone blocks within the Yarlung Zangbo suture zone were accumulated since the Guadalupian. Fossils within these blocks consist of mixed faunas. Such faunal characteristic is in contrast to those in the northern Gondwanan region. The Himalaya Tethys Zone in the peri-Gondwanan region were marked by glacio-marine deposits in the Cisuralian, with no Guadalupian deposits. Prevalent cold-water deposits were continuously accumulated in the Lopingian in this region, showing a remarkably different feature from those of the Cimmerian microcontinents.

The Paleo-Tethys Ocean is represented by the Longmu Co-Shuanghu suture zone. The North Qiangtang Block, north to this suture zone, contains basically warm-water faunas throughout the Permian. The Cimmerian microcontinents, including the South Qiangtang, Baoshan, Tengchong, and Lhasa blocks, collectively contains typical Gondwana-type cold-water faunas characterized by *Eurydesma*, *Bandoproductus*, *Spirelytha*, *Punctocyrtella*, and *Cimmeriella* in the lowest Cisuralian (Figure 4). In the early Cisuralian (~290–280 Ma), the Cimmerian microcontinents including the South Qiangtang, Baoshan, and Sibuma blocks in Myanmar-

Thailand rifted off and drifted northward from the northern Gondwana in a speed faster than the Lhasa, Tengchong, and Irrawaddy blocks. Such allometric northward drifting of the Cimmerian microcontinents resulted in the formation of the Meso-Tethys (Bangong-Nujiang Ocean) and Neo-Tethys oceans (Figure 8). In particular, the South Qiangtang and Baoshan blocks recorded warm-water faunas and widespread carbonate deposits from the late Artinskian. By contrast, the Lhasa, Tengchong, and Irrawaddy blocks contained strata with warm-water faunas from the Kungurian. The exotic limestone blocks within the Yarlung Zangbo suture zone contain warm-water and mixed faunas between cold- and warm-water faunas, which showed a progressive cooling trend from the east to the west blocks. These exotic limestone blocks commonly contain basalts, suggesting that they most likely represent seamount deposits in the Neo-Tethys Ocean. The Gondwana-type, cold-water faunas were widely documented in the entire Permian strata in the Himalaya Tethys Zone of northern India and all basins in Western Australia, reflecting a direct influence of high-latitude cold climate on these regions from Gondwana.

Correlations among various blocks in the Qinghai-Tibetan Plateau and its adjacent regions, such as the Karakoram, Central Pamir, and Southeast Pamir, remain controversial owing to the presences of the Karakoram fault zones. Depositional sequences and faunal compositions provided robust correlations among the Karakoram of Pakistan, Central Pamir, Southeast Pamir, and South Qiangtang blocks. By contrast, the Lhasa Block is exclusive, with no blocks to correlate with in the western part of the Karakorum Fault.

The blocks constructing the Qinghai-Tibetan Plateau were situated at mid- to high latitudes during the Permian. Among them, a couple of blocks in the Cimmerian microcontinents had drifted northward to the low latitude regions from the southern high latitude regions. A change in paleogeographic latitude superimposed by paleoclimatic change have led to synergistic effects on faunal evolutions of those blocks (Figure 8). The Artinskian warming event was remarkably archived in the northern Cimmerian regions; whereas the latest Permian warming event was more pronouncedly recorded in both the northern Gondwana and Lhasa blocks, and is marked by the widespread occurrences of conodont fossils during a rapid transgression.

**Acknowledgements** We thank Miao Desui for improving English. This work was supported by the the Second Tibetan Plateau Scientific Expedition and Research (Grant No. 2019QZKK0706), the National Natural Science Foundation of China (Grant Nos. 91855205, 42261144668, 42293280) and the Strategic Priority Research Program (B) of the Chinese Academy of Sciences (Grant No. XDB26000000).

## References

Ali S K, Janjuhah H T, Shahzad S M, Kontakiotis G, Saleem M H, Khan U, Zarkogiannis S D, Makri P, Antonarakou A. 2021. Depositional sedi-

- mentary facies, stratigraphic control, paleoecological constraints, and paleogeographic reconstruction of Late Permian Chhidru Formation (western salt range, Pakistan). *J Mar Sci Eng*, 9: 1372
- Angiolini L, Brunton H, Gaetani M. 2005. Early Permian (Asselian) brachiopods from Karakorum (Pakistan) and their palaeobiogeographical significance. *Palaeontology*, 48: 69–86
- Angiolini L, Bucher H, Pillevuit A, Platel J P, Roger J, Broutin J, Baud A, Marcoux J, Al Hashmi H. 1997. Early Permian (Sakmarian) brachiopods from southeastern Oman. *Geobios*, 30: 379–405
- Angiolini L, Zanchi A, Zanchetta S, Nicora A, Vezzoli G. 2013. The Cimmerian geopuzzle: New data from South Pamir. *Terra Nova*, 25: 352–360
- Angiolini L, Zanchi A, Zanchetta S, Nicora A, Vuolo I, Berra F, Henderson C, Malaspina N, Rettori R, Vachard D, Vezzoli G. 2015. From rift to drift in South Pamir (Tajikistan): Permian evolution of a Cimmerian terrane. *J Asian Earth Sci*, 102: 146–169
- Angiolini L. 1995. Permian brachiopods from Karakorum (Pakistan). Pt. 1. *Riv Ital Paleontol Stratigr*, 101: 165–214
- Archbold N W. 1999. Permian Gondwanan correlations: The significance of the western Australian marine Permian. *J African Earth Sci*, 29: 63–75
- Baioomy H, Anuar M N A B, Nordin M N M, Arifin M H, Al-Kahtany K. 2020. Source and origin of Late Paleozoic dropstones from Peninsular Malaysia: First record of Mississippian glaciogenic deposits of Gondwana in Southeast Asia. *Geol J*, 55: 6361–6375
- Bernardi M, Petti F M, Benton M J. 2018. Tetrapod distribution and temperature rise during the Permian-Triassic mass extinction. *Proc R Soc B*, 285: 20172331
- Brönnimann P, Whittaker J E, Zaninetti L. 1978. *Shanita*, a new Pillared Miliolacean foraminifera from the Late Permian of Burma and Thailand. *Riv Ital Paleontol Stratigr*, 84: 63–92
- Brookfield M E, Gregory Shellnutt J, Yui T F. 2022. Climatic fluctuations during a mass extinction: Rapid carbon and oxygen isotope variations across the Permian-Triassic (PT) boundary at Guryul Ravine, Kashmir, India. *J Asian Earth Sci*, 227: 105066
- Cai F, Ding L, Leary R J, Wang H, Xu Q, Zhang L, Yue Y. 2012. Tectonostratigraphy and provenance of an accretionary complex within the Yarlung-Zangpo suture zone, southern Tibet: Insights into subduction-accretion processes in the Neo-Tethys. *Tectonophysics*, 574-575: 181–192
- Chaodumrong P, Wang X D, Shen S Z. 2007. Permian lithostratigraphy of the Shan-Thai Terrane in Thailand: Revision of the Kaeng Krachan and Ratburi groups. In: International Conference on Geology of Thailand: Towards Sustainable Development and Sufficiency Economy. 229–236
- Chen B, Joachimski M M, Shen S Z, Lambert L L, Lai X, Wang X, Chen J, Yuan D. 2013. Permian ice volume and palaeoclimate history: Oxygen isotope proxies revisited. *Gondwana Res*, 24: 77–89
- Chen D, Luo H, Wang X, Xu B, Matsuoka A. 2019. Late Anisian radiolarian assemblages from the Yarlung-Tsangpo Suture Zone in the Jinlu area, Zedong, southern Tibet: Implications for the evolution of Neotethys. *Island Arc*, 28: E12302
- Chen G B. 1984. The Carboniferous System of the Baoshan region, western Yunnan (in Chinese). *J Strat*, 8: 129–135
- Chen J B, Xu X Y, Li W Q, Gong B. 2002. New advances in research of Permian-Carboniferous in the Kangmar region, southern Tibet (in Chinese). *Geoscience*, 16: 237–242
- Chen J, Shen S Z, Li X H, Xu Y G, Joachimski M M, Bowring S A, Erwin D H, Yuan D X, Chen B, Zhang H, Wang Y, Cao C Q, Zheng Q F, Mu L. 2016. High-resolution SIMS oxygen isotope analysis on conodont apatite from South China and implications for the end-Permian mass extinction. *Palaeogeogr Palaeoclimatol Palaeoecol*, 448: 26–38
- Chen J, Shen S Z, Zhang Y C, Angiolini L, Gorgij M N, Crippa G, Wang W, Zhang H, Yuan D X, Li X H, Xu Y G. 2020. Abrupt warming in the latest Permian detected using high-resolution in situ oxygen isotopes of conodont apatite from Abadeh, central Iran. *Palaeogeogr Palaeoclimatol Palaeoecol*, 560: 109973

- Chen Q H, Wang J P, Wang S L, Wu K Y. 1999. Discovery of the Upper Permian series in Cuoqin Basin, Xizang (Tibet) and its geological significance. *Chin Sci Bull*, 44: 1520–1523
- Chen W Y, Shellnutt J G, Bhat G M, Tejada M L G, Suzuki K, Denyszyn S W. 2023. Geochronology and geochemistry of the Panjal Traps from the southern Pir Panjal Range, Kashmir, India. *Lithos*, 436–437: 106967
- Chen Z Q, Shi G R, Shen S Z, Archbold N W. 2000. *Tethyochonetes* gen. nov. (Chonetida, Brachiopoda) from the Late Permian of China. *Proc R Soc Victoria*, 112: 1–15
- Cheng H, Zhang C, Vervoort J D, Lu H, Wang C, Cao D. 2012. Zircon U-Pb and garnet Lu-Hf geochronology of eclogites from the Lhasa Block, Tibet. *Lithos*, 155: 341–359
- Cheng L R, Li C, Zhang Y C, Wu S Z. 2005. The *Polydiexodina* (fusulinids) fauna from central Qiangtang, Tibet, China (in Chinese). *Acta Micropalaeontol Sin*, 22: 152–162
- Cheng L R, Wang T W, Li C, Wu S Z. 2002. Establishment of the Upper Permian Mujiu Co Formation and rugose coral assemblage in the Xainza area, northern Tibet (in Chinese). *Geol Bull Ch*, 21: 140–143
- Cheng X, Zhou Y N, Guo Q, Hou B N, Wu H N. 2015. Paleomagnetism of Triassic rocks in the western Lhasa terrane, Tibetan Plateau, and its tectonic implications (in Chinese). *Geol Bull Ch*, 34: 306–317
- Chernykh V V, Chuvashov B I, Shen S Z, Henderson C M, Yuan D X, Stephenson M H. 2020. The global stratotype section and point (GSSP) for the base-Sakmarian Stage (Cisuralian, Lower Permian). *Episodes*, 43: 961–979
- Close R A, Benson R B J, Saupe E E, Clapham M E, Butler R J. 2020. The spatial structure of Phanerozoic marine animal diversity. *Science*, 368: 420–424
- Crame J A, McGowan A J, Tomašových A. 2022. Origin of the tropical-polar biodiversity contrast. *Glob Ecol Biogeogr*, 31: 1207–1227
- Dan W, Wang Q, Murphy J B, Zhang X Z, Xu Y G, White W M, Jiang Z Q, Ou Q, Hao L L, Qi Y. 2021. Short duration of Early Permian Qiangtang-Panjal large igneous province: Implications for origin of the Neotethys Ocean. *Earth Planet Sci Lett*, 568: 117054
- Diener C. 1903. Permian fossils of the Central Himalayas. *Mem Geol Surv India, Paläontologia Indica, Series 15*, 1: 1–204
- Ding L, Kapp P, Cai F, Garzanti C N, Xiong Z, Wang H, Wang C. 2022. Timing and mechanisms of Tibetan Plateau uplift. *Nat Rev Earth Environ*, 3: 652–667
- Dong Z H, Wang W. 2006. The Cambrian-Triassic Conodont Faunas in Yunnan, China (in Chinese). Kunming: Yunnan Science and Technology Press. 1–347
- Douglass R C. 1970. Morphologic study of fusulinids from the Lower Permian of West Pakistan. US Geological Survey, Professional Paper, 643: 1–11
- Fan J C. 1993. Bryozoans of Late Carboniferous-Early Permian in Tengchong area of western Yunnan (in Chinese). *Yunnan Geol*, 12: 383–406
- Fan J J, Niu Y, Luo A B, Xie C M, Hao Y J, Liu H Y. 2021. Timing of the Meso-Tethys Ocean opening: Evidence from Permian sedimentary provenance changes in the South Qiangtang Terrane, Tibetan Plateau. *Palaeogeogr Palaeoclimatol Palaeoecol*, 567: 110265
- Fan J X, Shen S Z, Erwin D H, Sadler P M, MacLeod N, Cheng Q M, Hou X D, Yang J, Wang X D, Wang Y, Zhang H, Chen X, Li G X, Zhang Y C, Shi Y K, Yuan D X, Chen Q, Zhang L N, Li C, Zhao Y Y. 2020. A high-resolution summary of Cambrian to Early Triassic marine invertebrate biodiversity. *Science*, 367: 272–277
- Fan X L, Li X H, Mattern F, Wei Z, Zheng C Y, Wang J Y, Zhou M. 2023. Lithofacies, geochemistry, and sequences of basalt and carbonate rocks of a Middle Permian composite seamount (central Yarlung Zangbo Suture Zone, Tibet): Implications to the incipient opening of the Neotethys Ocean. *Lithos*, 448–449: 107175
- Fang R S, Fan J C. 1994. Middle to Upper Carboniferous-Early Permian Gondwana Facies and Palaeontology in Western Yunnan (in Chinese). Kunming: Yunnan Science and Technology Press. 1–121
- Fang R S. 1983. The early Permian brachiopoda from Xiaoxinzhai of Gengma Yunnan and its geological significance. In: CGQXP Editorial Committee, Ministry of Geology and Mineral Resources, ed. Contribution to the Geology of the Qinghai-Xizang (Tibet) Plateau (11) (in Chinese with English abstract). Beijing: Geologica Publishing House. 93–119
- Fielding C R, Frank T D, Isbell J L. 2008. The late Paleozoic ice age—A review of current understanding and synthesis of global climate patterns. *Geol Soc Am Spec Pap*, 441: 343–354
- Gaetani M, Angiolini L, Garzanti E, Jadoul F, Leven E Y, Nicora A, Sciunnach D. 1995. Permian stratigraphy in the Northern Karakorum, Pakistan. *Riv Ital Paleontol Stratigr*, 101: 107–152
- Gaetani M, Leven E J. 2014. The Permian succession of the Shaksgam Valley, Sinkiang (China). *Int J Geosci*, 133: 45–62
- Garzanti E, Le Fort P, Sciunnach D. 1999. First report of Lower Permian basalts in South Tibet: Tholeiitic magmatism during break-up and incipient opening of Neotethys. *J Asian Earth Sci*, 17: 533–546
- Gehrels G, Kapp P, DeCelles P, Pullen A, Blakey R, Weislogel A, Ding L, Guynn J, Martin A, McQuarrie N, Yin A. 2011. Detrital zircon geochronology of pre-Tertiary strata in the Tibetan-Himalayan orogen. *Tectonics*, 30: TC5016
- Ghazi S, Mountney N P, Sharif S. 2015. Lower Permian fluvial cyclicality and stratigraphic evolution of the northern margin of Gondwanaland: Warchha Sandstone, Salt Range, Pakistan. *J Asian Earth Sci*, 105: 1–17
- Ghazi S, Mountney N P, Butt A A, Sharif S. 2012. Stratigraphic and palaeoenvironmental framework of the Early Permian sequence in the Salt Range, Pakistan. *J Earth Syst Sci*, 121: 1239–1255
- Golonka J, Ford D. 2000. Pangean (Late Carboniferous–Middle Jurassic) paleoenvironment and lithofacies. *Palaeogeogr Palaeoclimatol Palaeoecol*, 161: 1–34
- Grunt T A, Dmitriev V Y. 1973. Permskie brachiopody Pamira. Moscow: Akademia Nauk SSSR, Paleontologicheskii Institut. 212
- Grunt T A, Novikov V P. 1994. Biostratigraphy and biogeography of the Early Permian in the Southeastern Pamirs. *Stratigr Geol Correl*, 2: 331–339
- Guo T Y, Liang D Y, Zhang Y Z, Zhao C H. 1991. Geology of Ngari, Tibet (Xizang) (in Chinese). Beijing: China University of Geosciences Press. 1–464
- Gupta V J. 1975. The stratigraphic position of the Boulder beds in the agglomeratic slate succession and their equivalents in the Tethyan Himalaya. *Bull Indian Geol Assoc*, 8: 35–49
- Haig D W, Mory A J, McCartain E, Backhouse J, Håkansson E, Ernst A, Nicoll R S, Shi G R, Bevan J C, Davydov V I, Hunter A W, Keep M, Martin S K, Peyrot D, Kossavaya O, Santos Z D. 2017. Late Artinskian–Early Kungurian (Early Permian) warming and maximum marine flooding in the East Gondwana interior rift, Timor and Western Australia, and comparisons across East Gondwana. *Palaeogeogr Palaeoclimatol Palaeoecol*, 468: 88–121
- He W, Bu J, Niu Z, Zhang Y. 2009. A new Late Permian brachiopod fauna from Tanggula, Qinghai-Tibet Plateau and its palaeogeographical implications. *Alcheringa*, 33: 113–132
- He W, Shi G R, Bu J J, Niu Z. 2008. A new brachiopod fauna from the Early to Middle Permian of Southern Qinghai Province, Northwest China. *J Paleontology*, 82: 811–822
- Hou Z S, Shen S Z, Henderson C M, Yuan D X, Zhang Y C, Fan J X. 2023. Cisuralian (Early Permian) paleogeographic evolution of South China Block and sea-level changes: Implications for the global Artinskian Warming Event. *Palaeogeogr Palaeoclimatol Palaeoecol*, 613: 111395
- Hu X, Ma A, Xue W, Garzanti E, Cao Y, Li S M, Sun G, Lai W. 2022. Exploring a lost ocean in the Tibetan Plateau: Birth, growth, and demise of the Bangong-Nujiang Ocean. *Earth-Sci Rev*, 229: 104031
- Huang B C, Yan Y G, Piper J D A, Zhang D H, Yi Z Y, Yu S, Zhou T H. 2018. Paleomagnetic constraints on the paleogeography of the East Asian blocks during Late Paleozoic and Early Mesozoic times. *Earth-Sci Rev*, 186: 8–36
- Huang H, Jin X C, Shi Y K, Yang X N. 2007. Middle Permian fusulinids from the Xainza area of the Lhasa Block, Tibet (in Chinese). *Acta Palaeontol Sin*, 46: 62–74
- Huang H, Jin X C, Shi Y K, Yang X N. 2009. Middle Permian western Tethyan fusulinids from southern Baoshan Block, western Yunnan,

- China. *J Paleontol*, 83: 880–896
- Huang H, Jin X, Shi Y, Wang H, Zheng J, Zong P. 2020. Fusulinid-bearing oolites from the Tengchong Block in western Yunnan, SW China: Early Permian warming signal in the eastern peri-Gondwana. *J Asian Earth Sci*, 193: 104307
- Huang H, Jin X, Shi Y. 2022. Distribution pattern of Middle Permian fusulinids in the Lhasa Block, Tibet and their paleogeographic implications. *Palaeogeogr Palaeoclimatol Palaeoecol*, 586: 110780
- Huang H, Shi Y K, Jin X C. 2017. Permian (Guadalupian) fusulinids of Bawei Section in Baoshan Block, western Yunnan, China: Biostratigraphy, facies distribution and paleogeographic discussion. *Palaeo-world*, 26: 95–114
- Huang H, Shi Y, Jin X. 2015. Permian fusulinid biostratigraphy of the Baoshan Block in western Yunnan, China with constraints on paleogeography and paleoclimate. *J Asian Earth Sci*, 104: 127–144
- Ingavat R, Douglass R C. 1981. Fusuline fossils from Thailand, part 14. The fusulinid genus *Monodiexodina* from Northwest Thailand. *Geol Palaeontol Southeast Asia*, 22: 23–34
- Ingavat-Helmcke R. 1993. Contribution to the Permian fusulinacean faunas of Peninsular Thailand. *J Southeast Asian Earth Sci*, 8: 67–75
- Isbell J L, Henry L C, Gulbranson E L, Limarino C O, Fraiser M L, Koch Z J, Ciccio P L, Dineen A A. 2012. Glacial paradoxes during the late Paleozoic ice age: Evaluating the equilibrium line altitude as a control on glaciation. *Gondwana Res*, 22: 1–19
- Ji W Q, Wu F Y, Chung S L, Li J X, Liu C Z. 2009. Zircon U-Pb geochronology and Hf isotopic constraints on petrogenesis of the Gangdese batholith, southern Tibet. *Chem Geol*, 262: 229–245
- Ji Z S, Yao J X, Jin X C, Yang X N, Wang Y Z, Yang H L, Wu G C. 2004. Early Permian conodonts from the Baoshan Block, Western Yunnan, China. *Acta Geol Sin-Engl Ed*, 78: 1179–1184
- Ji Z S, Yao J X, Wu G C, Liu G Z. 2006. Discovery of the conodont *Rabeignathus bucaramangus* fauna in Rutog, Tibet, China, and its significances (in Chinese). *Geol Bull Ch*, 25: 142–145
- Ji Z S, Yao J X, Wu G C, Zhan L P, Jiang Z T, Fu Y H. 2005. On the stratigraphic sequence, lithological characteristics and origin of the Lower Permian Pangduo Group in Linzhou County, northern Lhasa, Tibet (in Chinese). *Acta Geol Sin-Chin Ed*, 79: 433–443
- Ji Z S, Yao J X, Wu G C. 2007. Discovery of Permian and Triassic conodonts in the Shiquanhe area, Ngari, western Tibet, China and their significances (in Chinese). *Geol Bull Ch*, 26: 383–397
- Jin X C, Huang H, Shen Y, Wang Y Z. 2008. Subdivision and correlation of Mid-Late Permian successions of the Baoshan Block, western Yunnan: Status and problems (in Chinese). *Acta Geosci Sin*, 29: 533–541
- Jin X C, Huang H, Shi Y K, Zhan L P. 2011. Lithologic boundaries in Permian post-glacial sediments of the Gondwana-affinity regions of China: Typical sections, age range and correlation. *Acta Geol Sin-Engl Ed*, 85: 373–386
- Jin X C, Huang H, Shi Y K, Zhan L P. 2014. Permo-Carboniferous successions of the Tengchong Block, Western Yunnan, China: Status and Problems. *STRATI*, 2013: 767–771
- Jin X C, Huang H, Shi Y K, Zhan L P. 2015. Origin of Permian exotic limestone blocks in the Yarlung Zangbo suture zone, southern Tibet, China: With biostratigraphic, sedimentary and regional geological constraints. *J Asian Earth Sci*, 104: 22–38
- Jin X C. 1994. Sedimentary and paleogeographic significance of Permo-Carboniferous sequences in western Yunnan, China. *Geologisches Institut der universitat zu Koeln Sonderveroffentlichung*, 99: 1–136
- Jin X C. 2002. Permo-Carboniferous sequences of Gondwana affinity in southwest China and their paleogeographic implications. *J Asian Earth Sci*, 20: 633–646
- Jin Y G, Liang X L, Wen S X. 1977. Additional material of animal fossils from the Permian deposits on the northern slope of Mount Qomolangma Feng (in Chinese). *Chin J Geol*, 12: 236–249
- Jin Y G, Shen S Z, Zhu Z L, Mei S L, Wang W. 1996. The Selong section, candidate of the global stratotype section and point of the Permian-Triassic boundary. In: Yin H F, ed. *The Palaeozoic-Mesozoic Boundary Candidates of the Global Stratotype Section and Point of the Permian-Triassic Boundary*. Wuhan: China University of Geosciences Press. 127–137
- Jin Y G, Sun D L. 1981. Palaeozoic brachiopods from Xizang. In: Nanjing Institute of Geology and Palaeontology, ed. *Palaeontology of Xizang*, Book 3, The Series of the Scientific Expedition to the Qinghai-Xizang Plateau (in Chinese with English abstract). Beijing: Science Press. 127–176
- Jin Y G, Wang Y, Sun D L, Shi Q. 1985. Late Paleozoic and Triassic brachiopods from the east of the Qinghai-Xizang Plateau. In: Sichuan Regional Geological Survey, Nanjing Institute of Geology and Palaeontology, eds. *Stratigraphy and palaeontology in W. Sichuan and E. Xizang, China (Part 3)* (in Chinese with English abstract). Chengdu: Sichuan Science and Technology Press. 182–249
- Joachimski M M, Lai X, Shen S Z, Jiang H, Luo G, Chen B, Chen J, Sun Y. 2012. Climate warming in the latest Permian and the Permian-Triassic mass extinction. *Geology*, 40: 195–198
- Ju Q, Zhang Y C, Qiao F, Xu H P. 2019. Middle Permian fusuline faunas from the Zhabuye area, central Lhasa Block, Tibet and their palaeobiogeographic implications (in Chinese). *Acta Palaeontol Sin*, 58: 324–341
- Ju Q, Zhang Y C, Qiao F, Xu H P. 2021. A Middle Permian assemblage of smaller foraminifera (*Shanita-Hemigordiopsis* assemblage) from the central Lhasa Block and its paleobiogeographic implications. *Palaeogeogr Palaeoclimatol Palaeoecol*, 572: 110417
- Ju Q, Zhang Y, Qiao F, Xu H P. 2022b. First discovery of Wuchiapingian (Late Permian) foraminiferal fauna from the Zhari Namco area, central Lhasa Block, Tibet, and their palaeogeographic implications. *Geol J*, 57: 2564–2580
- Ju Q, Zhang Y C, Yuan D X, Qiao F, Xu H P, Zhang H, Zheng Q F, Luo M, Qie W K, Zhai Q G, Zhang Y J, Shen S Z. 2022a. Permian foraminifers from the exotic limestone blocks within the central Qiangtang Metamorphic Belt, Tibet and their geological implications. *J Asian Earth Sci*, 239: 105426
- Kapp P, Yin A, Manning C E, Harrison T M, Taylor M H, Ding L. 2003. Tectonic evolution of the early Mesozoic blueschist-bearing Qiangtang metamorphic belt, central Tibet. *Tectonics*, 22: 1043
- Ke Y, Shen S Z, Shi G R, Fan J X, Zhang H, Qiao L, Zeng Y. 2016. Global brachiopod palaeobiogeographical evolution from Changhsingian (Late Permian) to Raetian (Late Triassic). *Palaeogeogr Palaeoclimatol Palaeoecol*, 448: 4–25
- Keppie D F. 2015. How the closure of paleo-Tethys and Tethys oceans controlled the early breakup of Pangaea. *Geology*, 43: 335–338
- Kozur H. 1994. Permian pelagic and shallow-water conodont zonation. *Permophiles*, 24: 16–20
- Lan C H, Sun C, Fan J C, Fang R S. 1983. Carboniferous and Permian stratigraphy of the Zhenkang and Luxi region in western Yunnan. In: CGQXP Editorial Committee, Ministry of Geology and Mineral Resources, ed. *Contribution to the geology of the Qinghai-Xizang (Tibet) Plateau (11)* (in Chinese with English abstract). Beijing: Geologica Publishing House. 79–91
- Laurie J R, Bodorkos S, Nicoll R S, Crowley J L, Mantle D J, Mory A J, Wood G R, Backhouse J, Holmes E K, Smith T E, Champion D C. 2016. Calibrating the middle and late Permian palynostratigraphy of Australia to the geologic time-scale via U-Pb zircon CA-IDTIMS dating. *Aust J Earth Sci*, 63: 701–730
- Leven E J. 1967. Stratigrafiya i fuzulinidy permsskikh otlozheniy Pamira. Moscow: Ademiya Nauk SSSR, Geologicheskii Institut. 1–224
- Leven E J. 1991. Pervye nakhodki v SSSR foraminifer roda *Shanita* (Semeystvo Hemigordiopsidae). *Paleontol J*, 2: 102–104
- Leven E J. 1998. Permian fusulinid assemblages and stratigraphy of the Transcaucasia. *Riv Ital Paleontol Stratigr*, 104: 299–323
- Leven E J. 2003. The Permian stratigraphy and fusulinids of the Tethys. *Riv Ital Paleontol Stratigr*, 109: 267–280
- Leven E J. 2004. Fusulinids and Permian scale of the Tethys. *Stratigr Geol Correl*, 12: 139–151
- Leven E J, Leonova T B, Dmitriev V Y. 1992. *Permi Darvaz-Zaalauskoy zony Pamira: Fuzulinidy, ammonoidei, stratigrafiya*. Moscow: Ros-

- siyskaya Akademiya Nauk, Trudy Paleontologicheskogo Instituta. 203
- Li C, Cheng L R, Hu K. 1995. Researches on the Longmu Co-Shunghu Paleotethys Suture in Tibet. Beijing: Geological Publishing House. 1–131
- Li C. 1987. The Longmucuo-Shuanghu-Lancangjiang plate suture and the north boundary of distribution of Gondwana facies Permo-Carboniferous system in northern Xizang, China (in Chinese). *J Changchun Coll Geol*, 17: 155–166
- Li C., Xie C M, Wang M, Wu Y W, Hu P Y, Zhang X Z, Xu F, Fan J, Wu H, Liu Y M, Peng H, Jiang Q Y, Chen J W, Xu J X, Zhai Q G, Dong Y S, Zhang T Y, Huang X P. 2016. Geology of the Qiangtang Region (in Chinese). Beijing: Geological Publishing House. 1–681
- Li W Z, Shen S Z. 2005. Faunas from the Permian Limestone Blocks at the Yarlung Zangbo suture zone in southern Xizang (Tibet) and its palaeogeographical implications (in Chinese). *Geol Rev*, 51: 225–233
- Li X H, Wang C S, Li Y L, Wei Y S, Chen X. 2014. The disaggregation of the Permian Quga Formation in Zhongba area, southwestern Tibet (in Chinese). *Geol Bull Chin*, 33: 614–628
- Liang D Y, Nie Z T, Guo T Y, Zhang Y Z, Xu B W, Wang W P. 1983. Permo-Carboniferous Gondwana-Tethys facies in southern Karakoran, Ali, Xizang (Tibet) (in Chinese). *Earth Sci*, 19: 9–27
- Liao S Y, Wang D B, Tang Y, Yin F G, Cao S N, Wang L Q, Wang B D, Sun Z M. 2015. Late Paleozoic Woniusi basaltic province from Sibumasu terrane: Implications for the breakup of eastern Gondwana's northern margin. *GSA Bull*, 127: 1313–1330
- Lin B Y. 1983. Palaeozoic stratigraphy in Xainza County, Xizang (Tibet). In: CGQXP Editorial Committee, Ministry of Geology and Mineral Resources PRC, ed. Contribution to the Geology of the Qinghai-Xizang (Tibet) (8) (in Chinese with English abstract). Beijing: Geological Publishing House. 1–13
- Liu C Z, Chung S L, Wu F Y, Zhang C, Xu Y, Wang J G, Chen Y, Guo S. 2016. Tethyan suturing in Southeast Asia: Zircon U-Pb and Hf-O isotopic constraints from Myanmar ophiolites. *Geology*, 44: 311–314
- Liu C, An X, Algeo T J, Munneke A, Zhang Y, Zhu T. 2021. Hydrocarbon-seep deposits in the lower Permian Angie Formation, Central Lhasa Block, Tibet. *Gondwana Res*, 90: 258–272
- Liu F, Peng H, Bomfleur B, Kerp H, Zhu H, Shen S Z. 2020. Palynology and vegetation dynamics across the Permian-Triassic boundary in southern Tibet. *Earth-Sci Rev*, 209: 103278
- Liu G C. 1993. Age assignment of Kaixinling Group and Wuli Group in the middle Tanggula Mountain (in Chinese). *Qinghai Geol*, (1): 1–9
- Liu Y, Zhai Q, Hu P, Tang Y, Lee H. 2022. Evolution of the Paleo-Tethys Ocean: Constraints from detrital zircons of the Paleozoic to Triassic clastic rocks in the Qiangtang terrane, Tibetan Plateau. *J Asian Earth Sci*, 232: 105226
- Lucas S G, Henderson C M, Barrick J E, Krainer K. 2022. Conodonts and the correlation of the Lower Permian Yeso Group, New Mexico, USA. *Stratigraphy*, 19: 77–94
- Lys M, Colchen M, Bassoulet J P, Marcoux J, Mascle G. 1980. La biozone a *Colaniella parva* du Permian Supérieur et sa microfuna dans le bloc calcaire exotique de Lamayuru, Himalaya du Ladakh. *Rev de Micropaleontol*, 23: 76–108
- Lyu Z Y, Orchard M J, Golding M L, Henderson C M, Chen Z Q, Zhang L, Han C, Wu S L, Huang Y G, Zhao L S, Bhat G M, Baud A. 2021. Lower Triassic conodont biostratigraphy of the Guryul Ravine section, Kashmir. *Glob Planet Change*, 207: 103671
- Mannion P D, Upchurch P, Benson R B J, Goswami A. 2014. The latitudinal biodiversity gradient through deep time. *Trends Ecol Evol*, 29: 42–50
- Marchetti L, Forte G, Kustatscher E, DiMichele W A, Lucas S G, Roghi G, Juncal M A, Hartkopf-Fröder C, Krainer K, Morelli C, Ronchi A. 2022. The Artinskian Warming Event: An Euramerican change in climate and the terrestrial biota during the early Permian. *Earth-Sci Rev*, 226: 103922
- Mei S L. 1996. Restudy of conodonts from the Permian-Triassic boundary beds at Selong and Meishan and the natural Permian-Triassic boundary. In: Wang H Z, Wang X L, eds. Centennial Memorial Volume of Professor Sun Yunzhu: Stratigraphy and Palaeontology. Wuhan: China University of Geosciences Press. 141–148
- Meng Y, Xu Z, Xu Y, Ma S. 2018. Late Triassic granites from the Quxu Batholith shedding a new light on the evolution of the Gangdese Belt in Southern Tibet. *Acta Geol Sin-Engl Ed*, 92: 462–481
- Meng Z, Wang J G, Garzanti E, Han Z, Chen G. 2021. Late Triassic rifting and volcanism on the northeastern Indian margin: A new phase of Neotethyan seafloor spreading and its paleogeographic implications. *Palaeogeogr Palaeoclimatol Palaeoecol*, 570: 110367
- Mertmann D. 2003. Evolution of the marine Permian carbonate platform in the Salt Range (Pakistan). *Palaeogeogr Palaeoclimatol Palaeoecol*, 191: 373–384
- Metcalfe I. 2013. Gondwana dispersion and Asian accretion: Tectonic and palaeogeographic evolution of eastern Tethys. *J Asian Earth Sci*, 66: 1–33
- Metcalfe I. 2021. Multiple Tethyan ocean basins and orogenic belts in Asia. *Gondwana Res*, 100: 87–130
- Mitchell A H G. 1992. Late Permian-Mesozoic events and the Mergui group Nappe in Myanmar and Thailand. *J Southeast Asian Earth Sci*, 7: 165–178
- Mory A J, Crowley J L, Backhouse J, Nicoll R S, Bryan S E, López Martínez M, Mantle D J. 2017. Apparent conflicting Roadian-Wordian (middle Permian) CA-IDTIMS and palynology ages from the Canning Basin, Western Australia. *Aust J Earth Sci*, 64: 889–901
- Mory A J, Redfern J, Martin J R. 2008. A review of Permian-Carboniferous glacial deposits in Western Australia. *Geol Soc Am Spec Pap*, 441: 29–40
- Muttoni G, Gaetani M, Kent D V, Sciunnach D, Angiolini L, Berra F, Garzanti E, Mattei M, Zanchi A. 2009. Opening of the Neo-Tethys Ocean and the Pangea B to Pangea A transformation during the Permian. *GeoArabia*, 14: 17–48
- Muttoni G, Kent D V, Garzanti E, Brack P, Abrahamsen N, Gaetani M. 2003. Early Permian Pangea “B” to Late Permian Pangea “A”. *Earth Planet Sci Lett*, 215: 379–394
- Nakazawa K, Kapoor H M, Ishii K, Bando Y, Okimura Y, Tokuoka T. 1975. The upper Permian and the lower Triassic in Kashmir, India. *Mem Fac Sci*, 40: 1–106
- Nicoll R S, Metcalfe I. 1998. Early and Middle Permian conodonts from the Canning and Southern Carnarvon Basins, Western Australia: Their implications for regional biogeography and palaeoclimatology. *Proc R Soc Victoria*, 110: 419–461
- Nie Z T, Song Z M. 1983a. Fusulinids of Lower Permian Tunlonggongba Formation from Rutog of Xizang (Tibet), China (in Chinese). *Earth Sci*, 19: 43–55
- Nie Z T, Song Z M. 1983b. Fusulinids of Lower Permian Qudi Formation from Rutog of Xizang (Tibet), China (in Chinese). *Earth Sci*, 19: 29–42
- Nie Z T, Song Z M. 1983c. Fusulinids of Lower Permian Maokouian Longge Formation from Rutog, Xizang (Tibet), China (in Chinese). *Earth Sci*, 19: 57–67
- Nie Z T, Song Z M. 1985. Foeaminiferal assemblage of lower Permian Maokou'an Longge Formation in Rutog, Ngari area, Xizang (Tibet). In: CGQXP Editorial Committee, Ministry of Geology and Mineral Resources PRC, ed. Contribution to the Geology of the Qinghai-Xizang (Tibet) (17) (in Chinese). Beijing: Geological Publishing House. 199–222
- Niu Z J, Duan Q F, Wang J X, Bai Y S, Tu B, Bu J J. 2006b. Discovery of the upper part of the Permian Yanghsinian Series and establishment of the Garizaren and Suojia formations in the Zhidoi-Zadoi area, southern Qinghai, China (in Chinese). *Geol Bull Chin*, 25: 176–182
- Niu Z J, Duan Q F, Wang J X, Bai Y S, Zeng B F, Tu B, Bu J J. 2006a. On the Gadikao Formation in Zhidoi and Zadoi areas, southern Qinghai (in Chinese). *J Strat*, 30: 109–115
- Niu Z J, Duan Q F, Wang J X, He L Q, Bai Y S. 2010. Early Permian (Cisuralian) lithostratigraphical succession in volcanic-sedimentary setting from southern Qinghai (in Chinese). *Earth Sci*, 35: 11–21
- Niu Z J, Ma L Y, Zeng B F. 2003. Late Permian brachiopod faunas from Wuli Group of Geladandong Mountain area in the source region of the



- Yangtze River (in Chinese). *Acta Geosci Sin*, 24: 343–348
- Niu Z J, Wu J, Duan Q F, Bai Y S, Ma L Y, Zhao X M, He L Q. 2011. Permian tectonic setting of southern Qinghai and its tectonic evolution (in Chinese). *Geol Rev*, 57: 609–622
- Niu Z J, Wu J. 2016. Fusulinid Fauna of Permian Volcanic-Depositional Succession (Setting) in Southern Qinghai, Northwest China (in Chinese). Wuhan: China University of Geoscience Publishing House. 1–200
- Norin E. 1946. Geological Explorations in Western Tibet. Stockholm: Sino-Swedish Expedition Publications. 214
- Oo T, Hlaing T, Htay N. 2002. Permian of Myanmar. *J Asian Earth Sci*, 20: 683–689
- Orchard M J, Krystyn L. 1998. Conodonts of the Lowermost Triassic of Spiti, and new zonation based on Neogondolella successions. *Riv Ital Paleontol Stratigr*, 104: 341–368
- Orchard M J, Nassichuk W W, Rui L. 1994. Conodonts from the lower Griesbachian *Otoceras latilobatum* bed of Selong, Tibet and the position of the Permian-Triassic boundary. In: Pangea: Global Environments and Resources, Memoir Canadian Society of Petroleum Geologists. 17: 823–843
- Pakistan-Japanese Working Group. 1985. Permian and Triassic systems in the Salt range and Surghar Range, Pakistan. In: Nakazawa K, Dickens J M, eds. The Tethys: Her Paleogeography and Paleobiogeography from Paleozoic to Mesozoic. Tokyo: Tokai University Press. 221–312
- Pan G, Wang L, Li R, Yuan S, Ji W, Yin F, Zhang W, Wang B. 2012. Tectonic evolution of the Qinghai-Tibet Plateau. *J Asian Earth Sci*, 53: 3–14
- Qiao F, Xu H P, Zhang Y C. 2019. Changhsingian (Late Permian) foraminifers from the topmost part of the Xiala Formation in the Tsochen area, central Lhasa Block, Tibet and their geological implications. *Palaeoworld*, 28: 303–319
- Qiao F, Zhang Y C, Wang Y, Yuan D X, Ju Q, Xu H P, Zhang H, Zheng Q F, Cai Y F, Hou Z S, Shen S Z. 2021. An updated age of Permian strata in the Raggyorcaka and Qamdo areas, Tibet and their paleogeographic implications. *Palaeogeogr Palaeoclimatol Palaeoecol*, 582: 110660
- Qiao F, Zhang Y C, Xu H P, Ju Q. 2021. Late Permian foraminifers in the Xainza area, Lhasa Block, Tibet (in Chinese). *Acta Micropalaeontol Sin*, 38: 1–17
- Qu X M, Xin H B, Zhao Y Y, Wang R J, Fan X T. 2010. Opening time of Bangong Lake Middle Tethys oceanic basin of the Tibet Plateau: Constraints from petro-geochemistry and zircon U-Pb LAICPMS dating of mafic ophiolites (in Chinese). *Earth Sci Front*, 17: 53–63
- Rahman N U, Song H J, Xian B, Rehman S U, Rehman G, Majid A, Iqbal J, Hussain G. 2022. Middle-Late Permian and Early Triassic foraminiferal assemblages in the Western Salt Range, Pakistan. *Min Geol Pet Eng Bull*, 161–196
- Rao J G, Zhang Z G, Yang Z R. 1988. Silurian, Devonian and Permian Systems in Tibet (in Chinese). Chengdu: Sichuan Science and Technology Press. 68–121
- Ridd M F. 2015. East flank of the Sibumasu block in NW Thailand and Myanmar and its possible northward continuation into Yunnan: A review and suggested tectono-stratigraphic interpretation. *J Asian Earth Sci*, 104: 160–174
- Ridd M F. 2016. Should Sibumasu be renamed Sibuma? The case for a discrete Gondwana-derived block embracing western Myanmar, upper Peninsular Thailand and NE Sumatra. *J Geol Soc Lond*, 173: 249–264
- Roxy M K, Dasgupta P, McPhaden M J, Suematsu T, Zhang C, Kim D. 2019. Twofold expansion of the Indo-Pacific warm pool warps the MJO life cycle. *Nature*, 575: 647–651
- Saupe E E, Myers C E, Townsend Peterson A, Soberón J, Singarayer J, Valdes P, Qiao H. 2019. Spatio-temporal climate change contributes to latitudinal diversity gradients. *Nat Ecol Evol*, 3: 1419–1429
- Schneebeil-Hermann E, Kürschner W M, Hochuli P A, Bucher H, Ware D, Goudemand N, Roohi G. 2012. Palynofacies analysis of the Permian-Triassic transition in the Amb section (Salt Range, Pakistan): Implications for the anoxia on the South Tethyan Margin. *J Asian Earth Sci*, 60: 225–234
- Schneebeil-Hermann E, Kürschner W M, Kerp H, Bomfleur B, Hochuli P A, Bucher H, Ware D, Roohi G. 2015. Vegetation history across the Permian-Triassic boundary in Pakistan (Amb section, Salt Range). *Gondwana Res*, 27: 911–924
- Şengör A M C. 1979. Mid-Mesozoic closure of Permo-Triassic Tethys and its implications. *Nature*, 279: 590–593
- Shellnutt J G, Bhat G M, Wang K L, Brookfield M E, Jahn B M, Dostal J. 2014. Petrogenesis of the flood basalts from the Early Permian Panjal Traps, Kashmir, India: Geochemical evidence for shallow melting of the mantle. *Lithos*, 204: 159–171
- Shen S Z, Archbold N W, Shi G R, Chen Z Q. 2000b. Permian brachiopods from the Selong Xishan section, Xizang (Tibet), China Part 1: Stratigraphy, Strophomenida, Productida and Rhynchonellida. *Geobios*, 33: 725–752
- Shen S Z, Archbold N W, Shi G R, Chen Z Q. 2001a. Permian brachiopods from the Selong Xishan section, Xiang (Tibet), China. Part 2: Palaeobiogeographical and palaeoecological implications, Spiriferida, Athyridida and Terebratulida. *Geobios*, 34: 157–182
- Shen S Z, Archbold N W, Shi G R. 2001b. A Lopingian (Late Permian) brachiopod fauna from The Quburga Formation at Shengmi in the Mount Qomolangma Region of Southern Xizang (Tibet), China. *J Palaeontology*, 75: 274–283
- Shen S Z, Cao C Q, Henderson C M, Wang X D, Shi G R, Wang Y, Wang W. 2006. End-Permian mass extinction pattern in the northern perigondwanan region. *Palaeoworld*, 15: 3–30
- Shen S Z, Cao C Q, Shi G R, Wang X D, Mei S L. 2003b. Lopingian (Late Permian) stratigraphy, sedimentation and palaeobiogeography in southern Tibet. *Newsl Stratigr*, 39: 157–179
- Shen S Z, Cao C Q, Zhang Y C, Li W Z, Shi G R, Wang Y, Wu Y S, Ueno K, Henderson C M, Wang X D, Zhang H, Wang X J, Chen J. 2010. End-Permian mass extinction and palaeoenvironmental changes in Neotethys: Evidence from an oceanic carbonate section in southwestern Tibet. *Glob Planet Change*, 73: 3–14
- Shen S Z, Jin Y G. 1999. Brachiopods from the Permian-Triassic boundary beds at the Selong Xishan section, Xizang (Tibet), China. *J Asian Earth Sci*, 17: 547–559
- Shen S Z, Mei S L, Wang X D. 2003e. Latest biostratigraphical advances of the Permian System in the Salt Range, Pakistan (in Chinese). *Acta Palaeontol Sin*, 42: 168–173
- Shen S Z, Ramezani J, Chen J, Cao C Q, Erwin D H, Zhang H, Xiang L, Schoepfer S D, Henderson C M, Zheng Q F, Bowring S A, Wang Y, Li X H, Wang X D, Yuan D X, Zhang Y C, Mu L, Wang J, Wu Y S. 2019. A sudden end-Permian mass extinction in South China. *GSA Bull*, 131: 205–223
- Shen S Z, Shi G R, Archbold N W. 2003a. Lopingian (Late Permian) brachiopods from the Quburga Formation at the Qubu section in the Mt. Qomolangma region, southern Tibet (Xizang), China. *Palaeontogr Abt A*, 268: 49–101
- Shen S Z, Shi G R, Archbold N W. 2003c. A Wuchiapingian (Late Permian) brachiopod fauna from an exotic block in the Indus-Tsangpo suture zone, southern Tibet, and its palaeobiogeographical and tectonic implications. *Palaeontology*, 46: 225–256
- Shen S Z, Shi G R, Fang Z J. 2002. Permian brachiopods from the Baoshan and Simao Blocks in Western Yunnan, China. *J Asian Earth Sci*, 20: 665–682
- Shen S Z, Shi G R, Zhu K Y. 2000a. Early Permian brachiopods of Gondwana affinity from the Dingjiazhai Formation of the Baoshan Block, western Yunnan, China. *Riv Ital Paleontol Stratigr*, 106: 263–282
- Shen S Z, Sun D L, Shi G R. 2003d. A biogeographically mixed late Guadalupian (late Middle Permian) brachiopod fauna from an exotic limestone block at Xiukang in Lhaze county, Tibet. *J Asian Earth Sci*, 21: 1125–1137
- Shen S Z, Sun T R, Zhang Y C, Yuan D X. 2016. An upper Kungurian/lower Guadalupian (Permian) brachiopod fauna from the South Qiangtang Block in Tibet and its palaeobiogeographical implications. *Palaeoworld*, 25: 519–538

- Shen S Z, Zhang H, Shi G R, Li W Z, Xie J F, Mu L, Fan J X. 2013. Early Permian (Cisuralian) global brachiopod palaeobiogeography. *Gondwana Res*, 24: 104–124
- Shen S Z. 2018. Global Permian brachiopod biostratigraphy: an overview. *Geol Soc Spec Publ*, 450: 289–320
- Sheng H B. 1984. Late Early Permian ammonoids from the Xiukang Formation, Lhaze district, Xizang (Tibet) (in Chinese). In: Editorial Committee of Proceedings of Himalayan Geology, ed. Himalayan Geology II, Beijing: Geological Publishing House. 219–243
- Shi G R, Archbold N W, Zhan L P. 1995. Distribution and characteristics of mixed (transitional) mid-Permian (Late Artinskian—Ufimian) marine faunas in Asia and their palaeogeographical implications. *Palaeogeogr Palaeoclimatol Palaeoecol*, 114: 241–271
- Shi G R, Archbold N W. 1995. Permian brachiopod faunal sequence of the Shan-Thai terrane: Biostratigraphy, palaeobiogeographical affinities and plate tectonic/palaeoclimatic implications. *J Southeast Asian Earth Sci*, 11: 177–187
- Shi G R, Fang Z J, Archbold N W. 1996. An Early Permian brachiopod fauna of Gondwanan affinity from the Baoshan block, western Yunnan, China. *Alcheringa*, 20: 81–101
- Shi G R, Grunt T A. 2000. Permian Gondwana-Boreal antitropicality with special reference to brachiopod faunas. *Palaeogeogr Palaeoclimatol Palaeoecol*, 155: 239–263
- Shi G R, Metcalfe I, Lee S, Chu D, Wu H, Yang T, Zakharov Y D. 2022. Marine invertebrate fossils from the Permian-Triassic boundary beds of two core sections in the northern Perth Basin, Western Australia. *Alcheringa*, 46: 156–173
- Shi G R, Shen S Z, Zhan L P. 2003. A Guadalupian-Lopingian (Middle to Late Permian) brachiopod fauna from the Juripu Formation in the Yarlung-Zangbo suture zone, Southern Tibet, China. *J Paleontology*, 77: 1053–1068
- Shi G R, Shen S Z. 2001. A biogeographically mixed, Middle Permian brachiopod fauna from the Baoshan Block, western Yunnan, China. *Paleontology*, 44: 237–258
- Shi Y K, Huang H, Jin X C, Yang X N. 2011. Early Permian fusulinids from the Baoshan Block, western Yunnan, China and their paleobiogeographic significance. *J Paleontol*, 85: 489–501
- Shi Y K, Huang H, Jin X C. 2017. Depauperate fusulinid faunas of the Tengchong Block in western Yunnan, China, and their paleogeographic and paleoenvironmental indications. *J Paleontol*, 91: 12–24
- Shi Y K, Jin X C, Huang H, Yang X N. 2008. Permian fusulinids from the Tengchong Block, Western Yunnan, China. *J Paleontol*, 82: 118–127
- Shi Y K, Yang X N, Jin X C. 2005. Restudy of the “*Rugososchwagerina*” of the Middle Permian from Xiaoxinzhai of Gengma, western Yunnan (in Chinese). *Acta Palaeontol Sin*, 44: 535–544
- Shields C A, Kiehl J T. 2018. Monsoonal precipitation in the Paleo-Tethys warm pool during the latest Permian. *Palaeogeogr Palaeoclimatol Palaeoecol*, 491: 123–136
- Sichuan Regional Geological Survey, Nanjing Institute of Geology and Palaeontology. 1982. Stratigraphy and Palaeontology of Western Sichuan and Eastern Tibet, No.1 (in Chinese). Chengdu: Sichuan People's Publishing House. 1–341
- Skwarko S K, Kummel B. 1972. Marine Triassic molluscs of Australia and Papua New Guinea. Bureau Mineral Resources, Geology, Geophysics of Australia Bulletin, 150: 111–127
- Stampfli G M. 2000. Tethyan oceans. *Geol Soc Lond Spec Publ*, 173: 1–23
- Sugiyama T, Ueno K. 1998. Paleobiogeography of Gondwana-derived Terranes in Western Yunnan, South China (preliminary report). *J Geography (Chigaku Zasshi)*, 107: 549–558
- Sun D L, Hu Z X, Chen T E. 1981. Discovery of Late Permian strata in Lhasa area (in Chinese). *J Strat*, 5: 139–143
- Sun D L, Xu J T. 1991. Outline of Permian, Jurassic and Cretaceous strata from Rutog region, Xizang (Tibet). In: Sun D L, Xu J T, eds. Permian Jurassic and Cretaceous strata and palaeontology from Rutog region, Xizang (Tibet) (in Chinese with English abstract). Nanjing: Nanjing University Press. 1–41
- Sun D L. 1991. Permian (Sakmarian–Artinskian) brachiopod fauna from Gegyai County, northwestern Xizang (Tibet) and its biogeographic significance. In: Sun D L, Xu J T, eds. Permian Jurassic and Cretaceous strata and palaeontology from Rutog region, Xizang (Tibet) (in Chinese with English abstract). Nanjing: Nanjing University Press. 215–275
- Sun Y, Joachimski M M, Wignall P B, Yan C, Chen Y, Jiang H, Wang L, Lai X. 2012. Lethally hot temperatures during the early Triassic greenhouse. *Science*, 338: 366–370
- Thomas B M, Willink R J, Grice K, Twitchett R J, Purcell R R, Archbold N W, George A D, Tye S, Alexander R, Foster C B, Barber C J. 2004. Unique marine Permian-Triassic boundary section from Western Australia. *Aust J Earth Sci*, 51: 423–430
- Tibetan Plateau Scientific Expedition Team and Chinese Academy of Sciences. 1984. Stratigraphy of Tibet (in Chinese). Beijing: Geological Publishing House. 1–405
- Ueno K. 2001. *Jinzhangia*, a new staffellid Fusulinoidea from the Middle Permian Daaazi Formation of the Baoshan Block, west Yunnan, China. *J Foraminiferal Res*, 31: 233–243
- Ueno K. 2003. The Permian fusulinoidean faunas of the Sibumasu and Baoshan blocks: Their implications for the paleogeographic and paleoclimatologic reconstruction of the Cimmerian Continent. *Palaeogeogr Palaeoclimatol Palaeoecol*, 193: 1–24
- Ueno K. 2006. The Permian antitropical fusulinoidean genus *Mono-diexodina*: Distribution, taxonomy, paleobiogeography and paleoecology. *J Asian Earth Sci*, 26: 380–404
- Ueno K, Arita M, Meno S, Sardud A, Saesaengseerung D. 2015. An Early Permian fusuline fauna from southernmost Peninsular Thailand: Discovery of Early Permian warming spikes in the peri-Gondwanan Sibumasu Block. *J Asian Earth Sci*, 104: 185–196
- Ueno K, Mizuno Y, Wang X, Mei S. 2002. Artinskian conodonts from the Dingjiazhai Formation of the Baoshan Block, West Yunnan, Southwest China. *J Paleontol*, 76: 741–750
- Ueno K, Wang Y J, Wang X D. 2003. Fusulinoidean faunal succession of a Paleo-Tethyan oceanic seamount in the Changning-Menglian Belt, West Yunnan, Southwest China: An overview. *Isl Arc*, 12: 145–161
- Viaretti M, Crippa G, Posenato R, Shen S Z, Angiolini L. 2021. Lopingian brachiopods from the Abadeh section (Central Iran) and their biostratigraphic implications. *Boll Soc Paleontol Ital*, 60: 213–254
- Viaretti M, Heward A P, Gementi A, Angiolini L. 2022. Upper Cisuralian-Lower Guadalupian brachiopods from the Qarari Unit, Batain Plain, Northeast Oman: Systematics, palaeoecology and correlation. *Riv Ital Paleontol Stratigr*, 128: 643–693
- Wan B, Wu F Y, Chen L, Zhao L, Liao X F, Xiao W J, Zhu R X. 2019. Cyclical one-way continental rupture-drift in the Tethyan evolution: Subduction-driven plate tectonics. *Sci China Earth Sci*, 62: 2005–2016
- Wang C, Ding L, Cai F L, Wang H Q, Zhang L Y, Yue Y H. 2022. Evolution of the Sumdo Paleo-Tethyan Ocean: Constraints from Permian Luobadui Formation in Lhasa terrane, South Tibet. *Palaeogeogr Palaeoclimatol Palaeoecol*, 595: 110974
- Wang L, Wignall P B, Sun Y, Yan C, Zhang Z, Lai X. 2017. New Permian-Triassic conodont data from Selong (Tibet) and the youngest occurrence of *Vjalovognathus*. *J Asian Earth Sci*, 146: 152–167
- Wang Q H, Xu Z X, Wu R Z. 1988. Permian System in Gyainyima District of Zhada, Xizang (Tibet) (in Chinese). *J Chengdu College Geol*, 15: 42–47
- Wang W, Dong Z Z, Wang C Y. 2004. The conodont ages of the Dingjiazhai and Woniusi formations in the Baoshan area, western Yunnan (in Chinese). *Acta Micropalaeontol Sin*, 21: 273–282
- Wang X D, Hu K Y, Shi Y K, Chen J T, Yang S R, Ye X Y, Li X M, Song Y F, Chen B, Chang X L, Yao L, Zhang Y C, Fan J X, Shen S Z. 2021. The missing upper Carboniferous in the Cimmerian continent: A critical review. *Earth-Sci Rev*, 217: 103627
- Wang X D, Lin W, Shen S Z, Chaodumrong P, Shi G R, Wang X J, Wang Q L. 2013. Early Permian rugose coral *Cyathaxonia* faunas from the Sibumasu Terrane (Southeast Asia) and the southern Sydney Basin (Southeast Australia): Paleontology and paleobiogeography. *Gondwana Res*, 24: 185–191
- Wang X D, Shen S Z, Sugiyama T, West R R. 2003. Late Palaeozoic corals

- of Tibet (Xizang) and West Yunnan, Southwest China: Successions and palaeobiogeography. *Palaeogeogr Palaeoclimatol Palaeoecol*, 191: 385–397
- Wang X D, Ueno K, Mizuno Y, Sugiyama T. 2001. Late Paleozoic faunal, climatic, and geographic changes in the Baoshan block as a Gondwana-derived continental fragment in southwest China. *Palaeogeogr Palaeoclimatol Palaeoecol*, 170: 197–218
- Wang X J, Wang X D, Zhang Y C, Cao C Q, Lee D J. 2019. Late Permian rugose corals from Gyanyima of Drhada, Tibet (Xizang), Southwest China. *J Paleontol*, 93: 856–875
- Wang Y, Ueno K, Zhang Y C, Cao C Q. 2010. The Changhsingian foraminiferal fauna of a Neotethyan seamount: The Gyanyima Limestone along the Yarlung-Zangbo suture in southern Tibet, China. *Geol J*, 45: 308–318
- Wang Y, Ueno K. 2009. A new fusulinoid genus *Dilatofusulina* from the Lopingian (Upper Permian) of southern Tibet, China. *J Foraminiferal Res*, 39: 56–65
- Wang Y, Zhang Y, Zheng Q, Tian X, Huang X, Luo M. 2020. The early Wuchiapingian (late Permian) fusuline fauna from the Penglaitan Section, South China. *Pap Paleontol*, 6: 485–499
- Wang Y J, Sheng J Z, Zhang L X. 1981. Fusulinids from Xizang of China. In: Nanjing Institute of Geology and Palaeontology, ed. *Palaeontology of Xizang, Book 3* (in Chinese). Beijing: Science Press. 1–80
- Wang Y J, Zhou J P. 1986. New material of fusulinids from Xainza, Xizang (in Chinese with English abstract). *Bulletin of Nanjing Institute of Geology and Palaeontology, Academia Sinica*, No. 10: 141–156
- Wardlaw B R, Mei S L. 1999. Refined conodont biostratigraphy of the Permian and lowest Triassic of the Salt and Khizor ranges, Pakistan. In: Yin H F, Tong J N, eds. *Proceedings of the International conference on Pangea and the Paleozoic-Mesozoic transition*. Wuhan: China University of Geosciences Press. 154–156
- Wardlaw B R, Pogue K R. 1995. The Permian of Pakistan. In: Scholle P A, Peryt T M, Ulmer-Scholle D S, eds. *The Permian of North Pangea. Volume 2: Sedimentary Basins and Economic Resources*. New York: Springer-Verlag. 215–224
- Waterhouse J B. 1978. Permian Brachiopoda and Mollusca from northwest Nepal. *Palaeontogr Abt A*, 160: 1–175
- Waterhouse J B. 1981. Early Permian brachiopods from Ko Yao Noi and near Krabi, southern Thailand. *Geological Survey Memoir*, 4: 45–213
- Waterhouse J B. 1982. An early Permian cool-water fauna from pebbly mudstones in south Thailand. *Geol Mag*, 119: 337–354
- Wei B T, Cheng X, Domeier M, Jiang N, Wu Y Y, Zhang W J, Wu K, Wang B F, Xu P X, Xing L Y, Zhang D M, Li T, Deng X H, Liu F F, Zhou Y N, Wu H N. 2022. Placing another piece of the Tethyan Puzzle: The first paleozoic paleomagnetic data from the South Qiangtang Block and its paleogeographic implications. *Tectonics*, 41: e2022TC007355
- Win Z, Aung H H, Shwe K K. 2011. Shanita thawtinti, a new milioloid foraminifer from the Middle Permian of Myanmar. *Micropaleontology*, 57: 125–138
- Wu F Y, Wan B, Zhao L, Xiao W J, Zhu R X. 2020. Tethyan geodynamics (in Chinese). *Acta Petrol Sin*, 36: 1627–1674
- Wu G C, Ji Z S, Lash G G, Yao J X, Zhang S W, Li Y G. 2021. Newly discovered Wuchiapingian to Olenekian conodonts from the Longgar area, southern Lhasa Terrane and their palaeobiogeographical implications. *Lethaia*, 54: 723–735
- Wu G C, Ji Z S, Trotter J A, Yao J X, Zhou L Q. 2014. Conodont biostratigraphy of a new Permo-Triassic boundary section at Wenbudangang, north Tibet. *Palaeogeogr Palaeoclimatol Palaeoecol*, 411: 188–207
- Wu G C, Ji Z S, Yao J X, He J F, Sun Q, Shi Q Y, Li H, Zhong Z, Liu Z Y, Guo A C, Hou Z S, Li D Z, Shen B. 2017. Age revision of the dolomite to the west of Namtso and the significance of the discovered oil-immersed dolomite (in Chinese). *Acta Geol Sin-Chin Ed*, 91: 2867–2880
- Wu R Z, Lan B L. 1990. New material of Late Permian deposits from northwest Xizang (Tibet) (in Chinese). *J Strat*, 14: 216–221
- Wu R Z. 1991. The Permian stratigraphy in Duoma-Kongka Mountain mouth country, northwest of Xizang (Tibet) and southwest of Xinjiang (in Chinese). *J Chengdu College Geol*, 18: 37–47
- Xia D X. 1983. Palaeozoic stratigraphy of Xainza area, northern Xizang (Tibet). In: CGQXP Editorial Committee, Ministry of Geology and Mineral Resources PRC, ed. *Contribution to the Geology of the Qinghai-Xizang (2)* (in Chinese). Beijing: Geological Publishing House. 106–120
- Xia F S, Zhang B G. 1992. Age of the Selong Group in the Selong-Xishan Section, Tibet and the Permian-Triassic boundary (in Chinese). *J Strat*, 16: 256–263
- Xie C M, Duan M L, Song Y H, Wang B. 2021. Provenance and tectonic setting of the Sumdo Formation in the Lhasa Terrane, Tibet: Implications for early subduction evolution of the Sumdo Paleo-Tethys Ocean. *Palaeogeogr Palaeoclimatol Palaeoecol*, 584: 110712
- Xu H P, Aung K P, Zhang Y C, Shi G R, Cai F L, Zaw T, Ding L, Sein K, Shen S Z. 2021. A late Cisuralian (early Permian) brachiopod fauna from the Taungnyo Group in the Zweekabin Range, eastern Myanmar and its biostratigraphic, paleobiogeographic, and tectonic implications. *J Paleontol*, 95: 1158–1188
- Xu H P, Cao C Q, Yuan D X, Zhang Y C, Shen S Z. 2018. Lopingian (Late Permian) brachiopod faunas from the Qubuega Formation at Tulong and Kujianla in the Mt. Everest area of southern Tibet, China. *Riv Ital Paleontol Stratigr*, 124: 139–162
- Xu H P, Zhang Y C, Qiao F, Shen S Z. 2019. A new Changhsingian brachiopod fauna from the Xiala Formation at Tsochen in the central Lhasa Block and its paleogeographical implications. *J Paleontol*, 93: 876–898
- Xu H P, Zhang Y, Yuan D, Shen S Z. 2022. Quantitative palaeobiogeography of the Kungurian-Roadian brachiopod faunas in the Tethys: Implications of allometric drifting of Cimmerian blocks and opening of the Meso-Tethys Ocean. *Palaeogeogr Palaeoclimatol Palaeoecol*, 601: 111078
- Xu R. 1976. On the discovery of a *Glossopteris* flora in southern Xizang and its significance in geology and palaeogeography (in Chinese). *Chin J Geol*, 323–331
- Yang J S, Xu Z Q, Li Z L, Xu X Z, Li T F, Ren Y F, Li H Q, Chen S Y, Robinson P T. 2009. Discovery of an eclogite belt in the Lhasa block, Tibet: A new border for Paleo-Tethys? *J Asian Earth Sci*, 34: 76–89
- Yang J Y, Qin S, Zhang W, Ni M C. 2016. Glacial-marine diamictite of Gondwana facies in the Sêbrong, East Gangdisê (in Chinese). *Acta Geol Sichuan*, 36: 195–199
- Yang S, Liang X, Jiang M, Chen L, He Y, Thet Mon C, Hou G, Thant M, Sein K, Wan B. 2022. Slab remnants beneath the Myanmar terrane evidencing double subduction of the Neo-Tethyan Ocean. *Sci Adv*, 8: eabo1027
- Yang W P. 1999. Stratigraphic and phytogeographic palynology of Late Paleozoic sediments in western Yunnan, China. *Sci rep Niigata Univ Ser E: Geol*, 14: 15–99
- Yang Z Y, Hu C M, Xiong B. 1990. Carboniferous and Permian brachiopods of the Ngari area. In: Yang Z Y, Nie Z T, eds. *Paleontology of Ngari, Tibet (Xizang)* (in Chinese with English abstract). Wuhan: The China University of Geosciences Press. 80–88
- Yao J X, Ji Z S, Wu G C, Zhan L P, Liu G Z, Jiang Z T, Fu Y H. 2007. Deri'angma-Xiala section in the Xainza area, Tibet, China: A bridge for the stratigraphic and paleontological correlation between Gondwana and Tethys during the Late Carboniferous and Early Permian (in Chinese with English abstract). *Geol Bull Chin*, 26: 31–41
- Yao J X, Li Z S. 1987. Permian-Triassic conodont faunas in the Selong-Xishan Section, Nyalam County, Tibet and the Permian-Triassic Boundary (in Chinese). *Chin Sci Bull*, 32: 45–51
- Yin A, Harrison T M. 2000. Geologic evolution of the Himalayan-Tibetan Orogen. *Annu Rev Earth Planet Sci*, 28: 211–280
- Yin H, Jiang H, Xia W, Feng Q, Zhang N, Shen J. 2014. The end-Permian regression in South China and its implication on mass extinction. *Earth-Sci Rev*, 137: 19–33
- Yin J X, Guo S Z. 1976. On the discovery of the stratigraphy of Gondwana facies in northern slope of the Qomolangma Feng in southern Xizang, China (in Chinese). *Chin J Geol*, 11: 291–322

- Yin J X. 1997. Stratigraphic geology of Gondwana facies of Qinghai-Xizang (Tibet) plateau and adjacent areas (in Chinese with English abstract). Beijing: Geological Publishing House. 1–206
- Yuan D X, Aung K P, Henderson C M, Zhang Y C, Zaw T, Cai F, Ding L, Shen S Z. 2020. First records of Early Permian conodonts from eastern Myanmar and implications of paleobiogeographic links to the Lhasa Block and northwestern Australia. *Palaeogeogr Palaeoclimatol Palaeoecol*, 549: 109363
- Yuan D X, Zhang Y C, Qiao F, Xu H P, Ju Q, Shen S Z. 2022. A new late Kungurian (Cisuralian, Permian) conodont and fusuline fauna from the South Qiangtang Block in Tibet and their implications for correlation and paleobiogeography. *Palaeogeogr Palaeoclimatol Palaeoecol*, 589: 110822
- Yuan D X, Zhang Y C, Shen S Z, Henderson C M, Zhang Y J, Zhu T X, An X Y, Feng H Z. 2016. Early Permian conodonts from the Xainza area, central Lhasa Block, Tibet, and their palaeobiogeographical and palaeoclimatic implications. *J Systatic Palaeontol*, 14: 365–383
- Yuan D X, Zhang Y C, Shen S Z. 2018. Conodont succession and re-assessment of major events around the Permian-Triassic boundary at the Selong Xishan section, southern Tibet, China. *Glob Planet Change*, 161: 194–210
- Yuan D X, Zhang Y C, Zhang Y J, Zhu T X, Shen S Z. 2014. First records of Wuchiapingian (Late Permian) conodonts in the Xainza area, Lhasa Block, Tibet, and their palaeobiogeographic implications. *Alcheringa*, 38: 546–556
- Zhai Q G, Jahn B M, Su L, Ernst R E, Wang K L, Zhang R Y, Wang J, Tang S. 2013. SHRIMP zircon U-Pb geochronology, geochemistry and Sr-Nd-Hf isotopic compositions of a mafic dyke swarm in the Qiangtang terrane, northern Tibet and geodynamic implications. *Lithos*, 174: 28–43
- Zhan L P, Wu R Y. 1982. Early Permian brachiopods from Xainza district, Xizang (Tibet). In: CGQXP Editorial Committee, Ministry of Geology and Mineral Resources PRC, eds, Contribution to the Geology of the Qinghai-Xizang (Tibet) Plateau (16) (in Chinese with English abstract). Beijing: Geological Publishing House. 86–109
- Zhan L P, Yao J X, Ji Z S, Wu G C. 2007. Late Carboniferous- Early Permian brachiopod fauna of Gondwanic affinity in Xainza County, northern Tibet, China: Revisited (in Chinese). *Geol Bull Ch*, 26: 54–72
- Zhang C, Bucher H, Shen S Z. 2017. Griesbachian and Dienerian (Early Triassic) ammonoids from Qubu in the Mt. Everest area, southern Tibet. *Palaeoworld*, 26: 650–662
- Zhang F F, Shen S Z, Cui Y, Lenton T M, Dahl T W, Zhang H, Zheng Q F, Wang W, Krainer K, Anbar A D. 2020. Two distinct episodes of marine anoxia during the Permian-Triassic crisis evidenced by uranium isotopes in marine dolostones. *Geochim Cosmochim Acta*, 287: 165–179
- Zhang H R, Torsvik T H. 2022. Circum-Tethyan magmatic provinces, shifting continents and Permian climate change. *Earth Planet Sci Lett*, 584: 117453
- Zhang H, Zhang F F, Chen J B, Erwin D H, Syverson D D, Ni P, Rampino M, Chi Z, Cai Y F, Xiang L, Li W Q, Liu S A, Wang R C, Wang X D, Feng Z, Li H M, Zhang T, Cai H M, Zheng W, Cui Y, Zhu X K, Hou Z Q, Wu F Y, Xu Y G, Planavsky N, Shen S Z. 2021. Felsic volcanism as a factor driving the end-Permian mass extinction. *Sci Adv*, 7: eabh1390
- Zhang L X, Mu X N, Sun D L, Dong D Y. 1979. The new understanding of “Tuoba Coal” in Qamdo, Tibet (in Chinese). *J Stratigr*, 3: 231–232
- Zhang L X. 1991. Early-Middle Permian fusulinids from Ngari, Xizang (Tibet). In: Sun D L, Xu J T, eds. Permian Jurassic and Cretaceous Strata and Palaeontology from Rutog Region, Xizang (Tibet) (in Chinese with English abstract). Nanjing: Nanjing University Press. 42–67
- Zhang S H, Shen S Z, Erwin D H. 2022. Latitudinal diversity gradient dynamics during Carboniferous to Triassic icehouse and greenhouse climates. *Geology*, 50: 1166–1171
- Zhang S X, Jin Y G. 1976. Late Paleozoic brachiopods from the Mount Jolmo Lungma Region. In: A Report of Scientific Expedition in the Mount Jolmo Lungma Region (1966–68) (in Chinese). Beijing: Science Press. 159–242
- Zhang Y C, Aung K P, Shen S Z, Zhang H, Zaw T, Ding L, Cai F L, Sein K. 2020. Middle Permian fusulines from the Thitsipin Formation of Shan State, Myanmar and their palaeobiogeographical and palaeogeographical implications. *Pap Palaeontol*, 6: 293–327
- Zhang Y C, Cheng L R, Shen S Z. 2010. Late Guadalupian (Middle Permian) fusuline fauna from the Xiala Formation in Xainza County, central Tibet: Implication of the rifting time of the Lhasa Block. *J Paleontol*, 84: 955–973
- Zhang Y C, Shen S Z, Zhai Q G, Zhang Y J, Yuan D X. 2016a. Discovery of a *Sphaeroschwagerina* fusuline fauna from the Raggyorcaka Lake area, northern Tibet: Implications for the origin of the Qiangtang Metamorphic Belt. *Geol Mag*, 153: 537–543
- Zhang Y C, Shen S Z, Zhang Y J, Zhu T X, An X Y, Huang B X, Ye C L, Qiao F, Xu H P. 2019a. Middle Permian foraminifers from the Zhabuye and Xiadong areas in the central Lhasa Block and their paleobiogeographic implications. *J Asian Earth Sci*, 175: 109–120
- Zhang Y C, Shen S Z, Zhang Y J, Zhu T X, An X Y. 2016b. Middle Permian non-fusuline foraminifers from the middle part of the Xiala Formation in Xainza County, Lhasa Block, Tibet. *J Foramin Res*, 46: 99–114
- Zhang Y C, Shi G R, Shen S Z, Yuan D X. 2014. Permian fusuline fauna from the lower part of the Lugu Formation in the central Qiangtang Block and its geological implications. *Acta Geol Sin-Engl Ed*, 88: 365–379
- Zhang Y C, Shi G R, Shen S Z. 2013a. A review of Permian stratigraphy, palaeobiogeography and palaeogeography of the Qinghai-Tibet Plateau. *Gondwana Res*, 24: 55–76
- Zhang Y C, Wang Y, Shen S Z. 2009. Middle Permian (Guadalupian) fusulines from the Xilanta Formation in the Gyanyima area of Burang County, southwestern Tibet, China. *Micropaleontology*, 55: 463–486
- Zhang Y C, Wang Y, Zhang Y J, Yuan D X. 2012. Kungurian (Late Cisuralian) fusuline fauna from the Cuozheqiangma area, northern Tibet and its palaeobiogeographical implications. *Palaeoworld*, 21: 139–152
- Zhang Y C, Wang Y, Zhang Y J, Yuan D X. 2013b. Artinskian (Early Permian) fusuline fauna from the Rongma area in northern Tibet: Palaeoclimatic and palaeobiogeographic implications. *Alcheringa*, 37: 529–546
- Zhang Y C, Wang Y. 2018. Permian fusuline biostratigraphy. *Geol Soc Lond Spec Publ*, 450: 253–288
- Zhang Y C, Wang Y. 2019. Middle Permian foraminifers from the Xilanta Formation in the Gyanyima area, Burang County, Tibet and their geological implications (in Chinese). *Acta Palaeontol Sin*, 58: 311–323
- Zhang Y C, Zhang Y J, Yuan D X, Xu H P, Qiao F. 2019b. Stratigraphic and paleontological constraints on the openingtime of the Bangong-Nujiang Ocean (in Chinese). *Acta Petrol Sin*, 35: 3083–3096
- Zhang Y C. 2010. Late middle Permian (Guadalupian) fusuline fauna from the Gyanyima area of Burang County, Tibet, China and its paleobiogeographic implications (in Chinese with English abstract). *Acta Palaeontol Sin*, 49: 231–250
- Zhang Y J, Zhang Y C, Pang W H, Zhu T X. 2013c. The litho/sedimentary facies analysis of Lagar Formation, Xainza area, Tibet (in Chinese). *Acta Sedimentol Sin*, 31: 269–281
- Zhang Y J, Zhu T X, Zhang Y C, An X Y. 2014b. The stratigraphic division of Xiala Formation from Xainza area, Tibet and its facies (microfacies) (in Chinese). *Acta Geol Sin-Chin Ed*, 88: 273–284
- Zhang Z G, Chen J R, Yu H J. 1985. Early Permian stratigraphy and character of fauna in Xainza district, northern Xizang (Tibet), China (in Chinese with English abstract). In: CGQXP Editorial Committee, Ministry of Geology and Mineral Resources PRC, eds, Contribution to the Geology of the Qinghai-Xizang (Tibet) Plateau (16). Beijing: Geological Publishing House. 117–138
- Zheng C Z, Wang Y S, Zhang S Q. 2005. The Carboniferous-Permian biostratigraphic division of Deriangmato-Xialashan of the Xainza area, northern Tibet (in Chinese). *J Strat*, 29: 520–528
- Zheng J B, Jin X C, Huang H, Yan Z, Wang H F, Bai L Q. 2021. Sedimentology and detrital zircon geochronology of the Nanpihe Formation in the central zone of the Changning-Menglian Belt in western Yunnan, China: Revealing an allochthon emplaced during the closure of Paleo-

- Tethys. *Int J Earth Sci-Geol Rund*, 110: 2685–2704
- Zheng Y Y, Xu R K, Wang C Y, Ma G T. 2007. Discovery of Permian cold water conodont faunas in China (in Chinese). *Chin Sci Bull*, 52: 578–583
- Zhong Y T, Luo Z Y, Mundil R, Wei X, Liu H Q, He B, Huang X L, Tian W, Xu Y G. 2022. Constraining the duration of the Tarim flood basalts (northwestern China): CA-TIMS zircon U-Pb dating of tuffs. *GSA Bull*, 134: 325–334
- Zhong Y, Liu W L, Xia B, Liu J N, Guan Y, Yin Z X, Huang Q T. 2017. Geochemistry and geochronology of the Mesozoic Lanong ophiolitic mélange, northern Tibet: Implications for petrogenesis and tectonic evolution. *Lithos*, 292-293: 111–131
- Zhou W M, Aung K P, Liu L, Zhang Y C, Zaw T, Wang J, Shen S Z. 2020. First record of Cisuralian-Guadalupian plant fossils from the Shan Plateau, eastern Myanmar. *Palaeoworld*, 29: 108–116
- Zhou Y N, Cheng X, Yu L, Yang X F, Su H L, Peng X M, Xue Y K, Li Y Y, Ye Y K, Zhang J, Li Y Y, Wu H N. 2016. Paleomagnetic study on the Triassic rocks from the Lhasa Terrane, Tibet, and its paleogeographic implications. *J Asian Earth Sci*, 121: 108–119
- Zhu D C, Zhao Z D, Niu Y, Dilek Y, Hou Z Q, Mo X X. 2013. The origin and pre-Cenozoic evolution of the Tibetan Plateau. *Gondwana Res*, 23: 1429–1454
- Zhu R X, Zhao P, Zhao L. 2022. Tectonic evolution and geodynamics of the Neo-Tethys Ocean (in Chinese). *Sci China Earth Sci*, 52: 1–25
- Zhu T X, Pan G T, Feng X T, Zou G F, Li J Z. 2002. Discovery and tectonic significance of Permian Basic volcanic rocks in the Selong area on the northern slope of the Himalayas, southern Tibet (in Chinese). *Geol Bull Chin*, 21: 717–722
- Zhu X F. 1982a. Lower Permian fusulinids from Xainza county, Xizang (Tibet). In: CGQXP Editorial Committee, Ministry of Geology and Mineral Resources PRC, eds, Contribution to the Geology of the Qinghai-Xizang (Tibet) Plateau (16) (in Chinese with English abstract). Beijing: Geological Publishing House. 110–135
- Zhu X F. 1982b. Lower Permian fusulinids from Lhunzhub county, Xizang (Tibet). In: CGQXP Editorial Committee, Ministry of Geology and Mineral Resources PRC, eds, Contribution to the Geology of the Qinghai-Xizang (Tibet) Plateau (16) (in Chinese with English abstract). Beijing: Geological Publishing House. 110–135

(Editorial handling: Xiangdong WANG)